BOLT BERANEK AND NEWMAN INC

CONSULTING • DEVELOPMENT • RESEARCH

BBN Report No. 2304

31 August 1972

LINEAR PREDICTION AND THE SPECTRAL ANALYSIS OF SPEECH

by

John I. Makhoul

Jared J. Wolf

AD 749066

DDC
RECEIVED
SEP 29 1972
C

Technical Report

Submitted to:

Advanced Research Projects Agency
1400 Wilson Blvd.
Arlington, Virginia 22209

Attention: Dr. L. G. Roberts

Reproduced by
NATIONAL TECHNICAL
INFORMATION SERVICE
U S Department of Commerce
Springfield VA 22151

This research was supported by the Advanced Research Projects Agency of the Department of Defense under Contract No. DAHC-71-C-0088.

DISTRIBUTION STATEMENT A
Approved for public release;
Distribution Unlimited

Unclassified

Security Classification

DOCUMENT CONTROL DATA - R & D

Security classification of title, body of abstract and indexing annotation must be entered when the overall report is classified

1 ORIGINATING ACTIVITY (Corporate author)

Bolt Beranek and Newman Inc.
50 Moulton Street
Cambridge, Massachusetts 02138

2a. REPORT SECURITY CLASSIFICATION

Unclassified

2b GROUP

3 REPORT TITLE

Linear Prediction and the Spectral Analysis of Speech

4 DESCRIPTIVE NOTES (*Type of report and inclusive dates*)

Technical Report

5 AUTHOR(S) (*First name, middle initial, last name*)

1) John I. Makhoul
2) Jared J. Wolf

6 REPORT DATE	7a. TOTAL NO OF PAGES	7b NO OF REFS
31 August 1972	237	55

8a CONTRACT OR GRANT NO	9a ORIGINATOR'S REPORT NUMBER(S)
DAHC15-71-C-0088	BBN Report No. 2304
b. PROJECT NO	
c.	9b OTHER REPORT NO(S) (*Any other numbers that may be assigned this report*)
d.	none

10 DISTRIBUTION STATEMENT

Distribution of this document is unlimited.

11 SUPPLEMENTARY NOTES	12 SPONSORING MILITARY ACTIVITY
	Advanced Research Projects Agency 1400 Wilson Blvd. Arlington, Virginia 22209

13 ABSTRACT

This report gives a detailed treatment of the use of linear prediction in speech analysis. New concepts are developed and more familiar concepts are seen in a new way. The Covariance and Autocorrelation methods are derived in the time and frequency domains. Both methods are shown to be derivable from a more general concept, that of generalized analysis-by-synthesis, where a nonstationary two-dimensional spectrum is approximated by another model spectrum. Linear prediction analysis is a special case where the model spectrum is all-pole. Also, under the assumption of stationarity the general Covariance method reduces to the Autocorrelation method. The normalized error is defined. Its relation to the cepstral zero quefrency, its usefulness as a voicing detector and as a determiner of the optimum number of predictor coefficients are discussed. The application of linear prediction to pitch extraction and formant analysis is carefully examined. Specific issues discussed include the adequacy of an all-pole model for formant extraction, pitch-synchronous and pitch-asynchronous analysis, windowing, preemphasis, and formant extraction by peak picking.

DD FORM 1 NOV 65 1473 (PAGE 1)

S/N 0101-807-6811

Unclassified

Security Classification

Unclassified
Security Classification

14 KEY WORDS	LINK A		LINK B		LINK C	
	ROLE	WT	ROLE	WT	ROLE	WT
Linear Prediction						
Predictive Coding						
Prony's Method						
Time-Domain Analysis						
Spectral Analysis						
Nonstationary Spectral Analysis						
Two-Dimensional Short-Time Spectra						
Speech Analysis						
Analysis-by-Synthesis						
Generalized Analysis-by-Synthesis						
Inverse Filtering						
Signal Processing						
FFT Pruning						
Cepstral Analysis						
Minimum-Phase Sequences						
Voicing Detection						
Pitch Extraction						
Formant Extraction						
Windowing						

DD FORM 1 NOV 65 1473 (BACK)

S/N 0101-807-6811

Security Classification

A-31409

BBN Report No. 2304 31 August 1972

LINEAR PREDICTION AND THE SPECTRAL ANALYSIS OF SPEECH

by

John I. Makhoul

Jared J. Wolf

Bolt Beranek and Newman Inc.
50 Moulton Street
Cambridge, Mass. 02138

This research was supported by the Advanced Research Projects Agency of the Department of Defense under Contract No. DAHC-71-C-0088.

ABSTRACT

This report gives a detailed treatment of the use of linear prediction in speech analysis. New concepts are developed and more familiar concepts are seen in a new way. The Covariance and Autocorrelation methods are derived in the time and frequency domains. Both methods are shown to be derivable from a more general concept, that of generalized analysis-by-synthesis, where a nonstationary two-dimensional spectrum is approximated by another model spectrum. Linear prediction analysis is a special case where the model spectrum is all-pole. Also, under the assumption of stationarity the general Covariance method reduces to the Autocorrelation method. The normalized error is defined. Its relation to the cepstral zero quefrency, its usefulness as a voicing detector and as a determiner of the optimum number of predictor coefficients are discussed. The application of linear prediction to pitch extraction and formant analysis is carefully examined. Specific issues discussed include the adequacy of an all-pole model for formant extraction, pitch-synchronous and pitch-asynchronous analysis, windowing, preemphasis, and formant extraction by peak picking.

ACKNOWLEDGEMENTS

The authors wish to thank Dennis Klatt, John Markel, Kenneth Stevens and Victor Zue for reading portions of earlier versions of this report and making several useful suggestions. We have also benefited from the discussions that took place in the Time-Domain Analysis Workshop at Carnegie-Mellon University in Pittsburgh, Pa., on May 19, 1972.

We also wish to thank Gail Hedtler for her patience throughout the preparation of this report.

TABLE OF CONTENTS

CHAPTER I

INTRODUCTION

1.. Historical Overview

One of the most important methods of speech analysis has been the use of the short-time spectrum. This has been accomplished in different ways and to different ends during the past 25 years. The first major breakthrough was the invention of the sound spectrograph (Koenig, Dunn & Lacey, 1946) which is still used extensively for the spectral analysis of speech. In 1960, G. Fant published the classic Acoustic Theory of Speech Production which laid the foundations for many of the different methods of speech analysis that followed. As a direct result of the significant advances that occurred in understanding the acoustics of speech production, and with the aid of high-speed digital computers, the method of analysis-by-synthesis was given new impetus at M.I.T. (Bell, Fujisaki, Heinz, Stevens and House, 1961). A bank of 36 band-pass filters was used in their analysis. Another landmark was the pitch-synchronous analysis of voiced sounds as reported by Mathews, Miller and David (1961) at Bell Labs. They actually used analysis-by-synthesis on the spectrum of a single pitch period obtained by a Fourier analysis of the sampled waveform. In 1964, A.M. Noll introduced the cepstrum for the purpose of pitch extraction. The cepstrum was later used as the basis for a formant tracking system (Schafer and Rabiner, 1970). This very

brief review gives a representative sample of the ideas and methodologies that have had a definite effect on the types of speech analysis that many speech researchers have chosen to pursue. A more complete review can be found in Flanagan (1972).

1.2 Linear Prediction

The past two years have witnessed a surge of interest on the part of the speech community in a method of analysis known alternately as predictive coding, linear prediction, Prony's method, inverse filtering formulation, etc. This surge of interest has been also accompanied by an air of confusion. Two main reasons for this confusion are:

(1) A lack of exposition on the similarities and differences between different formulations.

(2) A resurfacing of some of the problems (e.g. windowing, preemphasis, etc.) associated with accepted methods for computation of short-time spectra.

We shall attempt, in this report, to deal with these problems by relating a few of these formulations to each other.

Let us first discuss what these formulations have in common. As far as we can ascertain, all the methods we have inspected have exactly one thing in common: they all assume that at a particular instant in time, a speech sample $s(nT)$ can be approximated by a linearly weighted summation of the past p samples, where p is

some integer.

$$s(nT) \cong \sum_{k=1}^{p} a_k \, s(nT-kT)$$

or

$$s_n \cong \sum_{k=1}^{p} a_k \, s_{n-k} \, , \qquad (1\text{-}1)$$

where T is the sampling interval, n is the sample number, and a_k, $1 \le k \le p$, are the weights. Equivalently, given p samples of a speech signal, the following sample can be predicted approximately by a linear summation of the p known samples. Hence the term "linear prediction". Henceforth we shall use the term "linear prediction" as a generic name for any method that makes an assumption equivalent to that in (1-1).

The problem at hand, as put forth by linear prediction, is to compute a set of predictor coefficients a_k such that (1-1) holds optimally over a specified period of time. It is in computing the set of coefficients a_k that different formulations of linear prediction have evolved.

The assumption in (1-1) could be made for any signal, be it speech or not. The reason that this assumption works well for speech is that it is based on a model of speech production which has been shown to work quite well in analysis-synthesis systems (Fant, 1960). Basically, the model assumes an all-pole transfer

function of the combined effects of the glottal source, the vocal tract and radiation. These poles can be computed by solving a polynomial in z with coefficients a_k. A more detailed description of this model is given in Chapter II.

Theoretically there exist an unlimited number of ways in which to compute the coefficients a_k. However, we shall initially limit our discussion to three formulations which we feel to be representative of the possible methods of analysis and which raise some interesting issues. We shall describe briefly each of the formulations and give representative references on each without attempting to give a complete bibliography. The three methods will be given mnemonic names for ease of reference.

Exact Method

This method assumes that:

(a) The signal is defined for exactly 2p consecutive values.

(b) A speech sample can be predicted exactly from the past p samples, and that

(c) This holds for the trailing p consecutive samples.

These assumptions are represented by the following set of equations:

$$\sum_{k=1}^{p} a_k \, s_{n-k} = s_n, \quad n=0,1,\ldots,p-1. \qquad (1\text{-}2)$$

These are p equations in p unknowns which in general can be solved for the coefficients a_k, $1 \le k \le p$.

Covariance Method

This method assumes that:

(a) The signal is defined for p+N consecutive values, where N is some integer.

(b) A speech sample can be approximately predicted from the past p samples, and that

(c) This holds for the trailing N consecutive samples.

(d) The total-squared error between the real signal and its predicted value is minimized over the N consecutive samples. (Some prefer to use the mean-squared error instead of total-squared error. The difference in this case is a division by a constant N which does not affect the results of minimization.)

The minimization of error results in the following set of equations (detailed derivation is shown in Section 3.1).

$$\sum_{k=1}^{p} a_k \phi_{ik} = \phi_{i0}, \quad i=1,2,\ldots,p \qquad (1\text{-}3)$$

where

$$\phi_{ik} = \sum_{n=0}^{N-1} s_{n-i} s_{n-k} . \qquad (1\text{-}4)$$

Again we have p equations in p unknowns which can be solved to obtain the coefficients a_k, $1 \leq k \leq p$. The coefficients ϕ_{ik} form a covariance matrix, hence the name "Covariance Method." Equations such as (1-3) are known in least-squares terminology as the normal equations of the process (Hildebrand, 1956, p. 260). In this case we shall call (1-3) the Covariance normal equations, or alternately the Covariance normal matrix equation.

Autocorrelation Method

The assumptions made in this method are:

(a) The signal is defined for all time such that it is identically zero outside a portion of the signal N samples long, where N is some integer. This is equivalent to multiplying the speech signal by a finite window of length N.

(b) Each sample can be approximately predicted from the past p samples, and that

(c) This is true for all time.

(d) The total-squared error between the actual signal and its predicted value is minimized for all time.

The minimization of error results in the following set of equations (the derivation is given in Section 3.1):

$$\sum_{k=1}^{p} a_k \, R_{|i-k|} = R_i \quad , \quad i=1,2,\ldots,p \qquad (1\text{-}5)$$

where $$R_i = \sum_{n=0}^{N-1-|i|} s_n \, s_{n+|i|}. \qquad (1\text{-}6)$$

Again (1-5) forms p equations with p unknowns to be solved for the coefficients a_k.

The R_i are autocorrelation coefficients of the signal. The coefficients $R_{|i-k|}$ form a special matrix which we shall call the autocorrelation matrix (as opposed to the covariance matrix in the Covariance method). Also, we shall call equations (1-5) the Autocorrelation normal equations or alternately the Autocorrelation normal matrix equation.

As we shall see in Chapter IV, there are other possible formulations for the Covariance and Autocorrelation methods. The assumptions made above do not all apply in the other formulations. However, all Covariance-type formulations have (1-3) in common, and all Autocorrelation-type formulations have (1-5) in common, but (1-4) and (1-6) will not necessarily apply.

This concludes our brief description of each of three formulations for linear prediction. Now, we shall relate the work of some researchers to these three methods. The so-called Prony's method (Hildebrand, 1956, p. 378) or the exponential approximation method is equivalent to the Exact method for N = p and to the Covariance method for N≥p. A paper by Atal and Hanauer (1971),

which deals comprehensively with applications of linear prediction in speech analysis and synthesis, makes use of the Covariance method. The Autocorrelation method can be traced back to the classic work by Wiener on linear prediction (Wiener, 1966). Itakura and Saito (1970) using a maximum-likelihood method with a statistical model of speech production, derive a formulation which is equivalent to the Autocorrelation method. The digital inverse filtering formulation given by Markel (1972) is also equivalent to the Autocorrelation method. Markel's report contains early references on the subject and explores formant tracking as an application. Weinstein and Oppenheim (1971) have used linear prediction in a homomorphic vocoder, and it seems from their paper that they used the Autocorrelation method also.

It should be pointed out that linear prediction has had extensive applications in other fields. For example, Flinn (1972) gives references on seismic and acoustic applications. We quote from the introduction to the special issue on the M.I.T. Geophysical Analysis Group Reports in Geophysics (Treitel and Robinson, 1967):

> "The applications [of predictive decomposition] to seismic exploration deal with the model in which a section of seismic trace is given as the convolution of a random spike series with a minimum-delay waveform."

As we shall see, the problem in the analysis of voiced speech is very similar except instead of a random spike series (i.e.

impulses) we have a quasi-periodic impulse series. These seismic applications have used the Autocorrelation method of linear prediction.

In this report we shall investigate in detail the properties of the Autocorrelation and Covariance methods of linear prediction. The Exact method will not be discussed in any detail because it does not seem to have wide applicability in speech analysis (see Section 2.2). Of all three methods of linear prediction, we believe that the Autocorrelation method gives the speech researcher a more intuitive feel for the properties of linear prediction in terms of traditional concepts such as Fourier transformation and analysis-by-synthesis. On the other hand, the Covariance method offers new and exciting possibilities in the analysis of speech as a nonstationary signal.

1.3 Chapter Summaries

Basic to the workings of linear prediction in speech analysis is an appreciation for the underlying speech production model. The all-pole discrete model is described in Chapter II, with a critical evaluation of its adequacy for different applications of speech analysis. The main parameters of the model are the predictor coefficients. These coefficients can be computed from the speech signal by one of the methods of linear prediction. The time-domain derivation of the Covariance and Autocorrelation

methods and methods of computing the predictor coefficients are the subject of Chapter III. The stability of the resulting linear predictor is also discussed.

Although linear prediction has become popular as a time-domain analysis, we show in Chapter IV that linear prediction can be considered equally validly, and perhaps better understood, as a frequency-domain analysis. (In reality, linear prediction is an autocorrelation-domain analysis, which can be approached either from the time or frequency domain.) The formulations for the Covariance and Autocorrelation methods given in Section 1.2 are shown to be as special cases of more general formulations. We introduce the concept of generalized analysis-by-synthesis where the 2D-spectrum (two-dimensional spectrum) of a nonstationary signal (i.e. its statistics change with time) is to be approximated by another 2D-spectrum, where the error to be minimized is proportional to the integral of the ratio of the original spectrum to the approximate spectrum. In the special case when the approximate spectrum is all-pole, the generalized method reduces to the general Covariance method of linear prediction. If, in addition, the signal is assumed to be stationary, the Covariance method reduces to the Autocorrelation method. The general Covariance and Autocorrelation methods thus derived are each divided further into a direct and an indirect method, depending on whether the autocorrelation coefficients are computed from an infinite

but windowed signal, or from a finite and unwindowed portion of the signal, respectively. The formulations given in Section 1.2 are then relabelled as the indirect Covariance and direct Autocorrelation methods.

In order to better understand the manner in which linear prediction operates, we analyze in Chapter V one of the methods in detail, namely the direct Autocorrelation method. We examine the manner in which the all-pole spectrum approximates the signal spectrum, and the relation between the all-pole transfer function and the signal transfer function, especially as the number of poles is increased indefinitely. The remainder of the chapter is devoted to a detailed analysis of the normalized error, its relation to the zero quefrency (zero coefficient of the transform of the log spectrum), and its possible usefulness as a voicing detector and as a determiner of the optimum number of predictor coefficients to be used for certain applications.

Finally, in Chapter VI, we study how linear prediction can be useful in pitch extraction and formant analysis. Specific issues discussed include the adequacy of an all-pole model for formant extraction, pitch-synchronous and pitch-asychronous analysis, windowing, preemphasis, and formant extraction by peak picking.

In this report we have attempted to be as analytical as possible, but without losing sight of the applied world. The theo-

is seen as a solid basis on which to build a better understanding of how best to apply linear prediction to the analysis of speech. Thus, instead of flooding the reader with examples of when a particular method works, we have analyzed in detail situations where that method fails, in order to give a better appreciation of the processes involved.

CHAPTER II

DISCRETE MODEL OF SPEECH PRODUCTION

We mentioned in Section 1.2 that the reason linear prediction works well in the analysis of the speech signal, is that it is based on a model of speech production which agrees, to a large extent, with existing theories of speech production (such as Fant, 1960), and which has proven to be a good practical model in speech synthesis. Here we shall describe this model of speech production (in the discrete domain) and relate it to the three methods of linear prediction described in Section 1.2.

2.1 Speech Production Model

Speech is produced as a result of the excitation of a time-varying vocal tract shape. The speech signal is in general a nonstationary process, i.e. its statistics change with time. The nonstationarity is a result of changes in the excitation as well as in the vocal tract shape. If both the excitation and the vocal tract shape remain fixed, the resulting speech signal can be considered to be stationary. For example, uttering the vowel [a] at a constant pitch and intensity level produces a signal that is stationary. Keeping the vocal tract shape fixed for [a] and changing the pitch with time (such as going up a musical scale) produces a signal that is nonstationary. In general, given that some process is the output of a linear system, the process is sta-

tionary if the system is time-invariant and the input (or excitation) is stationary. If either the input is nonstationary or the system is time-varying, or both, the output process is nonstationary. The importance of the question of stationarity of the speech signal will become evident later.

For the purposes of modeling speech production, we approximate the continuously-varying vocal tract shape by a discretely-varying vocal tract shape, i.e. a vocal tract whose shape changes at discrete time intervals. Such a time interval shall be called a "frame". Within a frame, the vocal tract shape is considered to be fixed and can be modeled by a linear time-invariant filter. This model of speech production has been used effectively in speech synthesis systems. In linear prediction the linear filter is restricted to be all-pole.

Thus, the model of speech production used in linear prediction consists of the following three assumptions:

(1) Within a short interval of time (on the order of 10-25 msec) the human vocal tract is assumed to be fixed in shape. We shall refer to such an interval as a "frame".

(2) Within any frame, we assume that the transfer function of the combined effects of the glottal flow, the vocal tract (including the oral and nasal cavities) and the radiation characteristic, can be modeled by a linear time-invariant all-pole filter with either a sequence of impulses or white noise (or a combination

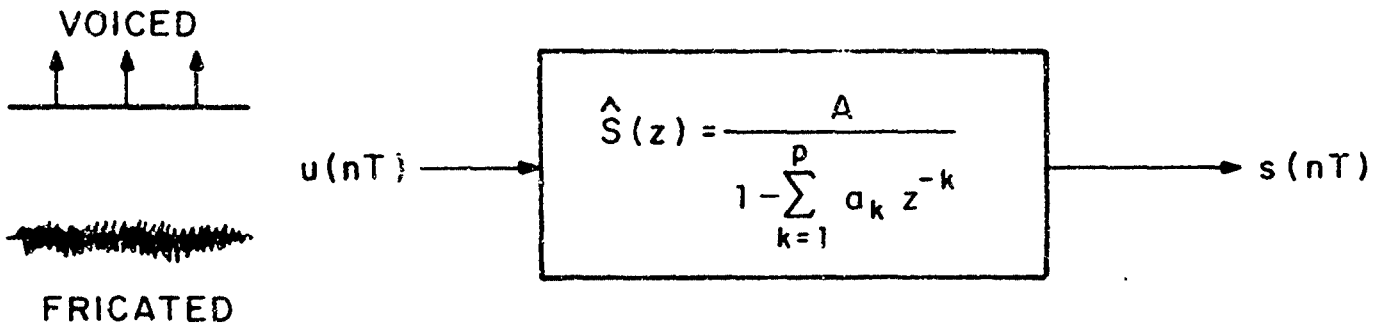

(a) FREQUENCY-DOMAIN MODEL

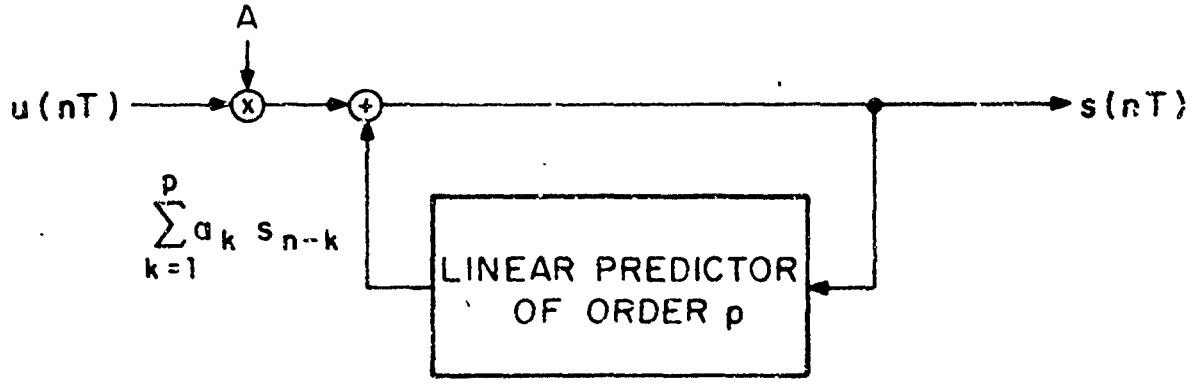

(b) TIME-DOMAIN MODEL

Fig. 2-1. Discrete model of speech production as employed in linear prediction methods.

of both) as input (see Fig. 2-1).

(3) The speech signal can be considered as the output of such an all-pole filter whose coefficients change at discrete intervals of time (on the order of 10 msec).

Below we shall focus our attention on a single frame where the all-pole filter is assumed to be time-invariant. Fig. 2-1a shows a schematic of the model in the frequency domain. The complex variable z is defined by:

$$z = e^{sT} = e^{(\sigma+j\omega)T}$$

where $s = \sigma+j\omega$ is the Laplace operator,

$\omega = 2\pi f$ is the radian frequency in rad/sec,

σ is the damping factor in rad/sec,

$T = \frac{1}{f_s}$ is the sampling interval in seconds,

and f_s is the sampling frequency in Hz.

(A brief presentation of z-transforms and their interpretation in terms of traditional Fourier series is given in Appendix A.) Figure 2-1a is interpreted as follows: Speech is either voiced, fricated, or both. (Throughout this report we shall assume that aspiration is a kind of frication.) Voiced speech is produced by applying a sequence of impulses, spaced at the pitch period, to a digital filter of the form:

$$\hat{S}(z) = \frac{A}{1-\sum_{k=1}^{p} a_k z^{-k}} = \frac{A}{H(z)} \qquad (2\text{-}2)$$

where a_k, $1 \le k \le p$ are the filter coefficients,

A is a multiplicative gain factor that controls the signal amplitude,

and $$H(z) = 1-\sum_{k=1}^{p} a_k z^{-k} \qquad (2\text{-}3)$$

is the inverse filter.

The output of the filter $\hat{S}(z)$ is s(nT), the speech samples. Fricated speech is produced by applying a sequence of white noise samples, spaced T seconds apart, to a filter of the form $\hat{S}(z)$. Voiced fricatives are produced by a combination of voicing and frication. The filter $\hat{S}(z)$ represents the combined transfer function of the glottal flow, the vocal tract and radiation. The poles of the filter $\hat{S}(z)$ can be determined by solving for the roots of the polynomial in z in the denominator of $\hat{S}(z)$.

Representing the z-transforms of s(nT) and u(nT) by S(z) and U(z), respectively, we can write from Fig. 2-1a:

$$S(z) = U(z)\ \hat{S}(z)$$

$$= \frac{A\ U(z)}{1-\sum_{k=1}^{p} a_k z^{-k}} . \qquad (2\text{-}4)$$

Equation (2-4) can be rewritten as:

$$S(z) = S(z) \sum_{k=1}^{p} a_k z^{-k} + A U(z) . \qquad (2\text{-}5)$$

Taking the inverse z-transform of (2-5) we obtain:

$$s(nT) = \sum_{k=1}^{p} a_k s(nT-kT) + A u(nT)$$

or

$$s_n = \sum_{k=1}^{p} a_k s_{n-k} + A u_n , \qquad (2\text{-}6)$$

where T, the sampling interval, has been omitted in (2-6) but is still implied.

Equation (2-6) is the time-domain counterpart to (2-4), and it represents the speech production model in the discrete time domain. A schematic of the time-domain model is shown in Fig.2-1b. It should be clear that the systems in Figs. 2-1a and 2-1b are equivalent.

2.2 Use of the Model in Linear Prediction

Note from (2-6) that except for contributions by the input u(nT), the signal s(nT) is produced by a linear summation of the past p samples. In trying to fit the model of Fig. 2-1 to a real speech signal we encounter the problem of not knowing what the input signal u(nT) looks like. For example, we don't know

a priori whether the speech signal is voiced or unvoiced. Even if we know that the signal s(nT) is likely to be voiced, we do not know the exact times of occurrence of the impulses in u(nT). Therefore, in linear prediction we first let u(nT) be an unknown (actually, the Exact method described in Section 1.2 assumes that u(nT)=0) and assume that (1-1) holds, i.e. we assume that s(nT) can be approximated by a linear summation of the past p samples. After the determination of the coefficients a_k, $1 \leq k \leq p$, we can then determine A by energy considerations, and we can also make certain statements about u(nT). (Normally, u(nT) is of interest only for voiced sounds since it gives information concerning the periodicity (pitch) of the speech signal.) Indeed, after some knowledge of the position of the pitch pulses in time, one could use that information to get a better estimate of the coefficients a_k.

As mentioned above, the Exact method of linear prediction assumes that u(nT)=0 for all n. In general, this is not a good assumption for speech unless one is sure, for example that there are no pitch pulses (in a voiced segment) during the time interval corresponding to the 2p speech samples needed for the analysis. For this reason one does not expect very good results using the Exact method of analysis. We know of no researcher who has used this method to analyze speech in any extensive manner.

On the other hand, both the Covariance and the Autocorrelation methods of analysis (see Section 1.2) admit that linear prediction produces an error which they proceed to minimize in the least-squares sense. The difference between the two methods lies in the definition of what the signal is and in the region of error minimization. This difference can be interpreted in terms of the stationarity of the speech signal. In the speech production model given in Section 2.1 the vocal tract was modeled by a linear time-invariant system for a single frame of speech. Within that frame, the signal s(nT) in Fig. 2-1 can still be either stationary or nonstationary depending on the input u(nT). As we shall see in Chapter IV, the Autocorrelation method assumes the signal s(nT) to be stationary, while the Covariance method assumes the signal to be nonstationary within a single frame.

2.3 Adequacy of the Model

We have mentioned that methods of linear prediction implicitly rely on the all-pole model of the vocal tract, glottal flow and radiation. The question is to what extent this model is adequate and for what applications. We shall compare this model with standard models of speech production described in Fant (1960) and Flanagan (1965).

For nonnasal sonorant sounds, the transfer function of the vocal tract is generally known to have only poles (resonances)

and no zeros (antiresonances). Therefore, for these sounds an all-pole model of the vocal tract is adequate. On the other hand, for nasal and fricative sounds the transfer function of the vocal tract is considered to have zeros as well as poles. This means that the zeros are being approximated by poles in the linear prediction model. Now, these zeros lie within the unit circle in the z-plane (Atal and Hanauer, 1971, p. 638), and each zero can be replaced theoretically by an infinity of poles. This is done by noting that a zero $(1-az^{-1})$ inside the unit circle (i.e. $|a|<1$), can be expanded (by long division into 1) as:

$$1-az^{-1} = \frac{1}{1+az^{-1}+a^2z^{-2}+\ldots} . \qquad (2-7)$$

Now, one could argue that the effect of a zero can be approximated by a finite number of poles and, hence, an all-pole model would also be adequate for nasal and fricative sounds. However, it is not clear how the poles that are approximating the zeros interact with the genuine poles (formants). What is likely to happen is that in trying to apply the all-pole model to nasals and fricatives, the antiresonances in those sounds will have the effect of shifting the positions and bandwidths of the formants as computed from the model. (This effect is discussed in Section 6.2.) For example, consider a particular all-pole transfer function (computed by some linear prediction method) which appro-

ximates that of the vocal tract for, say, a nasal. Not only is it unclear how one would go about locating the zeros (if any), but the computed positions and bandwidths of formants close to those zeros will be different from the "actual" values. In other words, if one is interested in locating the positions of the anti-formants as well as the formants in a nasal or fricative, then linear prediction may not be adequate. This can be important for applications such as speech recognition. On the other hand, if one is interested in using the results of the analysis for speech synthesis then the all-pole model is quite adequate. The reason for this lies partly in the fact that the human perceptual system is much more sensitive to the location of a pole than to the location of a zero (Matsuda, 1966; Flanagan, 1965, p. 215). Another reason may be that the human ear is sensitive to the general envelope of the spectrum, and it does not matter in what manner that spectrum was generated. As we shall see in Chapter IV, linear prediction guarantees a good spectral envelope fit to a short-time spectrum. Speech synthesizers that have used all-pole filters to generate sounds that normally contain zeros show that an all-pole model is quite adequate for speech production (Schafer and Rabiner, 1970; Atal and Hanauer, 1971; Klatt, 1972) although Mermelstein (1972) reports that an all-pole formulation introduces a noticeable decrease in naturalness. (The adequacy of an all-pole model for the purpose of speech recognition will be

discussed in Section 6.2.)

There remain the effects of radiation and glottal pulse shape. The effect of the radiation at the mouth and nostrils can be approximated by a zero at d.c. (Flanagan, 1965, p. 33), or in z-transform notation: $(1-z^{-1})$. The spectrum of the glottal volume velocity is characterized by a large number of zeros (Flanagan, 1965, p. 44; Mathews et al., 1961), but the general shape of the glottal spectrum can be approximated by two or three poles. Mártony (1965) found that the slope of the glottal spectrum between 500-3000 Hz varies between -12 and -18 dB/octave, depending on the individual. The net effect of the zero due to radiation and one of the poles approximating the glottal source can be approximated (in the z-plane) by a pole on the negative real axis inside the unit circle (Atal and Hanauer, 1971). (The effect on the spectrum of such a pole is described in Appendix A.) Hence, roughly speaking, the combined effects of radiation and glottal source can be approximated by two or three poles. Therefore, the linear prediction model seems to be adequate. It should be noted that the perceptual effect due to the glottal source is generally associated with the naturalness of speech and the characteristics of the speaker. Its effect on the identification of speech sounds does not seem to be of major importance (Flanagan, 1965, p. 199).

2.4 Determination of the Number of Poles p

In the linear prediction model of speech production shown in Fig. 2-1 the transfer function is assumed to have a certain number of poles p. Ideally, the value of p should change from one speech frame to another depending on the number of poles needed to represent each sound. In order to get an idea on the order of magnitude of p we shall take a specific example.

Generally for males, the average number of formants in a 5 kHz bandwidth is five. For example, for the sound [ə] the vocal (oral) tract can be approximated by a tube open at one end and closed at the other. If the length of the tract is 17 cm then the natural resonances of the tube will occur at $F_n = \frac{(2n-1)c}{4L}$, where c=340 meters/sec is the velocity of sound in air, and L=17 cm is the vocal tract length. Therefore in a 5 kHz region we have the five formants 500, 1500, 2500, 3500, and 4500 Hz. Since each formant comprises a pair of complex conjugate poles, the number of poles necessary to represent such a vocal tract is 10. [Atal and Hanauer (1971, p.630) derive the same number from a different point of view.] Now, we mentioned in Section 2.3 that two or three poles are adequate to represent the effects of the glottal flow and radiation. Therefore, the value of p should be approximately 12 or 13. However, we have so far neglected one other factor which should have an effect on the value of p, and that is

the fact that the poles are realized digitally. This has a side effect which is discussed below.

Theoretically, the number of resonances of the vocal tract is infinite. Analog formant synthesizers employing a fixed number of formants (usually 5) must compensate for higher frequency formants by what is known as the higher-pole correction (Fant, 1960). However, this higher-pole correction is not necessary in digital formant synthesizers because of the periodic frequency response of a digital formant network (Gold and Rabiner, 1968). As a result, the 10 poles necessary to represent the vocal tract transfer function in a 5 kHz bandwidth can be realized digitally without the need for compensation. On the other hand, the above reasoning cannot be applied validly to digital implementation of the poles representing the glottal flow and radiation. The periodicity of the digital network response is equivalent to an aliasing effect which can cause an error in the response of a single low-frequency pole by as much as 4 dB at 5 kHz (see Appendix A). On the average, the error is on the order of 2 dB at 5 kHz (Gold and Rabiner, 1968). This is true for each of the two or three poles representing the glottal flow and radiation. Therefore, in order to compensate for this cumulative error one must introduce at least one extra pole. The value of p now becomes approximately 13 to 14.

The above estimate for p assumes that the signal was sampled at 10 kHz. For other sampling frequencies the value of p is roughly equal to:

$$p = 2N_f + N_r \qquad (2\text{-}8)$$

where N_f is the number of formants expected in a frequency range equal to half the sampling frequency, and N_r is the number of real poles needed to represent the effects of the glottal flow and radiation. We have seen above that N_r is approximately equal to 3 or 4, independent of the sampling frequency. For nonnasal sonorants, formants occur at the rate of about one formant per 1 kHz of bandwidth (for male speakers). Therefore, (2-8) reduces to:

$$p = f_s \text{ (kHz)} + N_r \quad \text{(nonnasal sonorants)} \qquad (2\text{-}9)$$

where f_s is the sampling frequency in kHz, and N_r is equal to 3 or 4.

Equations (2-8) and (2-9) assume that the vocal tract can be approximated adequately by a number of poles. In particular, (2-9) is useful mainly for nonnasal sonorants. Other sounds, such as nasals and fricatives, are best represented by a combination of zeros and poles. Below, we shall discuss nasals as an example of sounds with zeros as well as poles.

Nasal poles correspond to the resonances of the nasal tract, while the zeros are due to the coupling to the mouth cavity. For an uncoupled nasal tract, there are no zeros and the average spacing of nasal formants is about 800 Hz for a male speaker. (Compare this with 1000 Hz for vowels; the difference is due to the fact that the nasal tract is longer than the oral tract.) These formants usually have higher bandwidths than vowel formants because of greater losses in the nasal cavity. From (2-8) we conclude that the number of poles needed to represent the uncoupled nasal system is approximately:

$$p = 1.2f_s \text{ (kHz)} + N_r. \qquad (2\text{-}10)$$

The velar nasal [ŋ] can be reasonably approximated by an uncoupled nasal tract up to 5 kHz, and (2-10) would be applicable. On the other hand, [m] and [n] have important antiformants in that frequency range. Each antiformant causes one of the nasal formants to split into two formants, thus forming what might be called a "formant cluster" (Fujimura, 1962). A nasal formant cluster, then, consists of two formants and one antiformant in the same region. In the frequency range up to 3000 Hz, [ŋ] has four formants; [m] is obtained when the second formant is replaced by a cluster consisting of two formants and one antiformant, and [n] is obtained when the third formant is replaced by a similar cluster (Fujimura, 1962). The position of the antiformant with respect to the two

formants in the cluster is quite variable, depending on the speaker and the phonetic context. If every antiformant happened to coincide with one of the two formants in its cluster, then (2-10) would still apply. However, in general, that is not the case; indeed the opposite is true. More importantly, a small shift in the position of a zero with respect to neighboring poles has drastic effects on the shape of the spectrum. This is important since linear prediction is basically a spectral matching process.

In trying to estimate a theoretical value for p in the case where zeros (or antiformants) exist, we attempted to approximate a spectral antiformant (complex conjugate pair of zeros) by a number of poles. We found that we needed at least 10 poles (10 kHz sampling) to get a rough spectral match to a single antiformant that is typical for nasals and fricatives. This number would have to be added to (2-10) in order to get a good estimate for what p should be to represent a nasal whose zero does not interact with neighboring poles. The number would have to be decreased with increased interaction. In the limit when the zero cancels a pole, (2-10) would apply as is. Since there is no a priori way to determine the position of a zero with respect to neighboring poles, there is no way of getting a good theoretical estimate for p. However, practical estimates for p do exist depending on the application. In Sections 5.6 and 6.2 we shall argue that, although the "optimum" value for p depends on the

type of sound as well as the individual speaker, a suboptimal value is usually adequate for many applications.

CHAPTER III

LINEAR PREDICTION ANALYSIS

In this chapter we shall derive in the time-domain the Covariance and Autocorrelation normal equations (1-3) and (1-5) and suggest algorithms for computing the predictor parameters. Given the normal equations, the minimum squared error is defined. The stability of the linear predictor, an important issue for speech synthesis, will then be examined for the three formulations of linear prediction. We then take a look at some autocorrelation-domain properties of linear prediction. A method for the computation of the gain factor A in $\hat{S}(z)$ will be specified.

3.1 Derivation of Covariance and Autocorrelation Normal Equations

Following the linear prediction speech production model described in Section 2.1 and represented by (2-6), we shall assume that a sampled speech signal s(nT) at time t=nT can be approximately predicted by a linear weighted summation of the past p samples. Let this approximation to s(nT) be $\tilde{s}(nT)$. We have:

$$\tilde{s}_n = \sum_{k=1}^{p} a_k \, s_{n-k} \,, \qquad (3\text{-}1)$$

where a_k, $1 \le k \le p$, is a set of real constants representing the predictor coefficients, and p is some integer whose value is determined as described in Sections 2.4 and 5.6.

Let the error between the actual value and the predicted value be given by e_n, where:

$$e_n = s_n - \tilde{s}_n$$

$$= s_n - \sum_{k=1}^{p} a_k \, s_{n-k} \, . \qquad (3\text{-}2)$$

The problem is to find a_k, $1 \le k \le p$, such that the error e_n is minimized in some sense over the desired range of signal samples. Both the Covariance and Autocorrelation methods employ a least-squares minimization procedure since it leads to a mathematically attractive solution. Denote the total-squared error by E, defined as:

$$E = \sum_n e_n^2 = \sum_n (s_n - \tilde{s}_n)^2 \, . \qquad (3\text{-}3)$$

The range over which the summation in (3-3) applies and the definition of s_n in that range is of importance. Indeed, this is exactly where the difference between the Covariance and Autocorrelation methods lies. However, let us first minimize E without specification of the range of the summation. Substituting (3-1) in (3-3) we obtain:

$$E = \sum_n (s_n - \sum_{k=1}^{p} a_k \, s_{n-k})^2 \, . \qquad (3\text{-}4)$$

The problem reduces to finding the condition that minimizes the total-squared error E with respect to a_k, $1 \le k \le p$. This condition is obtained by setting to zero the partial derivative of E with respect to each a_k:

$$\frac{\partial E}{\partial a_i} = \sum_n 2(s_n - \sum_{k=1}^{p} a_k \, s_{n-k})(-s_{n-i}) = 0, \qquad (3\text{-}5)$$

or,

$$\sum_n s_n s_{n-i} - \sum_n \sum_{k=1}^{p} a_k \, s_{n-k} \, s_{n-i} = 0, \quad 1 \le i \le p. \qquad (3\text{-}6)$$

Rearranging terms and interchanging summations we obtain:

$$\sum_{k=1}^{p} a_k \sum_n s_{n-k} \, s_{n-i} = \sum_n s_n \, s_{n-i}, \quad 1 \le i \le p. \qquad (3\text{-}7)$$

Equations (3-7) are known as the normal equations. For any definition of the signal s_n, (3-7) forms a set of p equations with p unknowns which can be solved for the predictor coefficients a_k. Now, we shall derive the Covariance and Autocorrelation normal equations from (3-7).

Covariance Normal Equations

Referring back to the assumptions of the Covariance method in Section 1.2, the summation over n in (3-3) and hence in (3-7) must go over N consecutive signal samples. Without loss of generality, we let the range of summation over n be: n=0,1,...,N-1.

We can now write (3-7) as:

$$\sum_{k=1}^{p} a_k \phi_{ik} = \phi_{i0} \ , \ i=1,2,\ldots,p \qquad (3\text{-}8)$$

where

$$\phi_{ik} = \sum_{n=0}^{N-1} s_{n-i} \, s_{n-k} \ . \qquad (3\text{-}9)$$

Note that (3-8) and (3-9) are identical to (1-3) and (1-4), and the derivation of the Covariance normal equations is complete. From (3-8) and (3-9) we note that values of s_n for n=-p,...,-1, 0,1,...,N-1, must be known. Therefore the signal s_n must be defined for p+N consecutive values, as stated in Section 1.2.

Autocorrelation Normal Equations

From the assumptions in Section 1.2 we can define the signal s_n as follows:

$$s_n = \begin{cases} \text{some sampled signal, } n=0,1,\ldots,N-1, \\ 0, \text{ otherwise.} \end{cases} \qquad (3\text{-}10)$$

The windowed signal s_n is defined for all n: $-\infty<n<+\infty$. Equation (3-7) becomes:

$$\sum_{k=1}^{p} a_k \sum_{n=-\infty}^{\infty} s_{n-k} \, s_{n-i} = \sum_{n=-\infty}^{\infty} s_n \, s_{n-i} \ , \ 1 \le i \le p \ . \qquad (3\text{-}11)$$

Substituting m = n-i in (3-11) we obtain:

$$\sum_{k=1}^{p} a_k \sum_{m=-\infty}^{\infty} s_m \, s_{m+i-k} = \sum_{m=-\infty}^{\infty} s_m \, s_{m+i} \,, \quad 1 \le i \le p. \qquad (3\text{-}12)$$

By definition, the autocorrelation function R_i of the signal s_n is given by

$$R_i = \sum_{n=-\infty}^{\infty} s_n \, s_{n+|i|} \,. \qquad (3\text{-}13)$$

and

$$R_{-i} = R_i \,. \qquad (3\text{-}14)$$

Therefore, (3-12) reduces to:

$$\sum_{k=1}^{p} a_k \, R_{|i-k|} = R_i, \quad i=1,2,\ldots,p. \qquad (3\text{-}15)$$

Now, since s_n is defined in (3-10) to be identically zero for $n<0$ and $n \ge N$, (3-13) reduces to:

$$R_i = \sum_{n=0}^{N-1-|i|} s_n \, s_{n+|i|} \,. \qquad (3\text{-}16)$$

Equations (3-15) and (3-16) are identical to (1-5) and (1-6), and the derivation of the Autocorrelation normal equations is complete.

3.2 Computation of Predictor Parameters

In each of the three formulations of linear prediction presented in Section 1.2 (eqs. 1-2, 3-8, 3-15), the predictor coefficients a_k, $1 \le k \le p$, can be computed by solving a set of p equations with p unknowns. There exist several standard methods for performing the necessary computations, e.g. the Gauss reduction or elimination method and the Crout reduction method (Hildebrand, 1956, pp. 428-434). These methods are general and can be used with the Exact, Covariance and Autocorrelation formulations. However, we note from the Covariance and Autocorrelation normal equations (3-8) and (3-15) that the matrix of coefficients in each case is a covariance matrix. The coefficients ϕ_{ik} in (3-8) form a typical covariance matrix and the coefficients $R_{|i-k|}$ in (3-15) form a special type of covariance matrix known as an autocorrelation matrix. A covariance matrix is symmetric and in general positive semidefinite, but in practice these covariance matrices are usually positive definite. Therefore, (3-8) and (3-15) can be solved more efficiently by the square-root method (Kunz, 1957, pp. 222-225). This method also requires about half the storage of the general methods. A similar method that does not employ the square root operation has been reported by Wilkinson and Reinsch (1971, pp. 9-30). Further reduction in storage and computation time is possible in solving the Autocorrelation normal equations because of their special form. Equation (3-15) can be

expanded in matrix form as:

$$\begin{bmatrix} R_0 & R_1 & R_2 & \cdots & R_{p-1} \\ R_1 & R_0 & R_1 & \cdots & R_{p-2} \\ R_2 & R_1 & R_0 & \cdots & R_{p-3} \\ \vdots & \vdots & \vdots & & \vdots \\ R_{p-1} & R_{p-2} & R_{p-3} & \cdots & R_0 \end{bmatrix} \begin{bmatrix} a_1 \\ a_2 \\ a_3 \\ \vdots \\ a_p \end{bmatrix} = \begin{bmatrix} R_1 \\ R_2 \\ R_3 \\ \vdots \\ R_p \end{bmatrix} \qquad (3\text{-}17)$$

Note that the p x p autocorrelation matrix is symmetric and the elements along any diagonal parallel to the principal diagonal are identical. This type of matrix is also known as a Toeplitz matrix (Grenander and Szegö, 1958). Equation (3-17) can be solved recursively by Robinson's method (Robinson, 1967b, pp. 274-279) which is a reformulation of a method by Levinson (1947). A flow chart for this method is given by Markel (1972). Robinson's method assumes the column matrix on the right hand side of (3-17) to be a general column matrix. By making use of the fact that this column matrix comprises the same elements found in the autocorrelation matrix, another method emerges which is twice as fast as Robinson's. This faster method has been derived by several people and was reported recently by Itakura and Saito (1971). A derivation and a flow chart of the Fast Autocorrelation method can be

found in Appendix B of this report. This derivation employs the theory of orthogonal polynomials in z, as developed by Grenander and Szegö (1958).

Figure 3-1 shows a comparison between the Gauss elimination method, the square-root method, and the Fast Autocorrelation method, in terms of storage and computation. The computation is represented by the total number of multiplications and divisions needed for the solution. (Each square root in the square-root method is represented by 3 computations.) The formulas for the Gauss and square-root methods were taken from Ralston (1965, pp. 401, 410, 452, 462). The formulas for the Fast Autocorrelation method were derived from the flow chart in Appendix B. For p=14, the computation comparisons between the Fast Autocorrelation method, the square-root method and the Gauss elimination method, are in the ratio of 1 : 3.2 : 5.3, while the storage requirements are in the ratio of 1 : 3.8 : 7. These values must of course be taken as approximate. It should be pointed out that the solution of the normal equations for the predictor coefficients a_k is usually only a small fraction of the total amount of computation that is involved in the analysis. For example, in order to compute the autocorrelation coefficients from the signal, it takes on the order of pN computations, where N is the number of samples in the signal. For a 10 kHz sampled signal, N could be anywhere between 100 and 300 depending on the application and the method

	Storage	Computation
Gaussian Elimination	p^2	$\frac{p}{6}(2p^2+6p-2)$
Square-Root Method	$\frac{p}{2}(p+1)$	$\frac{p}{6}(p^2+6p+11)$
Fast Autocorrelation Method	$2p$	$p(p+1)$

Fig. 3-1. Approximate storage and computational requirements for three methods of solving p simultaneous linear equations. The column under computation shows the total number of multiplications and divisions required. A square-root is represented by 3 computations.

of linear prediction used. If N=150 in the Autocorrelation method, then it takes 10 times as much computation to compute the autocorrelation coefficients as to compute the predictor coefficients using the Fast Autocorrelation method.

3.3 Minimum Total-Squared Error

The predictor coefficients a_k are determined such that the total-squared error E in (3-4) is minimized. After computation of the coefficients a_k using one of the methods mentioned in Section 3.2, one should be able to compute the minimum total-squared error E_p by substituting for the computed coefficients a_k in (3-4). (Note that there is no error criterion associated with the Exact method.) Thus:

$$E = \sum_n \left(s_n - \sum_{k=1}^{p} a_k \, s_{n-k} \right)^2$$

$$= \sum_n \left[s_n^2 - 2 \, s_n \sum_{k=1}^{p} a_k \, s_{n-k} + \sum_{k=1}^{p} \sum_{i=1}^{p} a_k a_i s_{n-k} s_{n-i} \right]$$

$$= \sum_n s_n^2 - 2 \sum_{k=1}^{p} a_k \sum_n s_n s_{n-k} + \sum_{k=1}^{p} a_k \sum_{i=1}^{p} a_i \sum_n s_{n-k} s_{n-i} \, .$$

Substituting (3-7), the condition for the minimization of E, and collecting terms, we obtain the minimum total-squared error E_p:

$$E_p = \sum_n s_n^2 - \sum_{k=1}^{p} a_k \sum_n s_n \, s_{n-k} \, . \qquad (3\text{-}18)$$

In particular, for the Covariance method, n ranges from 0 to N-1. Thus, substituting (3-9) in (3-18) we obtain the minimum total-squared error in the Covariance method:

$$E_p = \phi_{00} - \sum_{k=1}^{p} a_k \, \phi_{0k} \, . \text{ (Covariance Method)} \qquad (3\text{-}19)$$

In the Autocorrelation method n ranges from $-\infty$ to $+\infty$. Substituting (3-13) in (3-18) we have:

$$E_p = R_0 - \sum_{k=1}^{p} a_k \, R_k \, . \text{ (Autocorrelation Method)} \qquad (3\text{-}20)$$

We shall have the chance in Chapter V to discuss the behavior of this minimum error in the Autocorrelation method as a function of p and the autocorrelation function. In particular, we shall be interested in the normalized error V_p defined by:

$$V_p = \frac{E_p}{R_0} = \frac{\text{energy in the predictor error samples}}{\text{energy in the speech signal}} \qquad (3\text{-}21)$$

$$V_p = 1 - \sum_{k=1}^{p} a_k \, r_k \, , \qquad (3\text{-}22a)$$

where

$$r_k = \frac{R_k}{R_0} \, , \quad \text{for all } k \, , \qquad (3\text{-}22b)$$

and the samples r_k will be known as the normalized autocorrelation function. (Levinson (1947) uses the notation V, Markel (SCRL Mon., 1971) uses η, and Atal and Hanauer (1971) use ε for the normalized error. We have chosen the letter V because of the possible usefulness of the normalized error in the indication of voicing.) Note that dividing (3-15) by R_0 and using (3-22b) we obtain:

$$\sum_{k=1}^{p} a_k \, r_{|i-k|} = r_i \ , \ 1 \le i \le p \ . \qquad (3\text{-}23)$$

Equation (3-23) says that the predictor coefficients can also be computed using the normalized autocorrelation samples r_k. From (3-22b) and the fact that r_k is an autocorrelation function we have:

$$r_0 = 1$$

and $$|r_k| \le 1, \text{ for all } k. \qquad (3\text{-}24)$$

The signal total energy R_0 can vary widely for different signals, which might cause round-off problems in trying to solve (3-15) in a digital computer with only integer arithmetic capability. For such cases it would be useful to normalize the autocorrelation coefficients first by using (3-22b), and then solve for the a_k's using (3-23).

3.4 Stability of Linear Predictor

Given a frame of speech samples, the coefficients a_k of the linear predictor shown in Fig. 2-1 are determined as described in Section 1.2, 3.1, and 3.2. The all-pole transfer function $\hat{S}(z)$ is then completely specified except for the multiplicative constant A, which will be discussed in Section 3.5. One important question now is the stability of the filter $\hat{S}(z)$. This can be crucial if the recursive filter is to be used for speech synthesis. We know from Fig. 2-1b and (2-6) that $\hat{S}(z)$ is realizable. Therefore, the condition that $\hat{S}(z)$ must satisfy for stability is that all the poles should lie inside the unit circle. The poles of $\hat{S}(z)$ are simply the roots of the denominator polynomial $H(z)$, defined by (2-3), which depend completely on the values of the coefficients a_k. Of the three linear prediction formulations described in Section 1.2, only the Autocorrelation method guarantees the stability of $\hat{S}(z)$, i.e. for any stable signal, the poles of $\hat{S}(z)$ always lie inside the unit circle. [This result is well known from inverse filter theory and from the theory of orthogonal polynomials (see for example, Grenander and Szegö, 1958, pp. 40-41).] The implication for using the predictor coefficients in speech synthesis is clear: The coefficients a_k can be used directly for synthesis without having to check for the stability of the predictive filter since that is guaranteed in the Autocorrelation method.

In the Exact method and Covariance method the stability of $\hat{S}(z)$ cannot, in general, be guaranteed. However, in practical situations, the stability of $\hat{S}(z)$ can be improved in the Covariance method by increasing the number of samples in the frame; this is done by increasing N since p is normally fixed. This cannot be done in the Exact method since the number of samples is fixed at 2p samples. Atal and Hanauer (1971) describe a method for correcting the positions of the poles which lie outside the unit circle.

The above discussion assumes accurate computation of the predictor coefficients a_k. For a 36-bit computer with floating-point arithmetic, this has proved to be no problem. However, for computers with half as many bits or less per computer word, and with integer arithmetic capability only, round-off effects may produce coefficients which result in an unstable $\hat{S}(z)$, even with the Autocorrelation method (Markel and Gray, to be published).

3.5 Autocorrelation Analysis and Computation of Gain Factor A

There are several ways to determine A, the gain factor in $\hat{S}(z)$, depending on the application. The criterion we shall use in computing A is the following: The total energy in the impulse response of $\hat{S}(z)$ must equal the total energy in the signal in the frame of interest. This criterion is good for speech recognition applications, but may have to be modified for vocoder applications. We shall determine the total energy in the impulse

response of $\hat{S}(z)$ from the autocorrelation function $\hat{R}_i$ corresponding to the impulse response.

The impulse response is easily specified from (2-6) by setting $s_n = \hat{s}_n$ and $u_n = \delta_{n0}$, the input impulse:

$$\hat{s}_n = \sum_{k=1}^{p} a_k \hat{s}_{n-k} + A \delta_{n0} , \tag{3-25}$$

where

$$\delta_{nm} = \begin{cases} 1, & n = m , \\ 0, & \text{otherwise} . \end{cases} \tag{3-26}$$

Note from (3-25) that

$$\hat{s}_n = 0, \quad n<0, \tag{3-27}$$

$$\hat{s}_0 = A , \tag{3-28}$$

and

$$\hat{s}_n = \sum_{k=1}^{p} a_k \hat{s}_{n-k} , \quad n\geq 1. \tag{3-29}$$

By definition, the autocorrelation function $\hat{R}_i$ is given by:

$$\hat{R}_i = \sum_{n=-\infty}^{\infty} \hat{s}_n \hat{s}_{n+i} , \text{ for all } i. \tag{3-30}$$

We know that $\hat{R}_{-i} = \hat{R}_i$; therefore it is sufficient to compute $\hat{R}_i$ for $i\geq 0$. From (3-27) and (3-30) we have:

$$\hat{R}_i = \sum_{n=0}^{\infty} \hat{s}_n \hat{s}_{n+i} \quad , \; i \geq 0. \tag{3-31}$$

Now, <u>for i≥1</u>, n+i≥1 in (3-31). Therefore, we can substitute n+i for n in (3-29) and then substitute for the resulting $\hat{s}_{n+i}$ in (3-31):

$$\hat{R}_i = \sum_{n=0}^{\infty} \hat{s}_n \sum_{k=1}^{p} a_k \hat{s}_{n+i-k} \quad , \; i \geq 1$$

$$= \sum_{k=1}^{p} a_k \sum_{n=0}^{\infty} \hat{s}_n \hat{s}_{n+i-k}$$

$$\hat{R}_i = \sum_{k=1}^{p} a_k \hat{R}_{|i-k|} \quad , \; 1 \leq i < \infty \; . \tag{3-32}$$

Equation (3-32) is true for all i≠0. $\hat{R}_0$ is determined from (3-27) through (3-30) as follows:

$$\hat{R}_0 = \sum_{n=0}^{\infty} \hat{s}_n^2$$

$$= \hat{s}_0^2 + \sum_{k=1}^{\infty} \hat{s}_n \sum_{k=1}^{p} a_k \hat{s}_{n-k}$$

$$= A^2 + \sum_{k=1}^{p} a_k \sum_{m=1-k}^{\infty} \hat{s}_m \hat{s}_{m+k} \; .$$

Since $s_m = 0$, $m<0$, we have:

$$\hat{R}_0 = A^2 + \sum_{k=1}^{p} a_k \sum_{m=0}^{\infty} \hat{s}_m \hat{s}_{m+k}$$

$$\hat{R}_0 = A^2 + \sum_{k=1}^{p} a_k \hat{R}_k \quad . \qquad (3\text{-}33)$$

Equations (3-32) and (3-33) completely determine the autocorrelation function of the impulse response of $\hat{S}(z)$.

Now, the total energy in the impulse response of $\hat{S}(z)$ is given by $\hat{R}_0$. If we set $\hat{R}_0$ equal to the total energy of the signal, which we will denote by R_0, then A can be determined from (3-33) if $\hat{R}_k$, $1\leq k\leq p$, are also known. Atal and Hanauer (1971, p. 653) describe a recursive method for computing $\hat{R}_k$, $1\leq k\leq p$, from (3-32) with $\hat{R}_0$ normalized to 1. (We assume here that the coefficients a_k are known.) As we shall see in Section 3.51, there is a much simpler method for computing $\hat{R}_k$ in the Autocorrelation method. The only parameter that has not been specified mathematically yet is R_0, the total energy in the signal. In the Autocorrelation method this is done simply by summing the square of the sample values for all time. The problem in the Exact and Covariance methods is to specify the sample range whose total energy is to be computed. A reasonable specification includes the trailing p samples in the Exact method and the trailing N samples in the Covariance method.

Note that since (3-32) is of the same form as (3-15), the coefficients a_k can be uniquely determined from $\hat{R}_i$, $0 \le i \le p$. Actually, for a given A, there is a one-to-one relationship between the impulse response of $\hat{S}(z)$ (which is completely determined by a_k) and the corresponding autocorrelation function. We mentioned in Section 3.4 that the stability of $\hat{S}(z)$ is guaranteed if the coefficients a_k are computed from (3-15). One might conclude that the stability of $\hat{S}(z)$ is automatically guaranteed if the coefficients are computed from (3-32). This is true under one condition: that the autocorrelation coefficients be derived from a stable system. In other words, let us assume that the coefficients a_k were computed using the Exact or the Covariance method, and that the resulting $\hat{S}(z)$ was unstable. Then, one could compute the autocorrelation function $\hat{R}_i$ as mentioned above. Solving for the coefficients again using (3-32) will give values identical to the original coefficients and $\hat{S}(z)$ remains unstable. The reason that the stability of $\hat{S}(z)$ is guaranteed in the Autocorrelation method is that the autocorrelation coefficients R_i were derived from a stable system, namely the windowed speech signal.

3.51 A Special Case: The Autocorrelation Method

We already noted that (3-32) and (3-15) are of identical form, except that in (3-15) the range of i is limited. Therefore, both autocorrelation functions $\hat{R}_i$ and R_i obey the same matrix equation

(3-17). From the properties of (3-17) we conclude that $\hat{R}_i$ and R_i are related by the following equation:

$$\hat{R}_i = c\, R_i \ , \ 0 \le i \le p \ , \tag{3-34}$$

where c is a constant to be determined.

In order to conserve energy between the impulse response of $\hat{S}(z)$ and the actual signal, we must have $\hat{R}_0 = R_0$, as mentioned above. From (3-34) we conclude that c must equal 1, and we have the important result in the Autocorrelation method that:

$$\hat{R}_i = R_i \ , \ 0 \le i \le p. \tag{3-35}$$

This says that the first p coefficients (other than $\hat{R}_0$) of the autocorrelation function corresponding to the approximate spectrum, as computed from $\hat{S}(z)$, are identical to the first p coefficients of the autocorrelation function of the actual signal. The rest of the coefficients $\hat{R}_i$ are determined by (3-32). The problem of linear prediction using the Autocorrelation method can be stated in a new way as follows: Find a transfer function such that the first p values of its autocorrelation function are equal to the first p values of the signal autocorrelation function, and such that (3-32) applies.

Substituting (3-35) in (3-33) we have:

$$A^2 = R_0 - \sum_{k=1}^{p} a_k R_k \ . \tag{3-36}$$

The right-hand sides of (3-36) and (3-20) are identical. Therefore,

$$\begin{aligned} A^2 &= E_p \\ &= R_0 V_p = R_0 \left[1 - \sum_{k=1}^{p} a_k r_k\right] , \end{aligned} \tag{3-37}$$

and A^2 is equal to the minimum total-squared error. From (3-37) and (2-2) we have:

$$\hat{S}(z) = \frac{\sqrt{R_0 V_p}}{1 - \sum_{k=1}^{p} a_k z^{-k}} \ , \tag{3-38}$$

where R_0 is the total energy in the signal and V_p is the normalized error defined by (3-22).

The above findings will be very useful in discussing other properties of the Autocorrelation method in Chapter V, where we shall analyze the properties of the normalized error V_p and the behavior of different parameters as the number of predictor coefficients $p \to \infty$.

CHAPTER IV

SPECTRAL ESTIMATION AND ANALYSIS-BY-SYNTHESIS

In Chapter III the Covariance and Autocorrelation methods of linear prediction were derived from a time-domain formulation. In this chapter we shall show that the same normal equations can be derived from a frequency-domain formulation. It will become clear that linear prediction can be considered equally validly as either a time-domain or a frequency-domain type of analysis.

First, the Autocorrelation method is reinterpreted in terms of an inverse filter formulation. This leads directly to linear prediction analysis in the frequency domain. The Autocorrelation method is rederived from the spectral domain by approximating the signal short-time spectrum $P(\omega)$ by an all-pole power spectrum $\hat{P}(\omega)$. An error criterion between the two spectra is defined and minimized. The results are interpreted in terms of traditional methods of spectral analysis-by-synthesis. The Autocorrelation method is then reformulated in terms of a direct and an indirect method by relating to the corresponding methods of estimation of power spectra. An analogous reformulation of the Covariance method is derived from a generalized method of analysis-by-synthesis where the signal is assumed to be nonstationary and the two-dimensional short-time power spectrum $Q(\omega,\omega')$ is to be approximated by an all-pole two-dimensional spectrum $\hat{Q}(\omega,\omega')$.

A very brief introduction to nonstationary spectral analysis is included.

4.1 Inverse Filter Formulation

The linear prediction error e_n was defined by (3-2), and is repeated here for convenience:

$$e_n = s_n - \sum_{k=1}^{p} a_k s_{n-k} . \qquad (3-2)$$

Since the signal s_n is defined for all time, then e_n is also defined for all time. Therefore, we can take the z-transform of (3-2) by multiplying both sides of the equation by z^{-n} and summing over all n (see Appendix A for definition of z-transform). The result is:

$$E(z) = S(z) \left[1 - \sum_{k=1}^{p} a_k z^{-k}\right]$$

$$= S(z) H(z), \qquad (4-1)$$

where E(z) and S(z) are the z-transforms of e_n and s_n, respectively, and $H(z) = 1 - \sum_{k=1}^{p} a_k z^{-k}$ was already defined in (2-3) as the inverse filter.

From (4-1), the error signal e_n can be interpreted as the output of a filter H(z) whose input is s_n, as shown in Fig. 4-1.

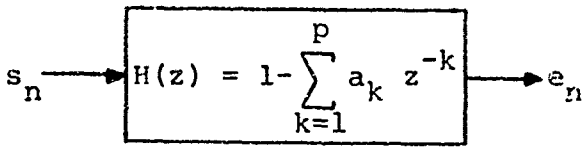

Fig. 4-1. The error sequence e_n as the output of an inverse filter H(z).

Therefore, another way to view the error minimization problem in Section 3.1 is to solve for the parameters a_k of the inverse filter H(z) which will minimize the energy $\sum_n e_n^2$ in the output error signal, for a given value of p. This is what Markel calls the inverse filter formulation (Markel, 1972).

Equation (4-1) can be solved for S(z) to obtain:

$$S(z) = \frac{E(z)}{H(z)} = \frac{E(z)}{1 - \sum_{k=1}^{p} a_k z^{-k}} \quad . \tag{4-2}$$

(4-2) is an exact equation. According to the speech production model described in Section 2.1, if the signal s_n is the vocal tract response due to a single pitch pulse, then the transfer function S(z) can be approximated by an all-pole filter $\hat{S}(z)$ given by (2-2) and shown below:

$$\hat{S}(z) = \frac{A}{H(z)} = \frac{A}{1 - \sum_{k=1}^{p} a_k z^{-k}} \quad . \tag{2-2}$$

Comparing (2-2) and (4-2) we conclude that E(z) is approximated by another function

$$\hat{E}(z) = A \ ,$$

which corresponds to a time-domain approximation $\hat{e}_n$ given by:

$$\hat{e}_n = A \, \delta_{n0} \ , \tag{4-3}$$

where δ_{nm} is the Kronecker delta defined by (3-26). $\hat{e}_n$ is just an impulse of magnitude A. Now, in order to conserve energy between $\hat{e}_n$ and e_n we must have

$$\sum_{n=-\infty}^{\infty} \hat{e}_n^{\,2} = \sum_{n=-\infty}^{\infty} e_n^{\,2} \ . \tag{4-4}$$

After the minimization of the total-squared error, the right-hand side of (4-4) is equal to the minimum total-squared error E_p given by (3-20). The left-hand side of (4-4) is determined easily from (4-3), and we have:

$$A^2 = E_p = R_0 - \sum_{k=1}^{p} a_k \, R_k \ .$$

The result is identical to (3-37) which was derived by energy conservation between the signal s_n and the impulse response of $\hat{S}(z)$.

The above analysis assumed that the vocal tract was excited

by a single pulse. The same results would be obtained if one assumed a white noise source excitation.

4.2 Error Minimization in the Spectral Domain

In this section we shall show that the Autocorrelation normal equations (3-15) can also be derived completely in the frequency domain. Before we proceed, we shall define the power spectrum of a transfer function Y(z) as the magnitude squared of Y(z) evaluated on the unit circle, i.e. $z = e^{j\omega T}$. Y(z) evaluated at $z = {}^{j\omega T}$ will be denoted by $Y(\omega)$, so that the power spectrum is given by:

$$\text{Power Spectrum} = Y(\omega)\ \bar{Y}(\omega) = |Y(\omega)|^2 , \tag{4-5}$$

where the over-bar denotes complex conjugate.

Let the power spectrum of $\hat{S}(z)$ be denoted by $\hat{P}(\omega)$, and of S(z) by $P(\omega)$, then:

$$\hat{P}(\omega) = |\hat{S}(\omega)|^2 = \frac{A^2}{\left|1-\sum_{k=1}^{p} a_k e^{-jk\omega T}\right|^2} , \tag{4-6a}$$

and

$$P(\omega) = |S(\omega)|^2 . \tag{4-6b}$$

We shall call $\hat{P}(\omega)$ the linear prediction or approximate spectrum and $P(\omega)$ the actual or signal spectrum. Methods for computing

$P(\omega)$ and $\hat{P}(\omega)$ are given in Appendix C.

Making use of Parseval's theorem (see Appendix A), the total-squared error E can be represented by:

$$E = \sum_{n=-\infty}^{\infty} e_n^2 = \frac{T}{2\pi} \int_{-\pi/T}^{\pi/T} |E(\omega)|^2 \, d\omega$$

$$= \frac{T}{2\pi} \int_{-\pi/T}^{\pi/T} P_e(\omega) \, d\omega \quad , \tag{4-7}$$

where $P_e(\omega)$ is the error power spectrum.

From linear system theory, we have from Fig. 4-1:

$$P_e(\omega) = P(\omega) \, |H(\omega)|^2 \quad , \tag{4-8}$$

where $H(\omega)$ is equal to $H(z)$ evaluated for $z = e^{j\omega T}$.

Substituting (4-8) in (4-7) we have:

$$E = \frac{T}{2\pi} \int_{-\pi/T}^{\pi/T} P(\omega) \, H(\omega) \, \bar{H}(\omega) \, d\omega, \tag{4-9}$$

$$= \frac{T}{2\pi} \int_{-\pi/T}^{\pi/T} P(\omega) \left[1 - \sum_{k=1}^{p} a_k \, e^{-jk\omega T}\right]\left[1 - \sum_{k=1}^{p} a_k \, e^{jk\omega T}\right] d\omega.$$

Following the same procedure in Section 3.1, E is minimized by setting $\frac{\partial E}{\partial a_i} = 0$, $1 \le i \le p$:

$$-\frac{\partial E}{\partial a_i} = \frac{T}{2\pi}\int_{-\pi/T}^{\pi/T} P(\omega)\left[-e^{-ji\omega T}\left(1-\sum_{k=1}^{p} a_k e^{jk\omega T}\right) - e^{ji\omega T}\left(1-\sum_{k=1}^{p} a_k e^{-jk\omega T}\right)\right] d\omega = 0$$

or $$\frac{T}{2\pi}\int_{-\pi/T}^{\pi/T} P(\omega)\left[\cos(i\omega T) - \sum_{k=1}^{p} a_k \cos\{(i-k)\omega T\}\right] d\omega = 0.$$

Interchanging integration and summation we have:

$$\sum_{k=1}^{p} a_k \left[\frac{T}{2\pi}\int_{-\pi/T}^{\pi/T} P(\omega)\cos\{(i-k)\omega T\} d\omega\right] = \frac{T}{2\pi}\int_{-\pi/T}^{\pi/T} P(\omega)\cos(i\omega T)\, d\omega, \quad 1\le i\le p. \tag{4-10}$$

We know that the autocorrelation function R(kT) is defined as the inverse Fourier transform of the power spectrum, i.e.

$$R_k = \frac{T}{2\pi}\int_{-\pi/T}^{\pi/T} P(\omega)\, e^{jk\omega T}\, d\omega, \tag{4-11a}$$

or $$R_k = \frac{T}{2\pi}\int_{-\pi/T}^{\pi/T} P(\omega)\cos(k\omega T)\, d\omega. \tag{4-11b}$$

(4-11b) follows from (4-11a) because the power spectrum is a real and even function of frequency. Substituting (4-11b) in (4-10) and noting that $R_{-k} = R_k$, we have:

$$\sum_{k=1}^{p} a_k R_{|i-k|} = R_i, \quad 1\le i\le p, \tag{4-12}$$

which are the same Autocorrelation normal equations as (3-15).

The minimum total-squared error E_p can be obtained by using (4-10) and (4-11) in (4-9). The answer can be shown to be equal to

$$E_p = A^2 = R_0 - \sum_{k=1}^{p} a_k R_k \ , \qquad (4\text{-}13)$$

which is identical to that given in (3-20) and (3-37).

The above derivation shows that, in the Autocorrelation method, the predictor parameters a_k can be determined if only the signal power spectrum is known. In fact all that is needed are the first p coefficients of the autocorrelation function, which can be computed either from the time signal (Section 3.1) or from the power spectrum as was shown above. The latter statement will be the basis for other formulations of the Autocorrelation method which are based on the idea of estimating the first p values of the autocorrelation function (see Section 4.4).

4.3 The Spectral Envelope and Analysis-by-Synthesis

We shall now interpret the minimization of error in the Autocorrelation method in terms of the estimation of the spectral envelope and in terms of analysis-by-synthesis.

From (2-2), H(z) can be written as:

$$H(z) = \frac{A}{\hat{S}(z)} ,$$

and

$$H(\omega) = \frac{A}{\hat{S}(\omega)} . \qquad (4\text{-}14)$$

Substituting (4-14) in (4-9) we obtain:

$$E = \frac{A^2 T}{2\pi} \int_{-\pi/T}^{\pi/T} \frac{P(\omega)}{|\hat{S}(\omega)|^2} \, d\omega . \qquad (4\text{-}15)$$

$|\hat{S}(\omega)|^2$ is the approximate power spectrum $\hat{P}(\omega)$ as defined in (4-6a), and (4-15) reduces to:

$$E = \frac{A^2 T}{2\pi} \int_{-\pi/T}^{\pi/T} \frac{P(\omega)}{\hat{P}(\omega)} \, d\omega. \qquad (4\text{-}16)$$

Therefore, minimizing the total-squared error E is equivalent to the minimization of the integrated ratio of the signal power spectrum $P(\omega)$ to its approximation $\hat{P}(\omega)$. Another way to look at this is that if one is interested in approximating a power spectrum $P(\omega)$ by an all-pole spectrum $\hat{P}(\omega)$ then (4-16) is an error measure that can be used in optimizing the approximation. We already know that this error can be minimized analytically resulting in the Autocorrelation normal equations (4-12) which can be solved for a_k, the parameters of the sought-for approximate spectrum $\hat{P}(\omega)$.

The question, then, is what are the properties of the error measure in (4-16), and are these properties commensurate with our stated goals? This is discussed below.

The model of speech production described in Chapter II approximates the transfer function of the glottal flow, the vocal tract and radiation by a single all-pole filter $\hat{S}(z)$ which is excited by a combination of sequences of impulses and white noise. Due to the nature of the excitation we conclude that $\hat{P}(\omega)$ attempts to approximate the envelope of the signal power spectrum $P(\omega)$. One important consideration in estimating the spectral envelope is the determination of an optimum value for p, the number of poles in the all-pole approximate spectrum $\hat{P}(\omega)$. This subject is discussed in Section 5.6. However, assuming that somehow we know this optimal value of p, there remains the question of whether the error measure in (4-16) will result in a good estimate of the spectral envelope. We note from (4-16) that spectral values of $P(\omega)$ that are greater than the corresponding values in $\hat{P}(\omega)$ will contribute to the total error in a significant manner, while spectral values of $P(\omega)$ that are much smaller than the corresponding values in $\hat{P}(\omega)$ will not affect the total error significantly. This means that, after the minimization of error, we expect a better fit of $\hat{P}(\omega)$ to $P(\omega)$ where $P(\omega)$ is greater than $\hat{P}(\omega)$ than where $P(\omega)$ is smaller. For example, if $P(\omega)$ is

the power spectrum of a quasi-periodic signal (such as a sonorant), then most of the energy in $P(\omega)$ will exist at the harmonics and very little energy will reside between harmonics. The error measure in (4-16) insures that the approximation of $\hat{P}(\omega)$ to $P(\omega)$ is far superior at the harmonics where the energy is greater, than between the harmonics where there is very little energy. Since $\hat{P}(\omega)$ is expected to be a smooth spectrum (this is insured by choosing an appropriate value for p), we conclude that minimization of the error measure in (4-16) results in an approximate spectrum $\hat{P}(\omega)$ that is a good estimate of the spectral envelope of the signal power spectrum $P(\omega)$. It should be clear from the above that the importance of the goodness of the error measure is much more crucial for voiced sounds than for unvoiced sounds where the variations of the signal spectrum from the spectral envelope are much less pronounced.

Another important property of this estimation procedure is that, because the contributions to the total error are determined by the ratio of the two spectra, the matching process should perform uniformly over the frequency range of interest, irrespective of the shaping of the speech spectral envelope. This property is reminiscent of the analysis-by-synthesis method of spectral reduction developed at M.I.T. (Bell, et.al., 1961), and was used by Paul et al. (1964) for the automatic reduction of vowel spectra, and by Fujimura (1962) for the analysis of nasal consonants.

A recent improvement in convergence strategy was introduced by Olive (1971) using a Newton-Raphson technique. Also, a pitch-synchronous analysis-by-synthesis was developed by Mathews et al. in 1961. The general idea behind the reduction of spectra using analysis-by-synthesis is that one has a spectral model consisting of poles and zeros, and the problem is to vary the positions of these poles and zeros such that some error criterion between the model spectrum and the signal spectrum is minimized. The error measure that was normally used is given (in our notation) by:

$$E' = \int_{\omega} W(\omega) \left[\log \frac{P(\omega)}{\hat{P}(\omega)}\right]^2 d\omega, \qquad (4\text{-}17)$$

where $W(\omega)$ is a weighting function, $\hat{P}(\omega)$ is the model spectrum, and the integration is over the frequency range of interest. In many cases the weighting function $W(\omega)$ was set equal to 1, and the integration was always approximated by a summation over discrete frequencies. The positions of poles and zeros of $\hat{P}(\omega)$ were varied such that the error E' was minimized.

It is [illegible] that the Autocorrelation method of linear prediction can be viewed as a method of analysis-by-synthesis where the model spectrum $\hat{P}(\omega)$ consists of poles only and the error measure is given by (4-16). The error measures in (4-16) and (4-17) are similar in that the contributions to the total error are

proportional to the ratio of the two spectra. We have already mentioned that this fact makes the matching process perform uniformly over the frequency range of interest (assuming $W(\omega)$ in (4-17) to be constant). However, the error measure E in linear prediction has two advantages over E': (1) The minimization of E in (4-16) can be done analytically and the resulting $\hat{P}(\omega)$ is computed simply by solving a set of simultaneous linear equations, while the minimization of E' has to be done iteratively and also approximately in that a summation is used instead of an integration. (2) E is a superior error measure to E' if a spectral envelope is desired. This is clear if you note from (4-17) that contributions to the total error E' are made equally whether $P(\omega)>\hat{P}(\omega)$ or $P(\omega)<\hat{P}(\omega)$, which means that energy at the harmonics (in voiced sounds) and the lack of energy between harmonics contribute equally to the total error. This, of course, will not lead to a good spectral envelope. But then, traditional analysis-by-synthesis methods have generally used already smoothed spectra, in which case it is probably of little consequence which error measure is used. The elegance of the linear prediction method is that it performs the smoothing (for a well-chosen p) as well as the analysis-by-synthesis type of computation all at once by simply solving a set of simultaneous linear equations. The price that one has to pay is that the approximate spectrum $\hat{P}(\omega)$ can have only poles.

By virtue of the above properties of linear prediction, it follows that any smoothing of the signal spectrum before the application of linear prediction is not only a waste of time, but may also introduce errors in the estimation of the predictor parameters. For example, preprocessing the speech signal by homomorphic analysis (Weinstein and Oppenheim, 1971) is unnecessary if one is interested in using linear prediction; better results would be obtained by using linear prediction on the original signal.

Figure 4-2 shows an example of the Autocorrelation method of analysis performed on a 25 msec portion of the vowel [æ] in the word "potassium". A Hamming window was used on the signal and the predictor had 14 poles. $\hat{P}(\omega)$ seems to be a good estimate of the spectral envelope of the signal power spectrum $P(\omega)$. (See Appendix C for methods of computing $P(\omega)$ and $\hat{P}(\omega)$.)

4.4 Reformulation of the Autocorrelation Method

We have shown above that the Autocorrelation method of linear prediction can be viewed as a process of spectral matching or approximation, where the envelope of the signal power spectrum $P(\omega)$ is approximated by an all-pole power spectrum $\hat{P}(\omega)$ given by (4-6a), and the error measure to be minimized is given by (4-16). So far in this report we have assumed $P(\omega)$ to be a short-time spectrum obtained by taking the power spectrum of a

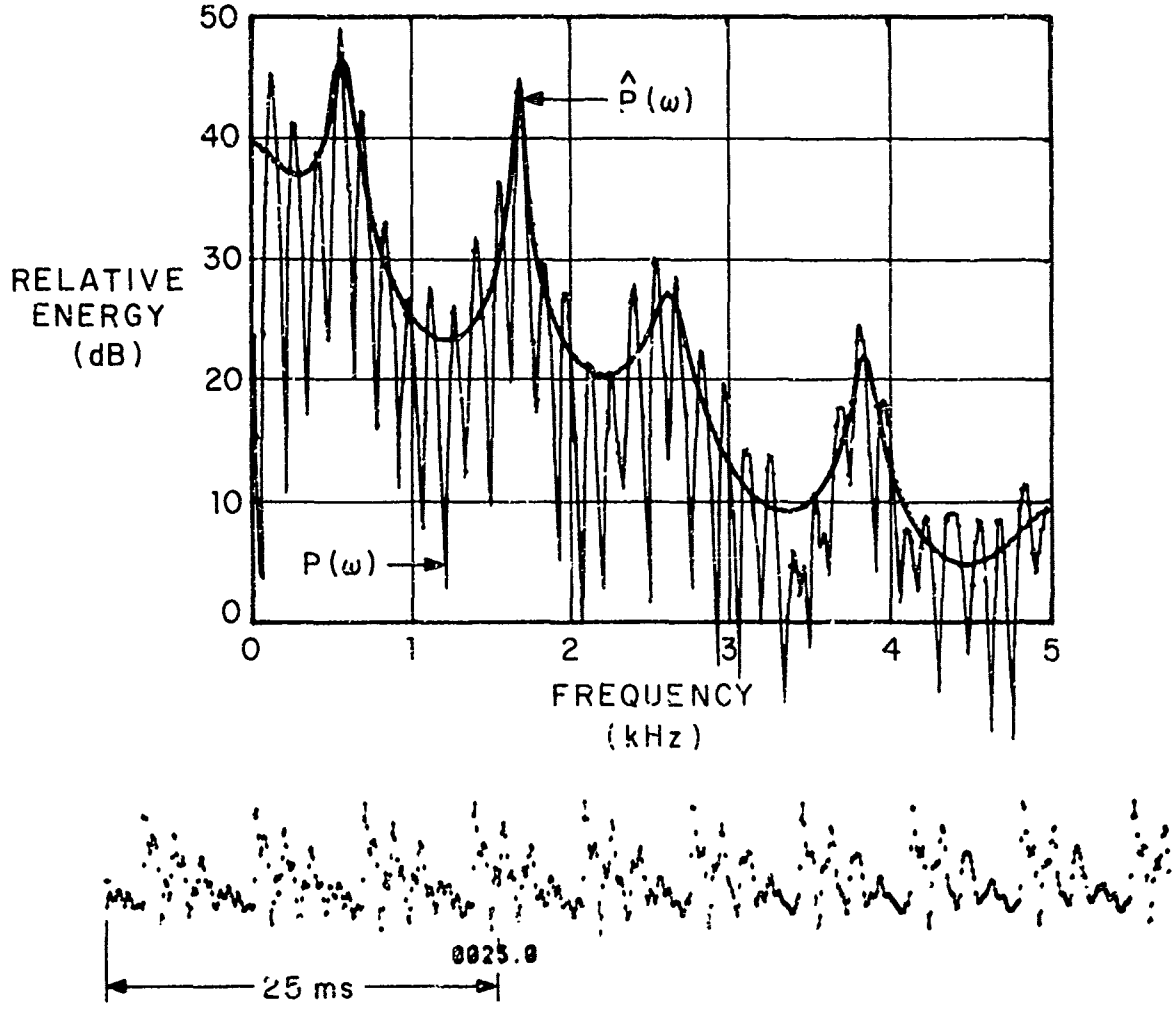

Fig. 4-2. Original spectrum P(ω) and linear prediction spectrum $\hat{P}(\omega)$ with p=14 for the sound [æ] in the word "potassium."

windowed signal. However, there is nothing in this chapter that restricts $P(\omega)$ to be defined in that particular manner. In general, there are two basic methods for the estimation of the power spectrum from a knowledge of a finite portion of a stationary signal (see Blackman and Tukey, 1958):

1. Direct Method - The power spectrum is estimated by:

$$P(\omega) = \left| \sum_{n=0}^{N-1} w(nT)\ s(nT)\ e^{-jn\omega T} \right|^2 , \qquad (4\text{-}18)$$

where $s(nT)$ is the original signal whose power spectrum is desired, and $w(nT)$ is a window function that is defined to be zero for $n<0$ and $n\geq N$. (A discussion of window functions is given in Section 6.2.) The spectrum defined by (4-18) is also known as the short-time spectrum, and it is the method we have used thus far to estimate the power spectrum of a short portion of the signal.

2. Indirect Method - The estimated power spectrum is computed as the Fourier series of a windowed apparent autocorrelation function:

$$P(\omega) = \sum_{k=-M}^{M} D(kT)\ \tilde{R}(kT)\ e^{-jk\omega T} , \qquad (4\text{-}19)$$

where $D(kT)$ is an even window defined to be zero for $|k|>M$, and $\tilde{R}(kT)$ is the apparent autocorrelation function, which is computed from the signal. The word "apparent" is used to indicate

that $\tilde{R}(kT)$ is not a true autocorrelation function since it is defined over a finite portion of the signal. We shall give two methods for the computation of $\tilde{R}(kT)$, yielding functions which will be labelled $\tilde{R}_k^{(1)}$ and $\tilde{R}_k^{(2)}$:

$$\text{(a)} \quad \tilde{R}_k^{(1)} = \frac{N}{N-|k|} \sum_{n=0}^{N-1-|k|} s_n \, s_{n+|k|} \quad , \quad |k| \leq M. \tag{4-20}$$

$$\text{(b)} \quad \tilde{R}_k^{(2)} = \sum_{n=0}^{N-1} s_n \, s_{n+|k|} \quad , \quad |k| \leq M. \tag{4-21}$$

In (4-20) the signal s(nT) is assumed to be known for N consecutive samples while in (4-21) s(nT) is assumed to be known for N+M samples. The signal is undefined outside these ranges. Note that we must have M<N, and for a stable spectral estimate of a noisy signal, M is usually taken to be a small fraction of N. See Blackman and Tukey (1958) for a thorough analysis of this subject.

Sometimes a single estimate of the power spectrum as described above may not be stable enough, i.e. the variability of the estimate with respect to the "true" spectrum is large. The stability can be improved (with a corresponding decrease in frequency resolution) by averaging over several estimates of the power spectrum taken over several (possibly overlapping) portions of the signal. The averaging can be alternately performed on

the autocorrelation function. One must be careful, however, that the basic assumption of stationarity still holds for the total signal span whose power spectrum is being estimated.

In speech research, the direct method of spectral analysis has been used almost exclusively. The method is computationally efficient and has proved to be quite adequate for many speech applications. Using the indirect method for computing the power spectrum is relatively inefficient, and may not be cost-effective for many applications.

Having computed the estimated signal power spectrum $P(\omega)$ by one of the methods described above, we can compute the parameters of the approximate power spectrum $\hat{P}(\omega)$ from the Autocorrelation normal equations (4-12), where the autocorrelation coefficients R_k are computed from $P(\omega)$ by using (4-11). But if the coefficients R_k can be computed directly from the time signal there is no need to estimate $P(\omega)$ in the first place. Indeed, using the direct method, we have already shown how to compute R_k from the windowed signal (see (3-16)). In the indirect method, from (4-19), the coefficients R_k are equal to:

$$R_k = D_k \tilde{R}_k \text{ , (Indirect Method)} \qquad (4\text{-}22)$$

where $\tilde{R}_k$ is either equal to $\tilde{R}_k^{(1)}$ in (4-20) or to $\tilde{R}_k^{(2)}$ in (4-21). The introduction of an autocorrelation window D_k may produce some distortion in estimating R_k. One method of avoiding the

use of such a window is to let R_k be the average of several values of $\tilde{R}_k$ computed from overlapping portions of the signal. If we replace s(nT) by s(nT+iT) in (4-20) and (4-21), we can say that $\tilde{R}_k^{(1)}$ and $\tilde{R}_k^{(2)}$ are functions of time t = iT, and they can be denoted by $\tilde{R}_k^{(1)}(iT)$ and $\tilde{R}_k^{(2)}(iT)$. Similarly $\tilde{R}_k$ at time t = iT will be denoted by $\tilde{R}_k(iT)$. The index i can be varied and the resulting values of the apparent autocorrelation can be averaged, yielding an estimated R_k. This can be written as:

$$R_k = \frac{1}{M} \sum_{i=0}^{M-1} \tilde{R}_k(iT). \qquad (4\text{-}23)$$

Alternatively, the number of values averaged could be made to depend on the index k of R_k. Thus,

$$R_k = \frac{1}{M-|k|} \sum_{i=0}^{M-1-|k|} \tilde{R}_k(iT) \quad , \; M>k, \; 0 \le k \le p. \qquad (4\text{-}24)$$

In (4-24) more values are used in computing R_k for low values of k than for large values of k. This is not unreasonable since the low-order autocorrelation coefficients are more important in determining the general shape of the spectrum, and therefore their values should be more "accurate" or stable.

The definitions for $\tilde{R}_k$ given by (4-20) and (4-21) are only two of several possible definitions. For example, two other

similar definitions are obtained by inversion of the time axis. This is done by substituting the index $(n-|k|)$ for $(n+|k|)$ in (4-20) and (4-21). Also, $\tilde{R}_k(iT)$ would be obtained by replacing $s(nT)$ by $s(nT-iT)$ in (4-20) and (4-21). In that case, $\tilde{R}_k$ in (4-21) becomes equal to

$$\tilde{R}_k = \phi_{0k} \ , \ 0 \le k \le p \ ,$$

where ϕ_{ik} are the covariance coefficients defined in (3-9). In fact, if we substitute $\tilde{R}_k$ for R_k in the equation for the minimum total-squared error in (3-20), then (3-19) and (3-20) become identical. Also, (4-24) for $N = p+1$ reduces to:

$$R_k = \frac{1}{p+1-|k|} \sum_{i=0}^{p-|k|} \sum_{n=0}^{N-1} s_{n-i} \, s_{n-i-|k|}$$

$$= \frac{1}{p+1-|k|} \sum_{i=0}^{p-|k|} \phi_{i,i+k} \ , \ 0 \le k \le p \ , \qquad (4\text{-}25)$$

which is the average of the covariance coefficients along each of the diagonals in the covariance matrix ϕ_{ik} (including the vector ϕ_{0k}). One way to look at the operation in (4-25) is that it is averaging out the nonstationarity inherent in the covariance matrix ϕ_{ik} (see Section 4.6), resulting in a stationary autocorrelation matrix. As we shall see below, the Covariance method and the indirect formulation of the Autocorrelation method share the property that the stability of the linear predictor cannot be

guaranteed.

Henceforth, we shall talk about the direct or indirect Autocorrelation method as referring to whether the coefficients R_k are computed from a windowed signal or from an apparent autocorrelation function $\tilde{R}_k$, respectively. Note that although the indirect method may be inefficient for computation of the power spectrum, the same is not true for the computation of (p+1) values of $\tilde{R}_k$.

4.41 Stability of Linear Predictor

In Section 3.4 we stated that of the different formulations of linear prediction, only the Autocorrelation method guarantees the stability of the linear predictor, i.e. all the poles of $\hat{S}(z)$ are inside the unit circle. This statement must be amended now to read: only the direct Autocorrelation method guarantees the stability of the linear predictor. The reason for this restriction is that the coefficients R_k are guaranteed to be those of an autocorrelation function only in the direct method. In the indirect method, the coefficients R_k are only estimates of some autocorrelation function, as can be seen from (4-20) to (4-24). These estimates may or may not form part of an autocorrelation function. In order for the coefficients R_k to be those of an autocorrelation function they must form a set that is positive-definite (Papoulis, 1965, p. 349). More formally, given an

arbitrary set of constants u_k, $0 \le k \le p$, the coefficients R_k, $0 \le |k| \le p$, form a positive-definite set if and only if the following condition holds (Papoulis, 1965, p. 349; Grenander and Szegö, 1958, pp. 17-19):

$$T_i = \sum_{n=0}^{i} \sum_{m=0}^{i} R_{n-m} u_n \bar{u}_m \ge 0 \ , \ 0 \le i \le p \ , \qquad (4\text{-}26)$$

where T_i, $0 \le i \le p$, are known as Toeplitz forms, and the over-bar denotes complex conjugate.

In particular, (4-26) should be true for $i = p$, and for the constants u_k equal to the impulse response of the inverse filter $H(z) = 1 - \sum_{k=1}^{p} a_k z^{-k}$. Let

$$u_k = \begin{cases} 1 \ , & k=0, \\ -a_k, & 1 \le k \le p \ . \end{cases} \qquad (4\text{-}27)$$

Substituting (4-27) in (4-26):

$$T_p = R_0 - \sum_{m=1}^{p} R_m a_m - \sum_{n=1}^{p} a_n \left[R_n - \sum_{m=1}^{p} R_{n-m} a_m \right].$$

But the terms in square brackets are zero, due to the Autocorrelation normal equations (4-12).

Hence,

$$T_p = R_0 - \sum_{k=1}^{p} a_k R_k = E_p \ge 0, \qquad (4\text{-}28)$$

and the Toeplitz form T_p is equal to the minimum total-squared error E_p which must be greater or equal to zero. Although (4-28) is a special case of (4-26), it can be shown that (4-28) is a necessary and sufficient condition for the set of coefficients R_k to be positive-definite, and hence result in a stable $\hat{S}(z)$ (see Appendix B). Therefore, in order to test for the stability of the linear predictor, given a set of coefficients R_k: Compute the predictor parameters a_k from (3-17) and check for the condition (4-28).

Another method to check for the positive-definiteness of the coefficients R_k is to make sure that the corresponding power spectrum is nonnegative for all frequencies (Papoulis, 1965, p. 349). But in order to do that, R_k must be defined for all k. Such a definition can be arbitrary for $|k|>p$. A convenient way of extending R_k is to make it periodic with period 2p, i.e.

$$R_{k+2p} = R_k \quad . \tag{4-29}$$

We can now apply the discrete Fourier transform (Gold and Rader, 1969, p. 162) to R_k and obtain the discrete power spectrum $P(n\omega_o)$:

$$P(n\omega_o) = \sum_{k=0}^{2p-1} R_k \, e^{-jkn\omega_o T} \quad , \tag{4-30}$$

where $$\omega_o = \frac{2\pi}{2pT} \quad .$$

Since R_k is discrete, real, even and periodic in 2p, $P(n\omega_o)$ is also discrete, real, even and periodic in 2p. Therefore, it is only necessary to compute p+1 values of $P(n\omega_o)$, e.g. $0 \leq n \leq p$. If these values of $P(n\omega_o)$ are all greater or equal to zero, we conclude that the set of coefficients R_k is positive-definite and that $\hat{S}(z)$ will be stable.

Suppose now that we have used one of the above methods (or any other method) to check for the stability of $\hat{S}(z)$ and found it to be unstable. The problem is what to do about the coefficients R_k to improve the stability of $\hat{S}(z)$. One method is to use a window D_k as shown in (4-22). The narrower the effective window width, the more stable $\hat{S}(z)$ is likely to be. A superior and highly recommended method is to take the average of $\tilde{R}_k$ for several overlapping portions of the signal, as shown in (4-23) and (4-24). Increasing the value of M in those equations increases the stability of $\hat{S}(z)$. A value of $M \geq p$ is usually sufficient.

Note that the methods that have been suggested for improving the stability of the linear predictor have the side effect of decreasing the frequency resolution in the corresponding power spectrum. Indeed, in the direct Autocorrelation method, the stability of the linear predictor is guaranteed by multiplying the speech signal s(nT) by a finite window: a process that results in loss of resolution in the signal power spectrum. However, for most applications this loss of resolution is not critical.

4.5 Nonstationary Spectral Analysis

So far in this chapter we have discussed the spectral analysis of speech by means of the Autocorrelation method of linear prediction. The main assumption underlying the whole discussion was that the predictor coefficients a_k, $1 \le k \le p$, are computed from a portion of the signal that can be considered as stationary. In the direct method, this stationarity was enforced by windowing the speech signal and considering the resulting infinite signal which has a well-defined, time-independent power spectrum and autocorrelation. In the indirect method, stationarity was enforced by assuming first that (3-17) holds, and then proceeding to estimate the autocorrelation coefficients. The averaging operations in (4-23) and (4-24) are only valid under the assumption of stationarity.

As we shall see in this section, the Covariance method assumes that the portion of the signal from which the predictor parameters are computed is nonstationary. It should be made clear that we are not discussing the stationarity of the running speech signal as such, but rather the stationarity of a single frame from which we wish to compute the predictor parameters. Both the Covariance and the Autocorrelation methods assume that the running speech signal is nonstationary. This is evident by the fact that the predictor parameters change from one frame to the next,

as was assumed in the model for speech production in Chapter II. However, within a single frame, the Autocorrelation method assumes that the signal is stationary while the Covariance method assumes that the signal is nonstationary.

Just as in Section 4.2 we derived the Autocorrelation normal equations in the frequency domain, we shall do the same to derive the Covariance normal equations. The only difference is that here we shall assume the signal to be nonstationary, in which case the power spectrum is a function of time. However, before we do the derivation we shall give some background information on spectral analysis of nonstationary signals. For references on the subject see, for example, Papoulis (1965, Ch. 12) and Bendat and Pierson (1966, Ch. 9).

The autocorrelation R(t,t') of a nonstationary process is a function of two time variables t and t'. A stationary process is then a special case where the autocorrelation becomes a function of only the time lag t'-t, i.e. R(t'-t). If we let

$$\tau = t'-t \tag{4-31}$$

be the time lag, then R(t'-t) = R(τ) for a stationary process, and R(t,t') = R(t,t+τ) for a nonstationary process. Here we shall assume that t, t' and τ take on discrete values only. For example, if we let τ = kT, then R(kT) would be an autocorrelation function

which we have seen repeatedly in this chapter.

The power spectrum of a nonstationary discrete process is defined as the Fourier series transform of the autocorrelation $R(t,t+\tau)$:

$$P(\omega,t) = \sum_{\tau=-\infty}^{\infty} R(t,t+\tau)\ e^{-j\omega\tau}. \qquad (4\text{-}32)$$

Note that the spectrum $P(\omega,t)$ is a function of time t. For a stationary process the autocorrelation is a function of τ only, and from (4-32) we see that the power spectrum becomes $P(\omega)$, which is time-independent. In speech analysis, $P(\omega,t)$ can be viewed as the running short-time spectrum (e.g. such as a spectrograph might produce). However, what is important in the Covariance method is that we wish to consider the spectrum $P(\omega,t)$ to be changing in time within a single frame of the signal, and that we wish to represent this change in some manner. This can be done by taking the Fourier transform of $P(\omega,t)$ with respect to time t. The result is a frequency correlation function which is the generalized (nonstationary) spectrum. It is defined by:

$$\Gamma(\omega,\Omega) = \sum_{t=-\infty}^{\infty} P(\omega,t)e^{-j\Omega t}. \qquad (4\text{-}33)$$

$\Gamma(\omega,\Omega)$ is also known as a double frequency spectrum. Since it

is defined as a two-dimensional transform, we shall call $\Gamma(\omega,\Omega)$ the 2D-spectrum. (The summation in (4-33) is for all time. However, we are only interested in t varying over a small range, namely that corresponding to the frame of interest. Therefore, just as we are interested in a short-time spectrum $P(\omega,t)$ we are also interested in a short-time 2D-spectrum $\Gamma(\omega,\Omega)$. That is, the short-time analysis is to be performed in two dimensions.)

From (4-32) and (4-33) we have:

$$\Gamma(\omega,\Omega) = \sum_{t=-\infty}^{\infty} \sum_{\tau=-\infty}^{\infty} R(t,t+\tau)\ e^{-j(\omega\tau+\Omega t)}. \qquad (4\text{-}34)$$

It can be shown that $R(t,t+\tau)$ can be computed from $\Gamma(\omega,\Omega)$ by a two-dimensional inverse Fourier transform:

$$R(t,t+\tau) = \left(\frac{T}{2\pi}\right)^2 \int_{-\pi/T}^{\pi/T} \int_{-\pi/T}^{\pi/T} \Gamma(\omega,\Omega)\ e^{j(\omega\tau+\Omega t)}\ d\omega\ d\Omega \qquad (4\text{-}35)$$

where T is the sampling interval. Note that $\Gamma(\omega,\Omega)$ is periodic in ω and Ω with period equal to the sampling radian frequency $\omega_s=\frac{2\pi}{T}$. Although $P(\omega,t)$ is real and even with respect to ω, $\Gamma(\omega,\Omega)$ is in general complex. It has the properties:

$$\Gamma(\omega+n\omega_s,\Omega+m\omega_s)=\Gamma(\omega,\Omega)\ ,\ -\infty<n,m<\infty, \qquad (4\text{-}36)$$

$$\Gamma(-\omega,\Omega) =\Gamma(\omega,\Omega)\ , \qquad (4\text{-}37)$$

and

$$\Gamma(\omega,-\Omega) =\bar{\Gamma}(\omega,\Omega)\ , \qquad (4\text{-}38)$$

where the over-bar denotes complex conjugate. Therefore, $\Gamma(\omega,\Omega)$ is even with respect to ω and hermitian with respect to Ω.

For a stationary process we know that the spectrum is time-independent, i.e. $P(\omega,t)=P(\omega)$. From (4-33) we have

$$\Gamma(\omega,\Omega)=P(\omega)\sum_{t=-\infty}^{\infty} e^{-j\Omega t}$$

$$=2\pi P(\omega)\sum_{n=-\infty}^{\infty} u_0(\Omega-n\omega_s)\ , \qquad (4\text{-}39)$$

where $u_0(x)$ is the impulse function defined by:

$$u_0(x)=0,\ x\neq 0\ ,$$

and

$$\int_{-\infty}^{\infty} u_0(x)dx = 1. \qquad (4\text{-}40)$$

Note that the impulse function $u_0(x)$ is different from the unit impulse (or unit sample) δ_{nm} defined in (3-26). Equation (4-39) says that for a stationary discrete process, the 2D-spectrum consists of a set of periodic "line masses" with density $2\pi P(\omega)$, where $P(\omega)$ is the power spectrum of the process. In the ω,Ω plane these line masses are parallel to the Ω-axis.

In order to make the analysis below more convenient we shall redefine the 2D-spectrum so that $Q(\omega,\omega')$ is the double

transform of R(t,t'). We substitute for τ from (4-31) into (4-34), and let

$$\omega' = \omega - \Omega. \tag{4-41}$$

Then we interchange t and t' and make use of the relation

$$R(t,t') = R(t',t). \tag{4-42}$$

Equation (4-34) then reduces to

$$Q(\omega,\omega') = \sum_{t'=-\infty}^{\infty} \sum_{t=-\infty}^{\infty} R(t,t')\, e^{-j(\omega t - \omega' t')}. \tag{4-43}$$

The inverse relation is:

$$R(t,t') = \left(\frac{T}{2\pi}\right)^2 \int_{-\pi/T}^{\pi/T} \int_{-\pi/T}^{\pi/T} Q(\omega,\omega')\, e^{j(\omega t - \omega' t')}\, d\omega\, d\omega'. \tag{4-44}$$

The 2D-spectrum $Q(\omega,\omega')$ is related to the 2D-spectrum $\Gamma(\omega,\Omega)$ by the relation

$$Q(\omega,\omega') = \Gamma(\omega,\omega-\omega'). \tag{4-45}$$

$Q(\omega,\omega')$ is periodic and hermitian in ω and ω'. It obeys the relations

$$Q(\omega+n\omega_s,\omega'+m\omega_s) = Q(\omega,\omega') \quad , \quad -\infty<n,m<\infty, \tag{4-46}$$

$$Q(-\omega,-\omega') = \bar{Q}(\omega,\omega') \quad , \tag{4-47}$$

and

$$Q(\omega',\omega) = \bar{Q}(\omega,\omega') \quad . \tag{4-48}$$

For a stationary process:

$$Q(\omega,\omega') = 2\pi P(\omega) \sum_{n=-\infty}^{\infty} u_0(\omega-\omega'-n\omega_s). \qquad (4\text{-}49)$$

Just as for $\Gamma(\omega,\Omega)$ in (4-39), $Q(\omega,\omega')$ consists of a set of periodic line masses with density $2\pi P(\omega)$. In the ω,ω' plane these lines would be diagonal lines compared to vertical lines in the ω,Ω plane.

We have introduced in this section two 2D-spectra, $\Gamma(\omega,\Omega)$ and $Q(\omega,\omega')$. $\Gamma(\omega,\Omega)$ was introduced first as a more intuitive definition of the 2D-spectrum starting from a time-varying power spectrum. However, as we shall see in the next section, the Covariance normal equations are easily derived by working with $Q(\omega,\omega')$ and $R(t,t')$ directly.

In the Autocorrelation method, $P(\omega)$ was considered to be the short-time spectrum for the particular frame of interest. Several methods for estimating $P(\omega)$ were mentioned in Section 4.4. However for the purposes of linear prediction, it was found that the estimation of a number of autocorrelation coefficients sufficed. Similarly, in the Covariance method we shall consider $Q(\omega,\omega')$ to be the short-time 2D-spectrum for the frame of interest. However, as we shall see shortly, we need not estimate $Q(\omega,\omega')$. All that is needed for the computation of the predictor parameters is the estimation of a set of nonstationary autocorrelation

coefficients.

4.6 Generalized Analysis-by-Synthesis and the Covariance Method

In Fig. 4-1 the signal s(nT) is passed through the inverse filter H(z) giving as output an error signal e(nT). Both s(nT) and e(nT) are now assumed to be nonstationary. The total energy E in the error signal is given by $R_e(0,0)$, where $R_e(t,t')$ is the nonstationary autocorrelation of the error signal e(nT). From (4-44) we conclude that:

$$E = \left(\frac{T}{2\pi}\right)^2 \int_{-\pi/T}^{\pi/T} \int_{-\pi/T}^{\pi/T} Q_e(\omega,\omega')\, d\omega\, d\omega', \qquad (4\text{-}50)$$

where $Q_e(\omega,\omega')$ is the 2D-spectrum of the error signal. From linear system theory (Papoulis, 1965, p.443), we can write for Fig. 4-1:

$$Q_e(\omega,\omega') = Q(\omega,\omega')\, H(\omega)\, \bar{H}(\omega'), \qquad (4\text{-}51)$$

where $Q(\omega,\omega')$ is the 2D-spectrum of the signal s(nT), and $H(\omega)$ has the same interpretation as before. Therefore, the total energy in the error signal is given by:

$$E = \left(\frac{T}{2\pi}\right)^2 \int_{-\pi/T}^{\pi/T} \int_{-\pi/T}^{\pi/T} Q(\omega,\omega')H(\omega)\, \bar{H}(\omega')d\omega\, d\omega'. \qquad (4\text{-}52)$$

(Compare (4-52) with (4-9) for the stationary case.)

Replacing the formula for H(ω) in (4-52) we obtain:

$$E = \left(\frac{T}{2\pi}\right)^2 \int_{-\pi/T}^{\pi/T} \int_{-\pi/T}^{\pi/T} Q(\omega,\omega') \left[1-\sum_{k=1}^{p} a_k\, e^{-jk\omega T}\right]\left[1-\sum_{k=1}^{p} a_k e^{jk\omega' T}\right] d\omega\, d\omega'. \tag{4-53}$$

In order to minimize E we take $\frac{\delta E}{\delta a_i} = 0$, $1 \le i \le p$.

The result of the differentiation is:

$$\left(\frac{T}{2\pi}\right)^2 \int_{-\pi/T}^{\pi/T} \int_{-\pi/T}^{\pi/T} Q(\omega,\omega') \left[e^{-ji\omega T} + e^{ji\omega' T} - \sum_{k=1}^{p} a_k e^{j(-i\omega+k\omega')T} - \sum_{k=1}^{p} a_k e^{j(-k\omega+i\omega')T}\right] d\omega\, d\omega' = 0.$$

Using (4-44) and the property that R(t,t') = R(t',t) we obtain

$$\sum_{k=1}^{p} a_k\, R(-iT,-kT) = R(-iT,0), \quad 1 \le i \le p. \tag{4-54}$$

We shall call (4-54) the <u>generalized normal equations</u>.

The minimum total-squared error E_p can be obtained by using (4-42), (4-44) and (4-45) in (4-53). The answer can be shown to be equal to:

$$E_p = R(0,0) - \sum_{k=1}^{p} a_k\, R(-kT,0). \tag{4-55}$$

For the special case when the signal is stationary, $R(t,t') = R(t'-t)$, (4-54) reduces to the Autocorrelation normal equations (4-12), and (4-55) reduces to (4-13).

What we shall show later in this section is that the Covariance normal equations (3-8) are the same as (4-54) with the nonstationary autocorrelation coefficients $R(iT,kT)$ being approximated by the covariance coefficients ϕ_{ik} defined in (3-9). First we shall interpret the above results in terms of generalized analysis-by-synthesis.

4.61 Generalized Analysis-by-Synthesis

Following a procedure analogous to that in Section 4.3, we can write from (4-52) and (4-14):

$$E = \left(\frac{AT}{2\pi}\right)^2 \int_{-\pi/T}^{\pi/T} \int_{-\pi/T}^{\pi/T} \frac{Q(\omega,\omega')}{\hat{S}(\omega)\ \hat{\bar{S}}(\omega')}\, d\omega\, d\omega'. \qquad (4\text{-}56)$$

We shall define the 2D-spectrum of the approximate transfer function $\hat{S}(z)$ as

$$Q(\omega,\omega') = \hat{S}(\omega)\ \hat{\bar{S}}(\omega'). \qquad (4\text{-}57)$$

Substituting in (4-54) we have:

$$E = \left(\frac{AT}{2\pi}\right)^2 \int_{-\pi/T}^{\pi/T} \int_{-\pi/T}^{\pi/T} \frac{Q(\omega,\omega')}{\hat{Q}(\omega,\omega')}\, d\omega\, d\omega'. \qquad (4\text{-}58)$$

The interpretation of (4-58) is analogous to that of (4-16) except that here the signal 2D-spectrum $Q(\omega,\omega')$ is being approximated by an all-pole 2D-spectrum $\hat{Q}(\omega,\omega')$. (Note that the 2D-spectrum is in general complex.) For a stationary signal, $Q(\omega,\omega')$ is given by (4-49), and

$$\hat{Q}(\omega,\omega') = \hat{Q}(\omega,\omega) = |\hat{S}(\omega)|^2 = \hat{P}(\omega). \qquad (4\text{-}59)$$

Substituting (4-59) and (4-49) in (4-58) we obtain:

$$E = \frac{A^2 T}{2\pi} \int_{-\pi/T}^{\pi/T} \frac{P(\omega)}{\hat{P}(\omega)}\, d\omega,$$

which is identical to (4-16). Therefore, (4-16) is a special case of (4-58) when the signal is stationary. In Section 4.3 we showed that the minimization of (4-16) can be considered as a method of analysis-by-synthesis. What we have in the minimization of (4-58) is a method of generalized analysis-by-synthesis where the signal is in general nonstationary. The properties given in Section 4.3 also apply to generalized analysis-by-synthesis. We note that the minimization of (4-58) results in the generalized normal equations given in (4-54).

4.62 Reformulation of the Covariance Method

All formulations of the Covariance method must now obey (4-54), where the nonstationary autocorrelation coefficients $R(t,t')$ are to be estimated in some fashion from the speech signal.

The development here will be analogous to that given in Section 4.4 for the Autocorrelation method. We shall define two basic formulations of the Covariance method: the direct and indirect method. In the direct method, the coefficients R(t,t') will be computed from an infinite signal that has been windowed by a moving window. In the indirect method, R(t,t') will be estimated from a finite unwindowed portion of the signal. (The words "direct" and "indirect" refer to whether the 2D-spectrum is computed directly from the signal, or indirectly through an estimated autocorrelation function.)

1. Direct Method

We shall define a nonstationary (time-varying) short-time spectrum P(ω,t) as:

$$P(\omega,t) = \left| \sum_{\tau=-\infty}^{\infty} w(\tau)\ s(\tau-t)\ e^{-j\omega\tau} \right|^2 \qquad (4\text{-}60a)$$

$$= \left| \sum_{\tau=0}^{(N-1)T} w(\tau)\ s(\tau-t)\ e^{-j\omega\tau} \right|^2 , \qquad (4\text{-}60b)$$

where s(t) is the original signal, and w(τ) is a window function that is defined to be zero for τ<0 and τ≥NT. This definition of P(ω,t) is consistent with the definition of P(ω) in (4-18) for the stationary (time-independent) case. P(ω,t) can be plotted

as a function of time in a manner similar to a spectrogram.

Equation (4-60a) can be expanded as:

$$P(\omega,t) = \sum_{x=-\infty}^{\infty} w(x)\ s(x-t)\ e^{-j\omega x} \sum_{y=-\infty}^{\infty} w(y)\ s(y-t)\ e^{j\omega y}$$

$$= \sum_{x=-\infty}^{\infty} \sum_{y=-\infty}^{\infty} w(x)\ w(y)\ s(x-t)\ s(y-t)\ e^{-j\omega(x-y)}. \quad (4-61)$$

Setting $x-y = \tau$, (4-61) reduces to:

$$P(\omega,t) = \sum_{\tau=-\infty}^{\infty} \sum_{x=-\infty}^{\infty} w(x)\ w(x-\tau)\ s(x-t)\ s(x-\tau-t)\ e^{-j\omega\tau}. \quad (4-62)$$

By comparing (4-62) and (4-32) we conclude that:

$$R(t,t+\tau) = \sum_{x=-\infty}^{\infty} w(x)\ w(x-\tau)\ s(x-t)\ s(x-\tau-t). \quad (4-63)$$

In order to obtain $R(t,t')$ we set $\tau = t'-t$ in (4-63):

$$R(t,t') = \sum_{x=-\infty}^{\infty} w(x)\ w(x-t'+t)\ s(x-t)\ s(x-t'). \quad (4-64)$$

Since $w(x) = 0$, $x<0$ and $x \geq NT$, (4-64) can be written as:

$$R(t,t') = \sum_{x=0}^{(N-1)T} w(x)\ w(x-t'+t)\ s(x-t)\ s(x-t') . \quad (4-65)$$

Setting $t = -iT$ and $t' = -kT$ in (4-55), we obtain:

$$R(-iT,-kT) = \sum_{n=0}^{N-1} w_n \, w_{n-i+k} \, s_{n+i} \, s_{n+k}. \qquad (4\text{-}66)$$

Equation (4-66) shows how to compute $R(-iT,-kT)$ for use in the normal equations (4-54) to solve for the predictor coefficients a_k. The coefficients w_n represent the sampled window function.

We note from (4-65), (4-66) and (4-54) that t varies between -pT and -T. From (4-60b) we see that, corresponding to $-pT \leq t \leq -T$, the time-varying spectrum $P(\omega,t)$ can be computed p consecutive times, and after each computation the window is moved one sample interval T. While the Autocorrelation method represents the properties of a single spectrum in each frame, the Covariance method represents the properties of p consecutive spectra in each frame.

2. Indirect Method

In this method the 2D-spectrum is computed from an estimated nonstationary autocorrelation function $\tilde{R}(t,t')$ that is computed from a finite unwindowed portion of the signal. Although several formulations could be defined, we shall give only one which is analogous to (4-21) in the indirect Autocorrelation method. Let us approximate the nonstationary autocorrelation $R(iT,kT)$ by:

$$\tilde{R}(iT,kT) = \sum_{n=0}^{N-1} s_{n+i} \, s_{n+k}, \quad 1 \leq i,k \leq p. \qquad (4\text{-}67)$$

Then $R(-iT,-kT)$ is approximated by:

$$\tilde{R}(-iT,-kT) = \sum_{n=0}^{N-1} s_{n-i}\, s_{n-k}\,, \quad 1 \le i,k \le p. \tag{4-68}$$

But the right-hand side of (4-68) is equal to the coefficients ϕ_{ik} defined by (3-9). Therefore,

$$\tilde{R}(-iT,-kT) = \phi_{ik} \tag{4-69}$$

and $$\tilde{R}(-iT, 0) = \phi_{i0}.$$

Substituting (4-69) in (4-54) we obtain:

$$\sum_{k=1}^{p} a_k\, \phi_{ik} = \phi_{i0}, \quad 1 \le i \le p,$$

which is identical to the Covariance normal equations (3-8). Also, substituting (4-69) in (4-55) results in an expression for E_p that is identical with (3-19).

We have shown that the Covariance method can be derived from a frequency-domain formulation where the short-time 2D-spectrum of a nonstationary signal is to be approximated by an all-pole 2D-spectrum. Under the assumption of a stationary signal, the generalized formulation reduces to the Autocorrelation method. The particular formulations presented in Chapters I and III can now be seen to be the direct Autocorrelation and indirect Covariance methods.

CHAPTER V

THE AUTOCORRELATION METHOD AND THE NORMALIZED ERROR

In Chapter IV it was shown that the Autocorrelation and Covariance methods of linear prediction can be considered to be methods of spectral analysis-by-synthesis, where the short-time spectrum $P(\omega)$ (or 2D-spectrum $Q(\omega,\omega')$) is approximated by an all-pole spectrum $\hat{P}(\omega)$ (or 2D-spectrum $\hat{Q}(\omega,\omega')$). We have also seen that in order to determine the parameters a_k of $\hat{P}(\omega)$ or $\hat{Q}(\omega,\omega')$, it was sufficient to know only a limited number of autocorrelation coefficients $R(kT)$ or $R(iT,kT)$; it was never necessary to know either $P(\omega)$ or $Q(\omega,\omega')$. However, in order to study how $\hat{P}(\omega)$ (or $\hat{Q}(\omega,\omega')$) approximates $P(\omega)$ (or $Q(\omega,\omega')$), one must be able to compute the signal spectrum $P(\omega)$ (or $Q(\omega,\omega')$). This is most easily done in the direct method (where the signal is defined for all time) by using (4-18) in the direct Autocorrelation method and (4-60) in the direct Covariance method. Since it is simpler to deal with one-dimensional rather than two-dimensional spectra, we have chosen to study the direct Autocorrelation method in detail. Moreover, in this way we take advantage of the body of knowledge that already exists in speech research.

In this chapter we shall examine analytically the manner in which the all-pole spectrum $\hat{P}(\omega)$ approximates the signal spectrum $P(\omega)$. For the reasons stated above, this will be done for the

direct Autocorrelation method only. We believe that much insight into linear prediction in general can be gained by analyzing this one method in detail.

First we examine the properties of the approximate spectrum $\hat{P}(\omega)$ and the transfer function $\hat{S}(z)$ when compared to the signal spectrum $P(\omega)$ and transfer function $S(z)$. Of particular interest is the analysis as $p \to \infty$ when $\hat{s}(nT)$ becomes the minimum-phase sequence corresponding to $s(nT)$. Different methods for computing the minimum-phase sequence for an arbitrary sequence are described. Next comes the analysis of the normalized error and its behavior as a function of different spectral shapes. The normalized error is related to the zeroth quefrency of the cepstrum and is interpreted in terms of the ratio of the geometric mean to the arithmetic mean of the spectrum. Properties of the zeroth quefrency follow from this analysis. Then, the usefulness of the normalized error as a voicing detector is discussed. Of importance are the properties of the first autocorrelation coefficient R_1. The chapter ends in a brief discussion on the role of the normalized error in determining the optimum number of predictor coefficients in estimating the spectral envelope.

5.1 Properties of the Approximate Spectrum $\hat{P}(\omega)$

In Section 3.5 we derived a relation between the autocorrelation function R_k of the windowed speech signal and the

autocorrelation function $\hat{R}_k$ of the impulse response of the transfer function $\hat{S}(z)$ defined in (2-2). This relation is given by (3-35) and is presented here with a change of subscripts:

$$\hat{R}_k = R_k \ , \quad 0 \le k \le p. \tag{5-1}$$

We know that the autocorrelation function has a one-to-one relationship with the power spectrum via the Fourier transform. Thus, R_k and $\hat{R}_k$ are the inverse Fourier transforms of $P(\omega)$ and $\hat{P}(\omega)$, respectively (see 4-11a). From (5-1) we see that as the number of predictor coefficients (or poles) p increases, $\hat{R}_k$ and R_k will be equal over a larger range, resulting in a better fit of $\hat{P}(\omega)$ to $P(\omega)$. In the limit, as $p \to \infty$, $\hat{R}_k$ becomes identical to R_k for all k, and hence the power spectra $\hat{P}(\omega)$ and $P(\omega)$ become identical:

$$\hat{P}(\omega) = P(\omega), \quad \text{as } p \to \infty \ . \tag{5-2}$$

One may not be interested in getting an exact replica of $P(\omega)$, but (5-1) and (5-2) give one a better understanding of the approximation process.

From (4-13) we have the minimum total-squared error $E_p = A^2$. Substituting for E_p in (4-16) we have:

$$\frac{T}{2\pi} \int_{-\pi/T}^{\pi/T} \frac{P(\omega)}{\hat{P}(\omega)} \, d\omega = 1. \tag{5-3}$$

Equation (5-3) is independent of p, the order of the linear predictor. In particular, we know from (5-2) that as $p \to \infty$, $\hat{P}(\omega) = P(\omega)$. In that case, (5-3) becomes an identity. In

Appendix B we show that (5-3) is a special case of a more general result, namely that the polynomials $H_0(z)$, $H_1(z)$,..., $H_p(z)$,... form a complete set of orthogonal polynomials with weight $P(\omega)$, where $H_n(z) = H(z)$ for p=n, and $H(z)$ is the inverse filter defined in (2-3).

5.2 Properties of the Transfer Function $\hat{S}(z)$

From (4-6) we have $\hat{P}(\omega) = |\hat{S}(\omega)|^2$, and $P(\omega) = |S(\omega)|^2$, where $S(z)$ is the z-transform of the speech signal $s(nT)$ and $\hat{S}(z)$ is the corresponding transfer function of the speech production model according to linear prediction. We wish to explore how $\hat{S}(z)$ might relate to $S(z)$. We have the definitions:

$$S(z) = \sum_{n=0}^{N} s_n z^{-n} , \qquad (5-4)$$

and

$$\hat{S}_p(z) = \frac{A_p}{1-\sum_{k=1}^{p} a_k z^{-k}} , \qquad (5-5)$$

where (5-5) is identical to (2-2) except that $\hat{S}(z)$ and the gain factor A have been subscripted to indicate the order of the predictor. The subscripts will be used only when necessary for disambiguation. Note that the upper limit on n in (5-4) is now N instead of (N-1); this was done here for convenience.

In light of (4-6) and (5-2), it is natural to ask how the

transfer functions $\hat{S}(z)$ and $S(z)$ are related as $p \to \infty$. Since $|\hat{S}_\infty(\omega)|^2 = |S(\omega)|^2$, it might seem that $\hat{S}_\infty(z)$ will be equal to $S(z)$. However, this is not true in general. As $p \to \infty$, $\hat{S}_\infty(z) = S(z)$ <u>if and only if</u> the windowed signal is minimum-phase, i.e. $S(z)$ has no zeros or poles outside the unit circle. We know in general that the speech signal is nonminimum-phase; it sometimes has zeros outside the unit circle due primarily to the glottal waveform (Flanagan, 1965, p. 140). We also know that $\hat{S}(z)$, in the direct Autocorrelation method, is always minimum-phase: all the poles are inside the unit circle and there are no zeros. Furthermore, there is a unique minimum-phase sequence whose spectrum is identical to $P(\omega)$. Since $\hat{S}_\infty(z)$ is minimum-phase and its spectrum $\hat{P}_\infty(\omega)$ is identical to $P(\omega)$, we conclude that $\hat{S}_\infty(z)$ is the transfer function of the minimum-phase sequence corresponding to the signal $s(nT)$. $\hat{S}_\infty(z)$ can be written as:

$$\hat{S}_\infty(z) = \frac{A_\infty}{1 - \sum_{k=1}^{\infty} a_k z^{-k}} = \sum_{n=0}^{M} \hat{s}_n z^{-n} \qquad (5\text{-}6a)$$

$$= \sum_{n=0}^{M} b_n z^{-n} = B(z) \ , \qquad (5\text{-}6b)$$

where $b(nT) = \hat{s}(nT)$ as $p \to \infty$, and it is equal to the minimum-phase sequence corresponding to the signal $s(nT)$, M is an integer to be determined, and $B(z)$ is the z-transform of $b(nT)$ and is

equal to $\hat{S}_\infty(z)$. Below we shall describe how to compute the sequence $b(nT)$. Of particular interest in Section 5.3 will be the computation of A_∞, which from (5-6) is equal to

$$A_\infty = b_0 \quad . \tag{5-7}$$

This is shown by long division of A_∞ into $1 - \sum_{k=1}^{\infty} a_k z^{-k}$ and equating terms in (5-6a) and (5-6b).

The determination of the minimum-phase sequence $b(nT)$ is equivalent to the classic problem of factorization of the spectrum $P(\omega)$ into

$$P(\omega) = B(\omega)\ \overline{B}(\omega) \quad , \tag{5-8}$$

where $B(\omega)$ is to be minimum-phase. Kolmogorov (1939) gave the general solution of this factorization problem. Fejér (1915) gave another solution for the special case of rational spectra. We shall give algorithms based on both methods. Our major source for this analysis is the 1954 Ph.D. thesis of Robinson, which was reprinted in Geophysics (Robinson, 1967a). The Fejér method can be found also in Grenander and Szegö (1958, pp. 20-26). A third method based on linear prediction will then be described.

A - Fejér Method

The Fejér method assumes only that the expression for $P(\omega)$ is known. However, in our problem we also know $S(z)$. The method described below is an adaptation of Fejér's with $S(z)$

assumed to be known.

Substituting z for $e^{j\omega T}$ in $P(\omega)$, we obtain

$$P(z) = S(z)\ S(z^{-1}) \quad , \tag{5-9}$$

which from (5-8) must also equal:

$$P(z) = B(z)\ B(z^{-1}) \quad . \tag{5-10}$$

Without loss of generality we shall assume that the samples s_0 and s_N of the signal are non-zero. (This can always be insured by defining the signal properly.) The polynomial $S(z)$ in (5-4) has N zeros, hence it can be written as:

$$S(z) = s_0 \prod_{k=1}^{u} (1-\alpha_k\ z^{-1}) \prod_{k=1}^{v} (1-\beta_k\ z^{-1}) \quad , \tag{5-11}$$

where α_k are the roots inside the unit circle,

β_k are the roots outside the unit circle,

and $$u + v = N \quad . \tag{5-12}$$

(We shall ignore cases with roots exactly on the unit circle, since they would rarely occur for an actual signal.) It is clear from (5-11) that $S(z^{-1})$ will have u roots α_k^{-1} outside the unit circle and v roots β_k^{-1} inside the unit circle. Therefore, $P(z)$ in (5-9) has a total of 2N roots, N roots inside the unit circle, and their reciprocals outside the unit circle. We conclude

from (5-10) that B(z) must have N roots. Therefore, M=N in (5-6b).

We wish to have all the roots of B(z) be inside the unit circle, hence

$$B(z) = \sum_{n=0}^{N} b_n z^{-n} \qquad (5\text{-}13)$$

$$= b_0 \prod_{k=1}^{u} (1-\alpha_k z^{-1}) \prod_{k=1}^{v} (1-\beta_k^{-1} z^{-1}), \qquad (5\text{-}14)$$

The roots of B(z) can be computed from the roots of S(z). There still remains the computation of b_0. Since the power spectra of B(z) and S(z) are identical, they must also have identical autocorrelation functions. In particular R_N, the Nth autocorrelation coefficient must be the same for both. From (1-6) (with N-1 replaced by N):

$$R_N = s_0 s_N = b_0 b_N . \qquad (5\text{-}15)$$

By equating the coefficients of z^{-N} in (5-13) and (5-14), we have

$$b_N = b_0 \prod_{k=1}^{u} \alpha_k \prod_{k=1}^{v} \beta_k^{-1} . \qquad (5\text{-}16)$$

Substituting for b_N in (5-15) we obtain:

$$b_0^2 = \frac{s_0 s_N}{\prod_{k=1}^{u} \alpha_k \prod_{k=1}^{v} \beta_k^{-1}} , \qquad (5\text{-}17)$$

From (5-11), (5-14) and (5-17), the specification of B(z) is

complete. From (5-6), $B(z) = \hat{S}_\infty(z)$, and we have now determined the transfer function $\hat{S}(z)$ as $p \to \infty$. Note in (5-13) that the sequence $b(nT)$ is of equal length to $s(nT)$, and $b(nT) = 0$ for $n<0$ and $n>N$.

Computational Considerations

The main problem in finding $\hat{S}_\infty(z)$ is computing the N roots of $S(z)$. For 25 msec of 10 kHz sampled speech, N=250. Finding the roots of a 250- or even a 100-degree polynomial is a major undertaking. To say the least, the method we have just outlined is highly impractical. The main reason for the above discussion was to show that although $\hat{S}_\infty(z)$ has an infinity of poles, it can be written as a polynomial with a finite number of zeros. Also, the minimum-phase sequence $b(nT)$ has the same length as the original sequence $s(nT)$.

B- Cepstral Method - (Kolmogorov Method)

Although Kolmogoroff did not use the word "cepstrum" to refer to the Fourier transform of the logarithm of the spectrum, the operation itself was used. A more recent analysis of this subject can be found in Oppenheim and Schafer (1968). We shall make use of the latter reference below.

The problem again is to compute the minimum-phase

sequence b(nT) corresponding to the speech sequence s(nT). The z-transform of b(nT) is $\hat{S}_\infty(z)$. Below we shall drop the subscript ∞ and simply use $\hat{S}(z)$ as the minimum-phase transfer function corresponding to S(z).

Let the cepstrum c(nT) of S(z) be defined as:

$$c_n = \frac{T}{2\pi} \int_{-\pi/T}^{\pi/T} \log|S(\omega)|^2 \, e^{jn\omega T} \, d\omega$$

$$= \frac{T}{2\pi} \int_{-\pi/T}^{\pi/T} \log P(\omega) \, e^{jn\omega T} \, d\omega \, . \qquad (5\text{-}18)$$

The cepstrum $\hat{c}(nT)$ of $\hat{S}(z)$ can be similarly defined. Since $|\hat{S}(\omega)|^2 = |S(\omega)|^2$ (the spectra are identical), we conclude that $\hat{c}_n = c_n$. We note from the properties of the spectrum and (5-18) that c_n is real and even.

Let the <u>complex</u> cepstrum c'(nT) of $\hat{S}(z)$ be defined as:

$$c_n = \frac{T}{2\pi} \int_{-\pi/T}^{\pi/T} \log \hat{S}(\omega) \, e^{jn\omega T} \, d\omega. \qquad (5\text{-}19)$$

$\hat{S}(\omega)$ can be written as:

$$\hat{S}(\omega) = |\hat{S}(\omega)| \, e^{j\theta(\omega)}$$

$$= |S(\omega)| \, e^{j\theta(\omega)} \, . \qquad (5\text{-}20)$$

Therefore, $\log \hat{S}(\omega) = \log|S(\omega)| + j\theta(\omega)$. (5-21)

$\text{Log}|S(\omega)|$ is an even function of frequency and $\theta(\omega)$ is a continuous odd function of frequency. Therefore, c'_n is a real function. Furthermore, since $\hat{S}(z)$ is minimum-phase we have (Oppenheim and Schafer, 1968):

$$c'_n = 0 , \quad n < 0 . \tag{5-22}$$

From (5-21), (5-19) and (5-18) we conclude that the even part of c'_n should be equal to $\frac{c_n}{2}$:

$$\text{Even}\left[c'_n\right] = \frac{1}{2}\left[c'_n + c'_{-n}\right] = \frac{1}{2} c_n ,$$

or

$$c'_n + c'_{-n} = c_n \quad . \tag{5-23}$$

From (5-22) and (5-23) we have:

$$c'_n = \begin{cases} 0, & n<0, \\ \frac{1}{2} c_0, & n=0, \\ c_n , & n>0 . \end{cases} \tag{5-24}$$

The sequence b(nT) is then computed from c'(nT) as follows:

$$\hat{S}(\omega) = \exp\left[\sum_{n=0}^{\infty}{}' c'_n e^{-jn\omega T}\right] , \tag{5-25}$$

and

$$b_n = \frac{T}{2\pi} \int_{-\pi/T}^{\pi/T} \hat{S}(\omega) e^{jn\omega T} d\omega . \tag{5-26}$$

Equations (5-18), (5-24), (5-25) and (5-26) specify the sequence of computations needed to find the minimum-phase sequence b(nT). Of particular interest is the value of b_0 which from (5-26), (5-25) and (5-24) is equal to:

$$b_0 = e^{c_0'} = e^{c_0/2}$$

or

$$b_0^2 = e^{c_0} \quad . \tag{5-27}$$

This result will be important in the next section.

Computational Considerations

The power spectrum $P(\omega) = |S(\omega)|^2$ is a continuous function of frequency and so is log $P(\omega)$. The cepstrum c(nT), which is the inverse transform of log $P(\omega)$, is potentially infinite in extent. In practice, the cepstrum becomes negligibly small at high cepstral values (or quefrencies). Therefore, $P(\omega)$ must be computed to have enough resolution such that no cepstral aliasing occurs. This criterion is realized by trial and error.

We shall give the whole algorithm in machine-implementable form. We assume that we are given the sequence s(nT).

(1) Take the FFT of s(nT) with enough zeros appended to give sufficient spectral resolution, giving $S(\omega)$ at a finite number of equispaced frequencies. Let this number be M.

(2) Compute M values of $C(\omega) = \log|S(\omega)|^2$.

(3) Take the inverse M-point FFT of C(ω) to obtain M points of c(nT).

(4) Compute c'_n from c_n as follows:

$$c'_n = \begin{cases} \frac{1}{2} c_0 & , n = 0 , \\ c_n & , 0<n<\frac{M}{2} , \\ \frac{1}{2} c_{M/2} & , n = \frac{M}{2} , \\ 0 & , \frac{M}{2}<n\leq M-1 . \end{cases} \qquad (5\text{-}28)$$

Note the differences between (5-28) and (5-24). The changes are necessary in order to deal with a finite instead of the theoretically infinite sequence.

(5) Take the FFT of c'_n, to obtain $\log \hat{S}(\omega) = \log |S(\omega)| + j\theta(\omega)$ at M frequency values.

(6) Compute $\hat{S}(\omega) = |S(\omega)| \cos[\theta(\omega)] + j |S(\omega)| \sin[\theta(\omega)]$.

(7) Take the inverse FFT of $\hat{S}(\omega)$ to obtain b(nT).

M must be greater than N, the number of samples in the signal. A value of M = 2N gives good results for a windowed signal with large N(~250). b(nT) should come out to be zero for n>N, but, in practice it will have small values in that region.

Another occasional source of problems in this method is when one of the values of P(ω) approaches zero, the logarithm approaches -∞. For a speech signal this problem is most likely

to occur when the d.c. value is zero. This problem will be discussed further in Section 5.4 in connection with the computation of c_0.

C - Linear Prediction Method

From (5-6), the sequence b(nT) can be obtained by long division of A_∞ into $1-\sum_{k=1}^{\infty} a_k z^{-k}$. However, one must first know A_∞ as well as a_k for all k. This, of course, is not possible, but one can make an approximation to $\hat{S}_\infty(z)$ by considering $\hat{S}_p(z)$ in (5-5) for a large value of p. The computation of the predictor parameters a_k is then possible by the Fast Autocorrelation method (see Appendix B), and A_p is computed from (3-36). Dividing A_p by $1-\sum_{k=1}^{p} a_k z^{-k}$ gives a polynomial whose coefficients approximate the minimum-phase sequence b(nT).

Figure 5-1a shows a windowed signal s(nT) of duration 25.6 msec (10 kHz sampling rate). The minimum-phase sequence b(nT) corresponding to s(nT) was computed by two methods: the cepstral method and the linear prediction method. Figure 5-1b shows the approximation to b(nT) as computed by the cepstral method using 512-point FFT's (256 zeros were appended to s(nT)). Figure 5-1c shows the approximation to b(nT) as computed by the linear prediction method with p = 250. All the figures are normalized to the same maximum amplitude. For a given accuracy, the cepstral method is more efficient than the linear prediction method.

(a)

(b) Cepstral Method

(c) Linear Prediction Method

Fig. 5-1 Computation of the minimum-phase sequence b(nT) corresponding to the windowed signal s(nT).
(a) s(nT) - 25.6 msec, 10 kHz sampled speech.
(b) Cepstral method using 512-point FFT.
(c) Linear Prediction method using p=250.

5.3 Analysis of the Normalized Error

We mentioned in Section 5.1 that as $p \to \infty$, $\hat{P}(\omega)$ becomes identical to $P(\omega)$. In this section we shall examine this process of approximation by analyzing the behavior of the normalized minimum total-squared error V_p, or simply the normalized error.

The normalized error was defined in Section 3.3 as the minimum total-squared error divided by the energy of the signal $s(nT)$:

$$V_p = \frac{E_p}{R_0} = \frac{A_p^2}{R_0} , \tag{5-29}$$

or

$$V_p = 1 - \sum_{k=1}^{p} a_k r_k , \tag{5-30}$$

where

$$r_k = \frac{R_k}{R_0} \tag{5-31}$$

are the normalized autocorrelation coefficients, which have the property that $|r_k| \leq 1$, for all k. The sum $\sum_{k=1}^{p} a_k r_k$ on the right-hand side of (5-30) cannot be negative since the choice $a_k = 0$, $1 \leq k \leq p$, would reduce V_p. This is not possible because V_p is already a minimum. Therefore, $\sum_{k=1}^{p} a_k r_k \geq 0$ must always hold and $V_p \leq 1$. By an argument similar to the above one can show that $V_{p+1} \leq V_p$, and hence that V_p is a monotonically decreasing function of p. As $p \to \infty$, V_p approaches a minimum value $V_\infty = V_{min} \geq 0$. The latter condition is true because V_p is a normalized squared error and therefore $V_p \geq 0$. Hence,

$$0 \leq V_p \leq 1 . \tag{5-32}$$

This result will be shown in a different way later.

Figure 5-2 shows normalized error curves as a function of p for the unvoiced fricative [s] in the word "list" and the vowel [æ] in the word "potassium". The speech signal was lowpassed at 4.5 kHz and sampled at 10 kHz. Each of the two error curves decreases monotonically towards its own asymptote V_{min} as $p \to \infty$. The largest single drop in both error curves occurs for p=1. Thus V_1 is indicative of the eventual levels of the error curves. It is instructive to examine the behavior of V_1 for different sounds. From the flow chart in Appendix B we note that for p=1, $a_1 = R_1/R_0 = r_1$.

Therefore,

$$V_1 = 1 - \left(\frac{R_1}{R_0}\right)^2 = 1 - r_1^2 \ . \qquad (5\text{-}33)$$

From (4-11b) we have:

$$R_0 = \frac{T}{2\pi} \int_{-\pi/T}^{\pi/T} P(\omega)\ d\omega \qquad (5\text{-}34)$$

and

$$R_1 = \frac{T}{2\pi} \int_{-\pi/T}^{\pi/T} P(\omega) \cos(\omega T)\ d\omega \ . \qquad (5\text{-}35)$$

R_0 is the integral of the spectrum, which is equal to the total energy in the signal. R_1 is the integral of the cosine-weighted spectrum. The cosine weighting is shown in Fig. 5-3. Low frequencies are weighted positively, high frequencies are weighted negatively, while mid frequencies do not contribute much to the value

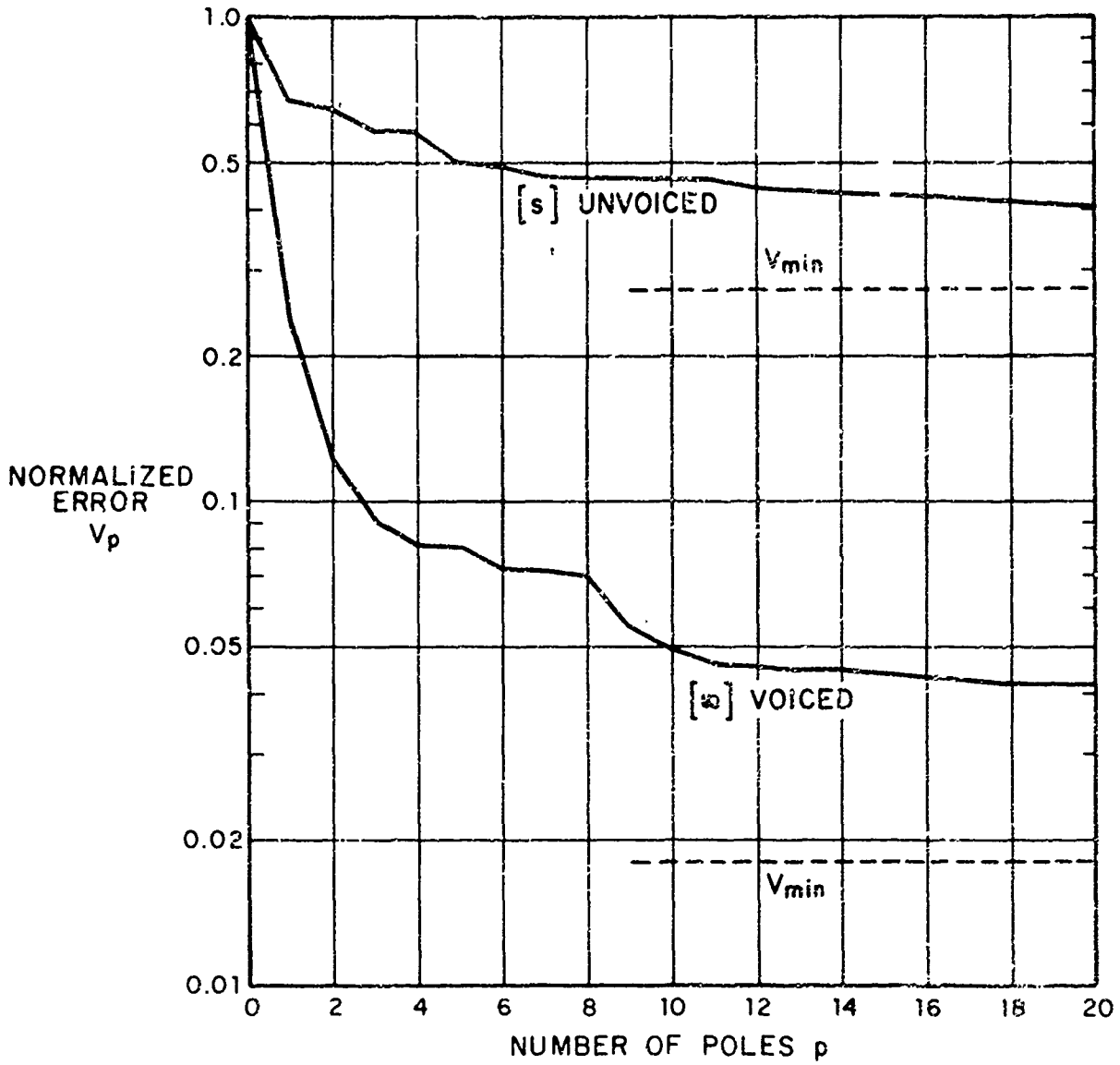

Fig. 5-2. Normalized error curves for [s] in the word "list" and [æ] in the word "potassium".

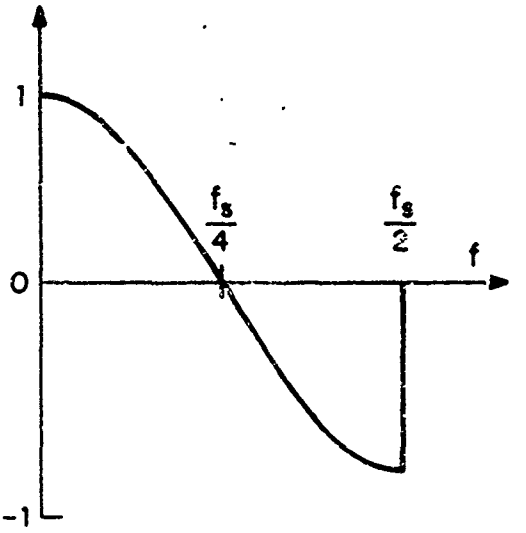

Fig. 5-3. Cosine weighting in computing R_1.

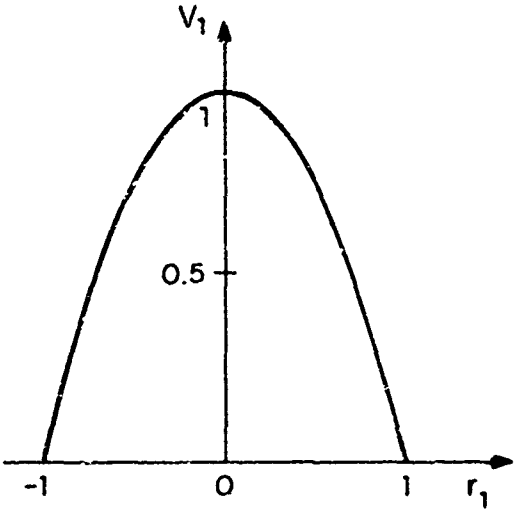

Fig. 5-4. A plot of $V_1=1-r_1^2$, the normalized error for p=1.

of R_1. So, what is important in determining the value of R_1 is the energy balance between low and high frequencies. For example, sonorants usually have most of their energy concentrated at low frequencies, resulting in a value of R_1 very close to R_0. Typically $r_1>.85$ for sonorants, and from (5-33) $V_1<.25$. On the other hand, unvoiced frication has the energy either distributed over the whole frequency range or is more concentrated at high frequencies. Typical values of R_1 are such that $-.5<r_1<.5$, with negative values being more likely for strident fricatives. This results in a $V_1>.75$. Note that it is the absolute value of r_1 that is important in determining the value of V_1. Figure 5-4 shows a plot of V_1 as a function of r_1. If most of the energy in the spectrum is concentrated at high frequencies then r_1 becomes close to -1 and V_1 becomes very small. In general, any particular spectrum and its mirror image (low and high frequencies interchanged) have identical values for V_1.

Above we tried to make three points: 1) One can get insight into the general level of the normalized error curve by examining the behavior of V_1. 2) The value of V_1 depends on the absolute value of the normalized first autocorrelation coefficient $r_1=R_1/R_0$. 3) The value of R_1 depends on the relative energy distribution in the spectrum. In order to get more insight into the behavior of the normalized error curve, we must examine V_p as p varies. This requires that we examine the autocorrelation

function since V_p is a function of only the autocorrelation coefficients R_k, $1 \leq k \leq p$. This can be seen from (5-30) and the fact that the predictor coefficients are computed from the autocorrelation coefficients by solving (3-17). The expression for V_p in terms of the autocorrelation coefficients becomes very complicated as p increases, and very little insight can be gained in that direction. On tne other hand, we know that there is a one-to-one relationship between the autocorrelation function and the spectrum. Therefore, an alternate course is to examine V_p as a function of the spectrum. This relation could be obtained from the results of Section 5.2 on minimum-phase sequences, but we shall give a more direct derivation below. The expression for V_p will be in terms of $\hat{c}_0$, the zeroth coefficient (quefrency) of the cepstrum corresponding to $\hat{P}(\omega)$. An expression for V_{min} then follows directly.

Substituting $\hat{P}(\omega)$ for $P(\omega)$ and $\hat{c}_n$ for c_n in (5-18), and letting n=0, we obtain:

$$\hat{c}_0 = \frac{T}{2\pi} \int_{-\pi/T}^{\pi/T} \log \hat{P}(\omega)\, d\omega \,. \qquad (5\text{-}36)$$

$\hat{c}_0$ is just the integral of the logarithm of the approximate spectrum $\hat{P}(\omega)$. $\hat{c}_0$ is a function of p since $\hat{P}(\omega)$ is a function of p.

The approximate spectrum $\hat{P}(\omega)$ in (4-6a) can be rewritten as:

$$\hat{P}(\omega) = \frac{A_p^2}{\prod_{k=1}^{p} \left| 1 - z_k e^{-j\omega T} \right|^2} \qquad (5\text{-}37)$$

$$= \frac{A_p^2}{\prod_{k=1}^{p} \left(1 + |z_k|^2 - 2[z_{kr}\cos(\omega T) + z_{ki}\sin(\omega T)] \right)}$$

where $z_k = z_{kr} + jz_{ki}$, $1 \le k \le p$, are the poles of the transfer function $\hat{S}(z)$, and z_{kr} and z_{ki} are the real and imaginary parts of the poles, respectively. Since the logarithm of a product is equal to the sum of the logarithms of its elements, (5-37) can be substituted in (5-36) to obtain (after interchanging integration and summation):

$$\hat{c}_0 = \log A_p^2 - \sum_{k=1}^{p} \frac{T}{2\pi} \int_{-\pi/T}^{\pi/T} \log \left(1 + |z_k|^2 - 2[z_{kr}\cos(\omega T) + z_{ki}\sin(\omega T)] \right) d\omega. \qquad (5\text{-}38)$$

Since all the poles of $\hat{S}(z)$ are guaranteed to be inside the unit circle, we have $|z_k| < 1$, $1 \le k \le p$. For this special case, the integral in (5-38) is equal to zero (Gradshteyn and Ryzhik, 1963, p.542). (For $|z_k| \ge 1$, the integral multiplied by $\frac{T}{2\pi}$ is equal to $\log |z_k|^2$.) Therefore:

$$\hat{c}_0 = \log A_p^2 = \log E_p . \qquad (5\text{-}39)$$

The zeroth coefficient of the approximate cepstrum is equal to the logarithm of the minimum total-squared error. Substituting (5-39) in (5-29) we obtain the desired result:

$$V_p = \frac{e^{\hat{c}_0}}{R_0} = \frac{e^{\hat{c}_0}}{\hat{R}_0} \quad . \tag{5-40}$$

(Note that $\hat{R}_0 = R_0$ for all p.)

From (5-2) we know that as $p \to \infty$, $\hat{P}(\omega)$ becomes equal to $P(\omega)$. Substituting $P(\omega)$ for $\hat{P}(\omega)$ in (5-36) and the result in (5-40), we obtain an expression for the minimum normalized error $V_{min}=V_\infty$:

$$V_{min} = \frac{e^{c_0}}{R_0} \quad , \tag{5-41}$$

where c_0 is the zeroth coefficient of the signal cepstrum, and R_0 is the energy in the signal.

Equation (5-41) can also be derived from the results of Section 5.2. From (5-29), (5-7) and (5-27) we have:

$$V_{min} = V_\infty = \frac{A_\infty^2}{R_0} = \frac{b_0^2}{R_0} = \frac{e^{c_0}}{R_0} \quad .$$

Also, since the impulse response $\hat{s}_n$ corresponding to $\hat{S}(z)$ is minimum-phase, and $\hat{s}_0 = A_p$ from (3-28), we have:

$$V_p = \frac{A_p^2}{\hat{R}_0} = \frac{\hat{s}_0^2}{\hat{R}_0} = \frac{e^{\hat{c}_0}}{\hat{R}_0} \quad .$$

It is instructive to write (5-41) as a function of $P(\omega)$:

$$V_{min} = \frac{\exp\left[\frac{T}{2\pi}\int_{-\pi/T}^{\pi/T} \log P(\omega)\, d\omega\right]}{\frac{T}{2\pi}\int_{-\pi/T}^{\pi/T} P(\omega)\, d\omega} . \qquad (5\text{-}42)$$

It is clear from (5-42) that V_{min} depends completely on the shape of the signal spectrum. Similarly, from (5-40), V_p depends completely on the shape of the approximate spectrum. This fact is very important in interpreting the behavior of the normalized error curve for the spectra of different sounds. For example, in Fig. 5-2 the error curve for the unvoiced fricative [s] is much higher than that for the vowel [æ]. On the whole, unvoiced sounds have a high error curve while voiced sounds have a much lower error curve. This property of voiced versus unvoiced sounds has been observed before (Atal and Hanauer, 1971; Markel, SCRL Mon. 1971), and V_p has been suggested as a possible parameter for the detection of voicing. However, with our result showing that the error curves are dependent only on the shape of the spectrum, it is clear that what makes this apparent dichotomy between voiced and unvoiced sounds has nothing to do with the fact of voicing itself, but rather with the shapes of the spectra corresponding to these sounds.

By examining the behavior of V_{min} in (5-42) one gains insight into how the error curves change for different shapes of the spectrum. For example, it is easy to show that if the spectrum is perfectly flat, then $V_{min} = 1$, and the error curve is the highest possible. On the other hand, if all the energy is concentrated in certain regions of the spectrum and the rest of the spectrum contains zero energy, then $V_{min} = 0$, and the error curve is the lowest possible. Speech sounds lie somewhere between these two extremes. In general, voiced sounds (especially sonorants) have most of the energy concentrated in one region at low frequencies, resulting in low error curves. Unvoiced sounds, on the other hand, have the energy more evenly distributed across the spectrum, resulting in higher error curves. However, this property cannot be relied upon all the time. As an example, Fig. 5-5a shows the error curve for the burst [k] in the word "concentration". The error curve is low although the sound is unvoiced. In this case, this was due to the fact that the [k] spectrum had a single sharp peak where most of the energy was concentrated (see Fig. 5-5b).

An interesting way to look at V_{min} in (5-42) is to view it as the ratio of the geometric mean to the arithmetic mean of the spectrum, where the notions of the geometric and arithmetic means have been extended to the continuous case. This becomes clear if one assumes that the spectrum $P(\omega)$ is approximated by a staircase spectrum with N distinct values P_k over the frequency range $\frac{-\pi}{T}$

(a)

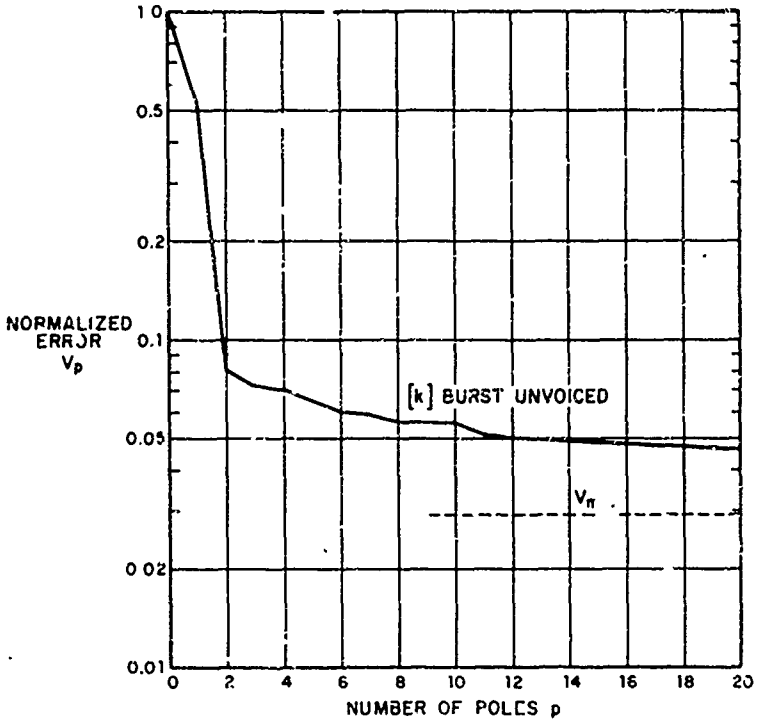

(b)

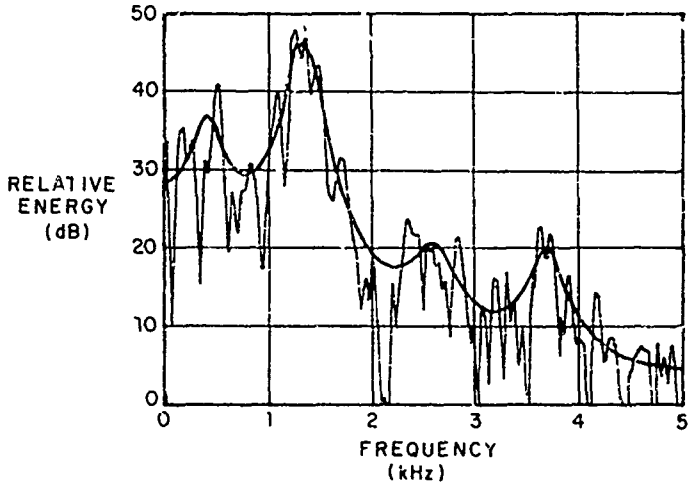

Fig. 5-5. (a) Normalized error curve for the [k] burst in the word "concentration".
(b) Burst spectrum.

and $\frac{\pi}{T}$. In that case, (5-42) reduces to:

$$V_{min} = \frac{\exp\left[\frac{1}{N}\sum_{k=1}^{N} \log P_k\right]}{\frac{1}{N}\sum_{k=1}^{N} P_k} = \frac{\left(\prod_{k=1}^{N} P_k\right)^{1/N}}{\frac{1}{N}\sum_{k=1}^{N} P_k}, \qquad (5\text{-}43)$$

which is the ratio of a geometric mean to an arithmetic mean. Such a ratio has been useful in acoustic signal processing in getting bounds on the difference between averaging logarithms versus taking the logarithm of the average of measured data samples (Cox, 1966; Hershey, 1972). (This difference is simply the logarithm of V_{min} in our case.) It is well known that the ratio in (5-43) is equal to 1 if all the data are equal, and the value decreases as the spread of the data increases. A larger spread is equivalent to heavy concentrations in certain regions and a simultaneous lack of energy in the other regions of the spectrum, i.e. the spectrum has a large dynamic range.

In order to get a better feel on how V_{min} varies with different spectral shapes, we shall compute the ratio in (5-42) for three models of the spectrum: (a) a two-level model, (b) a single-pole model, and (c) a double-pole model. Below, we shall refer to the ratio in (5-42) simply as V; it is the ratio of the geometric mean of a function to its arithmetic mean.

A. Two-Level Model

The two-level model is shown in Fig. 5-6a. The spectrum consists of two levels: a high level labeled H, and a low level labeled L. In Fig. 5-6a, for y = 0 or y = 1 , the spectrum is flat and from (5-42), V = 1. For $0<y<1$, $0<V<1$. Therefore, for fixed H and L, there must exist some y_m for which V has a minimum value V_m. We shall find this value of V_m as a function of H and L.

From (5-42) and Fig. 5-6a:

$$V = \frac{e^{[y \log H + (1-y) \log L]}}{yH + (1-y) L} \quad . \tag{5-44}$$

y_m can be shown to be equal to:

$$y_m = \frac{1}{\log d} - \frac{1}{d-1} \quad , \tag{5-45}$$

$$\text{where} \quad d = \frac{H}{L} \tag{5-46}$$

will be known as the dynamic range.

Substituting (5-45) and (5-46) in (5-44) we obtain V_m, the lower bound on V:

$$V_m = \gamma \, e^{(1-\gamma)} \quad , \tag{5-47}$$

$$\text{where} \quad \gamma = \frac{\log d}{d-1} \quad . \tag{5-48}$$

(5-47) is the expression for the lower bound on V for a particular value of the dynamic range d. Figure 5-6b shows a plot of V_m versus the dynamic range D in dB, where

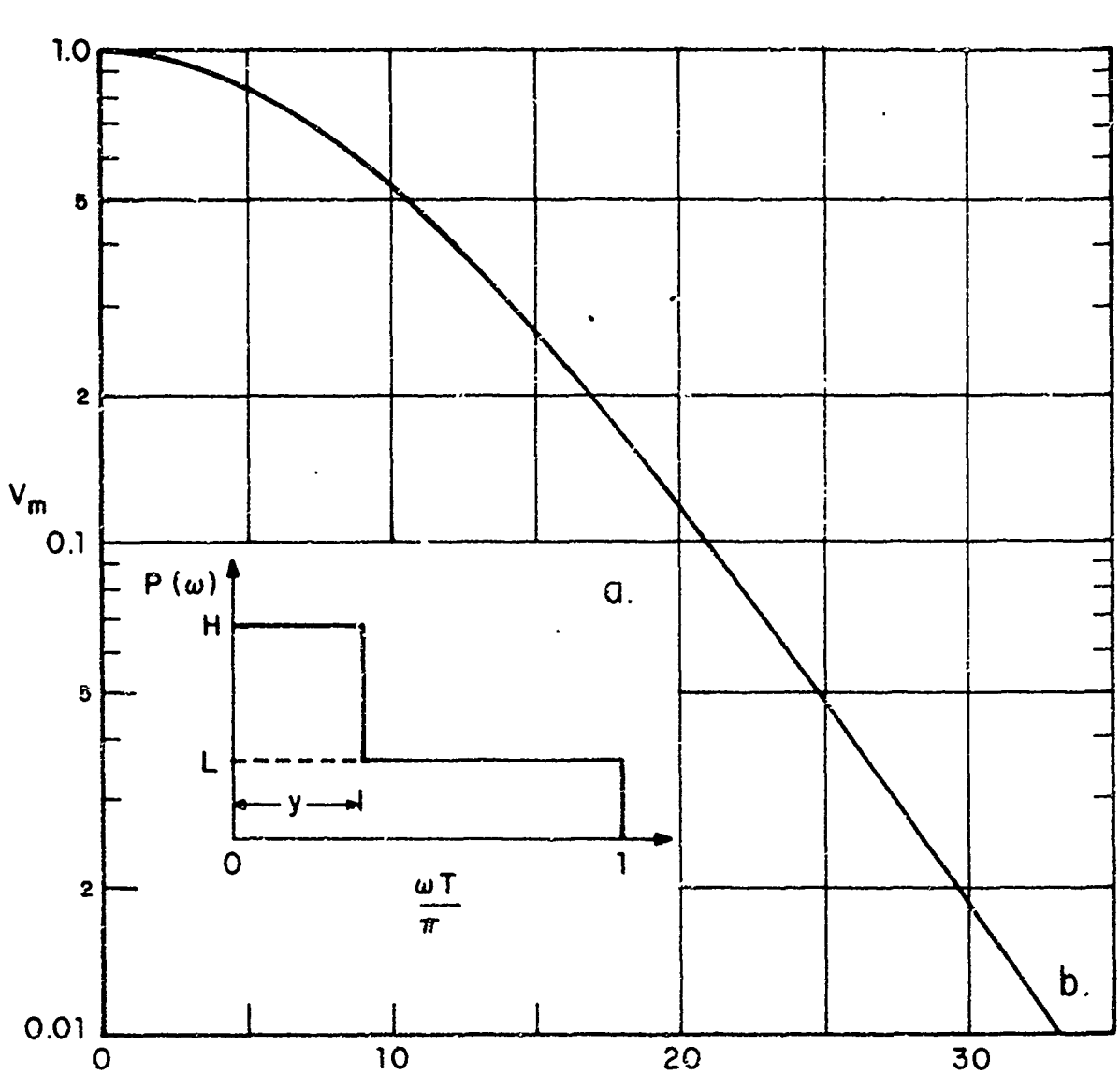

Fig. 5-6. (a) Two-level spectral model.
(b) A plot of V_m, the lower bound on the ratio V, versus the dynamic range of the spectrum.

$$D = 10 \log_{10} d = 10 \log_{10} \frac{H}{L} . \qquad (5\text{-}49)$$

For example, for a dynamic range D = 20 dB, we read from Fig. 5-6b that the lower bound on the value of V for any two-level spectrum with dynamic range of 20 dB is 0.12.

In terms of the value of V, it is clear from the properties of the integrals in (5-42) that the two-level model in Fig. 5-6a also applies to any other spectral shape that has only two values (levels). The importance of the two-level model to other multi-valued spectral shapes is in providing a lower bound on V for all other shapes. This is made explicit by the following lemma and theorem.

Lemma : Let H and L be the highest and lowest spectral values for any spectrum with total energy R_0. There exists a unique two-level spectrum, such as shown by Fig. 5-6a, whose two levels are H and L and whose total energy is equal to R_0. This two-level spectrum has:

$$y = \frac{R_0 - L}{H - L} . \qquad (5\text{-}50)$$

Theorem 1: For a given H, L and R_0, the value of V for the two-level spectrum determined by (5-50) is a lower bound on the value of V for any spectrum with maximum and minimum values H and L, and total energy R_0.

The derivation of (5-50) is straightforward. However, the proof of the theorem is more involved and will not be given here. The

method of proof is to make a perturbation to the shape in Fig. 5-6a, keeping R_0 constant, and proving that the resultant spectrum has a higher V than that for the original two-level spectrum.

Another way to state Theorem 1 is to say that for a certain dynamic range D and energy R_0, the two-level spectrum gives the minimum value for V. Moreover, we have seen that for a particular dynamic range D there is a particular two-level spectrum determined by (5-45) which gives a value V_m that is a lower bound for all two-level spectra with dynamic range D. This leads us to the following theorem:

Theorem 2: The value given by V_m in (5-47) is an absolute lower bound on the value of V for any spectrum with a given dynamic range D.

By equating the value of y in (5-50) and (5-45) one can solve for R_0, resulting in the following corollary:

Corollary: A spectrum with maximum and minimum values, H and L, and total energy R_0 given by

$$R_0 = \frac{H-L}{\log \frac{H}{L}} \qquad (5\text{-}51)$$

has an equivalent two-level spectrum as determined by (5-50) whose value for V is given by V_m in (5-47).

How close the value of V for a particular spectrum comes to V_m depends on how well that spectrum can be approximated by a two-level spectrum and how close R_0 is to the value given by (5-51). As an example of the latter condition, if the dynamic range D = 20 to 30 dB, then the total energy R_0 must be approximately 7-8 dB

below H for (5-51) to apply. For actual speech spectra, if H and L are those of the spectral envelope then the general shape of the curve in Fig. 5-6b applies, though the actual values of V are usually higher than those in the figure. As a general statement one can say that the value of the normalized error decreases as the spectral dynamic range increases.

B. Single and Double-Pole Models

The two-level model concentrated on the effect of the spectral dynamic range on the value of V. Here we shall examine the effect of the general slope of the spectrum on the value of V.

First we shall derive V for an arbitrary pair of poles, then we deal with special cases. Let the two poles be at z=a and z=b, both inside the unit circle. The transfer function for the two poles can be represented by

$$X(z) = \frac{1}{(1-az^{-1})(1-bz^{-1})}, \quad |a|<1, |b|<1. \tag{5-52}$$

The impulse response corresponding to X(z) is given by x(nT), the inverse z-transform of X(z). It can be shown that:

$$x_n = \begin{cases} 0, & n<0, \\ \frac{1}{a-b}\,(a^{n+1}-b^{n+1}), & n\geq 0. \end{cases} \tag{5-53}$$

The total energy R_0 can be obtained from (5-53) as:

$$R_0 = \sum_{n=0}^{\infty} x_n^2 = \frac{1+ab}{(1-ab)(1-a^2)(1-b^2)}. \tag{5-54}$$

In computing V from (5-42) we also need the numerator, which is equal to e^{c_0}. Following a derivation similar to that in Section 5.2 (equations 5-36 to 5-39) we conclude that $c_0 = 0$ for X(z), and hence $e^{c_0} = 1$. Therefore,

$$V = \frac{1}{R_0} = \frac{(1-ab)(1-a^2)(1-b^2)}{1+ab} \quad . \tag{5-55}$$

(5-55) is true for any pair of poles inside the unit circle.

Complex-Conjugate Pair of Poles: Here b is the complex conjugate of a, $b = \bar{a}$. Therefore,

$$V = \frac{1-r^2}{1+r^2}\left[1 + r^4 - 2r^2 \cos(2\omega T)\right] . \tag{5-56}$$

where $r = |a| = |b|$

and ωT = angular position of a or b.

Double Real Poles: a = b, both real.

$$V = \frac{(1-b^2)^3}{1+b^2} . \tag{5-57}$$

Single Real Pole: a = 0, b is real.

$$V = 1-b^2 . \tag{5-58}$$

Note that b could be either positive or negative. Recall that a positive real pole corresponds to the usual real pole in the analog domain, while a negative real pole in the z-plane behaves like a pair of complex conjugate poles at half the sampling frequency (see

Appendix A). The spectrum of a negative real pole is just the mirror image of the spectrum of a positive real pole. While the spectrum of a positive real pole slopes down at approximately 6 dB/octave, that of a negative real pole slopes up at the same rate. Note, however, that the value of V in (5-58) is the same whether the pole is positive or negative. The same goes for the double real poles in (5-57).

Using linear prediction we approximated the spectra of several sounds from a single male speaker by single and two-pole spectra. The speech signal was low-pass filtered at 4.5 kHz and sampled at 10 kHz. The results showed that most sonorants were well approximated by a complex pair of poles with a Q (ratio of frequency to bandwidth of resonance) of between .5 and 2. The frequency of the resonance ranged from about 200 to 700 Hz for different sonorants. [t] bursts were approximated by a complex pair of poles at around 7 kHz with a Q of 1.5. (Most of the high frequency energy in the burst had been filtered out.) The fricative [š] was also modeled by a complex pair at about 2700 Hz with a Q of 2. On the other hand, the fricative [s] was approximated by two real poles: one negative and one positive. When the approximation was restricted to a single pole, the pole was negative and positioned around the real frequency 1000 Hz (i.e. the pole is at 5 kHz with a half bandwidth of 1000 Hz).

The values of V in (5-56) for complex pairs of poles with low Q is quite close to that for a double pole in (5-57) at the same frequency. Therefore we shall give the values of V in (5-57) for different frequencies. This is shown as a graph in Fig. 5-7. For sonorants, values of V are seen to range from about .01 to .1. Also shown in Fig. 5-7 is a graph of V in (5-58) for a single real pole (positive or negative) with real frequency as the abscissa. The value for [s] would be on that graph around 1000 Hz. In order to convert between real frequency and the value of b in (5-57) and (5-58) use the formula

$$|b| = e^{-\sigma T} = e^{-2\pi f_r T}$$

where f_r is the real frequency and T is the sampling interval (in this case T = 100 μsec).

These graphs have two main properties. First, at any one frequency, V is less for a double pole than for a single pole. This is to be expected since the spectrum of the double pole has a larger dynamic range than that of the single pole, and we have learned that, other things being equal, a larger dynamic range results in a lower V. Second, for each of the two curves, as the frequency of the pole increases, V increases. Again, this is to be expected since as the pole frequency increases the dynamic range of the corresponding spectrum decreases which causes an increase in V.

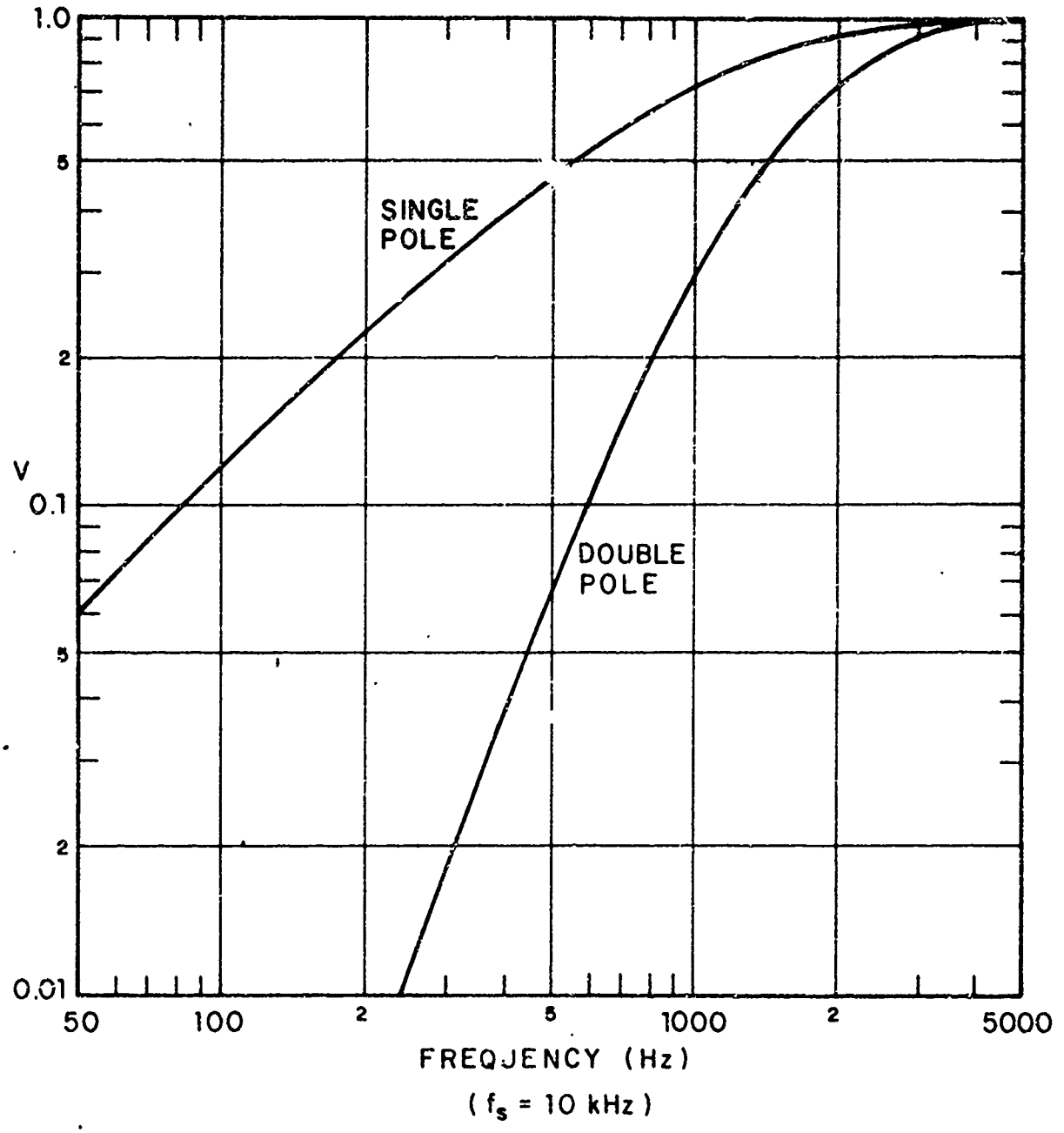

Fig. 5-7. The ratio V for single and double pole models of the spectrum.

This concludes our exposition of the behavior of V_{min} as a function of different spectral models. For real speech spectra V_{min} must be computed from (5-42) in an approximate manner. This is discussed in the next section where we deduce properties of the zeroth quefrency c_0.

5.4 The Zeroth Quefrency

It is clear from (5-41) that $V = \frac{e^{c_0}}{R_0}$ depends completely on the zeroth quefrency c_0 and the total energy R_0 of the signal. Therefore, all the properties of V that were discussed in Section 5.3 are actually a reflection on the properties of c_0. We shall not repeat these properties here, but we would like to examine another possible usefulness of c_0 in speech analysis.

Given two signals such that one is a constant multiple of the other, their cepstra are identical except at the origin (i.e. at c_0). This property led Mersereau and Oppenheim (1972) to suggest the possibility of using c_0 as a measure of signal amplitude. They presented plots of c_0 for several utterances and compared them with plots of log R_0. They noticed that the two curves had similar gross features except that for some fricatives c_0 had definite peaks while log R_0 did not. These differences between c_0 and log R_0 can be easily explained from the properties of V. Indeed, the difference between c_0 and log R_0 is simply given by

$$\log V = c_0 - \log R_0. \qquad (5\text{-}59)$$

This difference can be measured in dB if we take 10 $\log_{10}$ V in which case:

$$10 \log_{10} V = 4.34\, c_0 - 10 \log_{10} R_0$$

or
$$V(dB) = c_0(dB) - R_0(dB) , \qquad (5\text{-}60)$$

where V(dB) is V measured in dB, $R_0(dB)$ is the energy measured in dB, and $c_0(dB) = 4.34c_0$. Since $V \leq 1$ must always hold, log V is always negative (or equal to zero). Therefore,

$$c_0(dB) \leq R_0(dB) . \qquad (5\text{-}61)$$

How much $c_0(dB)$ is less than $R_0(dB)$ depends on the shape of the spectrum. From the analysis in Section 5.3 it is clear that $c_0(dB)$ could be as much as 20 dB less than $R_0(dB)$ for certain sonorants. On the other hand, for some fricatives that difference could be as low as 3 or 4 dB. This is why, relative to the general trend of c_0 versus log R_0, some fricatives were marked by sharp peaks. From our experience, even within the sonorants themselves V(dB) varied by as much as 10 dB.

Our conclusion is that the zeroth quefrency c_0 indeed does carry information concerning the energy in the signal, but that information is coupled with other information about the general shape of the signal spectrum. The energy information can be factored out by dividing e^{c_0} by R_0, leaving the information on the spectral shape, and that is simply V. c_0 (more accurately e^{c_0}) is

a measure of the geometric mean of the spectrum, while R_0 is a measure of the arithmetic mean. Thus, the information that c_0 carries about R_0 is the same information that a geometric mean carries about the corresponding arithmetic mean, no less and no more. The relation between the two means is represented by V.

Computational Considerations

If c_0 is to be computed for a speech signal using a digital computer, then the integral of the log spectrum must be approximated by a summation. This is usually no problem, unless one of the spectral values happens to be zero. This is most likely to happen at d.c. especially since many people remove the d.c. component from the signal before computing the spectrum. The problem, of course, is that the logarithm of zero is normally considered to be $-\infty$. Anything added to $-\infty$ keeps the sum at $-\infty$ and c_0 will have the value $-\infty$. This result is incorrect since we know that the integral of the log spectrum for any signal with finite non-zero energy must always be finite. The fact that the spectrum $P(\omega)$ is zero at one point (causing $\log P(\omega) \to -\infty$) does not mean that the integral of $\log P(\omega)$ is also infinite. As a simple illustration, it can be verified that

$$\int_0^{\varepsilon} \log \omega \, d\omega = \varepsilon \log \varepsilon - \varepsilon \, . \qquad (5\text{-}62)$$

Note that at $\omega=0$, $\log \omega \to -\infty$, but the integral in (5-62) is finite for an arbitrarily small ε. In particular, as $\varepsilon \to 0$, the integral approaches zero, and thus the fact that the logarithm is infinite at $\omega=0$ did not contribute to the integral at that point.

It should be clear that the above problem in computing c_0 arose only because we are approximating the integration by a summation. Indeed, if the integral in (5-62) is to be approximated by a summation and the value at $\omega=0$ is used, the same problem would occur. If we assume that this problem is likely to arise only at d.c., then a good solution is to remove the d.c. from the signal and then ignore the spectrum at d.c. in computing c_0.

5.5 Detection of Voicing

In Section 5.3 we pointed out the possible usefulness of the normalized error V_p as a voicing detector. This could be implemented by setting a threshold on the normalized error for a particular value of p. If V_p is less than the threshold, the sound is judged to be voiced; otherwise it is judged to be unvoiced. For speech recorded in a quiet room using a high quality system, we have found that the normalized error can be used in this manner a large portion of the time for the detection of voicing. (More precisely, it is useful in differentiating sonorants from nonsonorants. In the cases of stops and fricatives,

the normalized error does not work particularly well as a voicing detector.) It should be reiterated that this behavior of the normalized error has nothing to do with the fact of voicing itself, but rather with the shapes of the spectra corresponding to voiced vs. unvoiced (or sonorant vs. nonsonorant) sounds. We will point out some of the common conditions under which the normalized error works less than ideally as a voicing detector.

Background Noise - During stop gaps and other periods of silence, the signal being analyzed is the background noise. During these periods, irrespective of how low the noise level is, the normalized error curve could be low or high, depending on the shape of the noise spectrum. If the noise spectrum is rather flat, the error curve will be high and the spectrum will be judged to be unvoiced. However, in many real life situations there is a heavy energy concentration at very low frequencies, which causes the error curve to be low and may cause the spectrum to be judged as voiced. A possible solution is to high-pass the speech signal to get rid of these low frequency components (which are usually below 250 Hz), but this filtering would also filter out the low frequency components in all other sounds to an undesirable extent. A better solution would be to detect periods of silence from energy considerations (e.g. R_0) and then avoid making a voicing decision based on V_p during these periods.

Telephone Speech - The telephone is an example of a medium for extensive vocal communication which distorts the speech signal in many ways. For example, the energy below 300 Hz and above 3 kHz is filtered out. This keeps much of the formant structure relatively untouched, but it filters out much of the energy for sonorants and fricatives. This, in addition to other important factors (such as noise), reduces the spectral dynamic range of the signal. The overall effect on the normalized error is that it becomes higher. For some vowels the normalized error can be as much as an order of magnitude higher. The result, of course, is that it becomes more difficult to use the normalized error to differentiate between voiced and unvoiced sounds.

Effects of Preemphasis - Preemphasis is often used in speech analysis to compensate for the spectral slope of voiced sounds, which falls at 6 dB/octave or more. In the digital domain, preemphasis is conveniently accomplished by differencing the signal (i.e. subtracting adjacent samples). We shall go into some detail on the properties of differencing and its effects on the normalized error. Some of these properties will be useful in the next chapter on formant extraction.

Let the first difference of the signal s_n be defined by:

$$s'_n = s_n - s_{n-1} = d(s_n) \qquad (5\text{-}63)$$

where s'_n is the differenced signal and d^i is an operator that takes the ith difference of its argument.

Taking the z-transform of (5-63) we obtain:

$$S'(z) = (1-z^{-1})\ S(z) = D(z)\ S(z) \qquad (5\text{-}64)$$

where $$D(z) = 1-z^{-1} \qquad (5\text{-}65)$$

is the differencing operator in the frequency domain. It introduces a digital zero at z=1, which corresponds to zero frequency. The power spectrum of the differenced signal is:

$$\begin{aligned} P'(\omega) = |S'(\omega)|^2 &= |D(\omega)|^2\ P(\omega) \\ &= |1 - e^{-j\omega T}|^2\ P(\omega) \\ &= 4\ \sin^2\left(\frac{\omega T}{2}\right)\ P(\omega)\ , \end{aligned} \qquad (5\text{-}66)$$

where $$|D(\omega)| = 2\ \sin\left(\frac{\omega T}{2}\right) \qquad (5\text{-}67)$$

is the magnitude of the frequency response of the differencing operator. Therefore, the effect of differencing in the time domain is to multiply the power spectrum by $4\ \sin^2\left(\frac{\omega T}{2}\right)$, which is the spectral response of the zero z=1. Figure 5-8 shows a plot of $|D(\omega)|$ in (5-67) versus ωT. ($\omega T = \pi$ corresponds to half the sampling frequency, which would be 5 kHz for a 10 kHz sampled signal.) Also shown in Fig. 5-8 is a plot of the transfer function for the analog zero at zero frequency. The analog zero corresponds to differentiation in the continuous time domain.

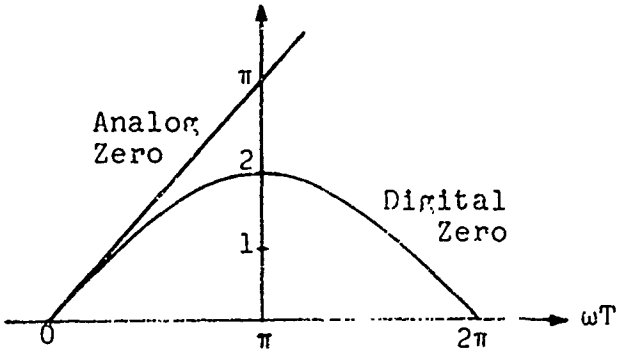

Fig. 5-8 The frequency response of a digital zero at z=1 as compared to the corresponding analog zero at zero frequency.

The response of the analog zero climbs at 6 dB/octave for all frequencies. The response of the digital zero climbs at 6 dB/octave at low frequencies, but becomes flat at $\omega T = \pi$. Between $\omega T = \frac{\pi}{2}$ and $\omega T = \pi$ (which corresponds to the octave 2.5 kHz to 5 kHz) there is a rise of only 3 dB. At $\omega T = \pi$, the digital response is 3.92 dB lower than the analog response.

Therefore, differencing greatly attenuates the energy at very low frequencies and enhances the energy at high frequencies. These major effects on the shape of the spectrum have strong effects on the normalized error curves. As an example, Fig. 5-9 shows the error curves for the same two signals shown in Fig. 5-2, except that in this case the signals were preemphasized by

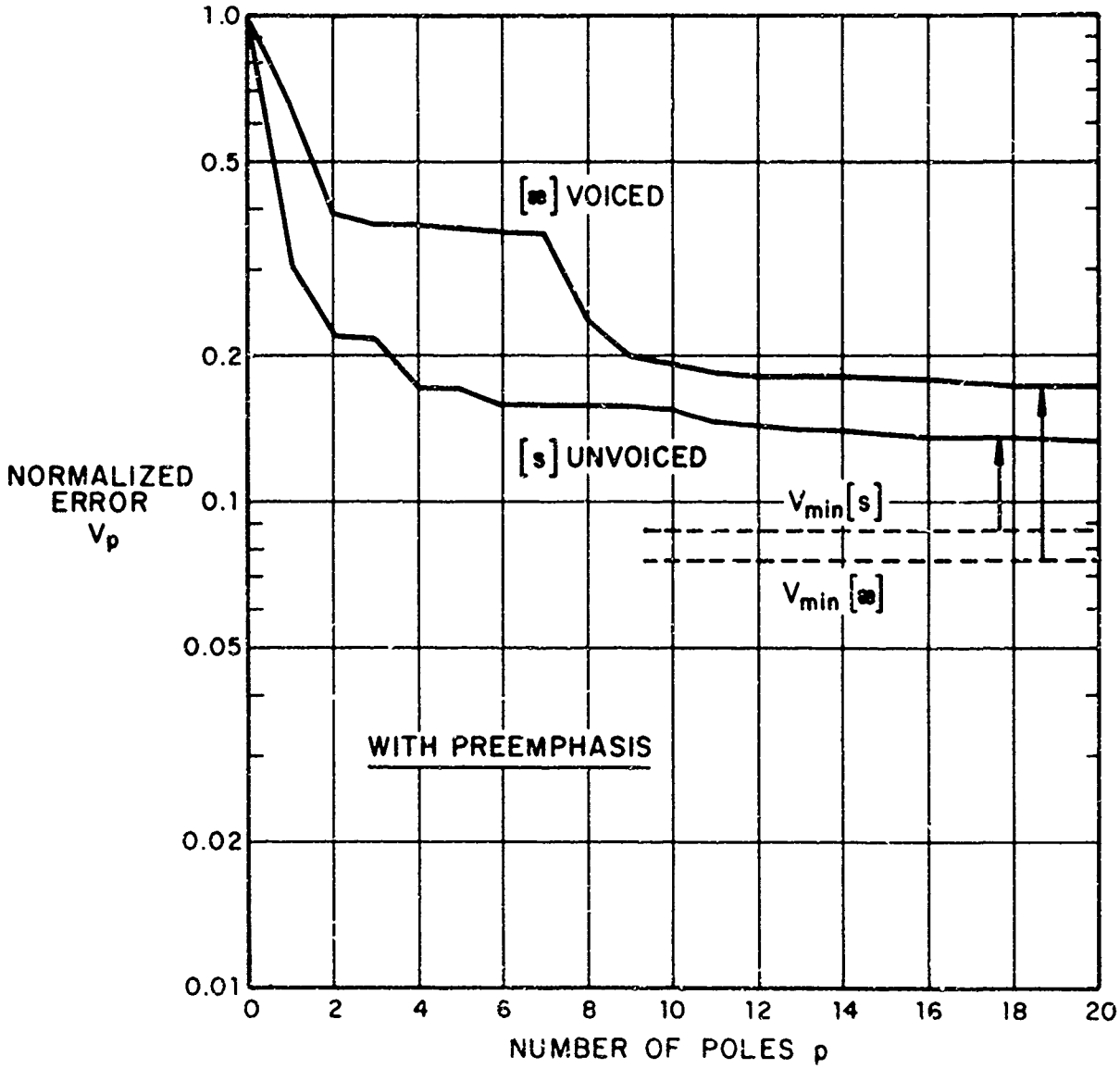

Fig. 5-9. Normalized error curves for the same two sounds as in Fig. 5-2, except that the speech signals were preemphasized by simple differencing.

differencing. The error curve for the unvoiced fricative [s] became lower while that for the vowel [æ] became much higher, so much so that the [æ] curve starts higher than the [s] curve, but as $p \to \infty$, V_{min} for [æ] becomes lower than V_{min} for [s]. (This means that the two curves must have crossed at some point. In this case the curves cross at p = 122.) In general, preemphasis causes a marked increase in the value of the normalized error for sonorants. The effects of preemphasis on unvoiced sounds such as stop bursts and fricatives are less predictable; the normalized error could go either up or down depending on the particular spectrum. These effects can be understood better by examining how the autocorrelation coefficient R_1 is affected by differencing the signal, and then using Fig. 5-4 to make statements about the behavior of V_1, which, as we have argued before, is a good indication of the general level of the error curve.

As we pointed out in Section 5.3, R_1 is the result of a cosine weighting on the spectrum which weights low frequencies positively and high frequencies negatively. Since preemphasis attenuates low frequencies and emphasizes high frequencies, the effect is to lower the value of R_1 relative to R_0, i.e. to lower r_1. From Fig. 5-4, decreasing r_1 could either increase or decrease V_1 depending on the value of r_1 and how much it decreases. Most sonorants have $r_1 > .9$, and differencing causes a decrease of between .1 and .7 so that the resulting r_1 is still greater than zero.

From Fig. 5-4 we see that V_1 always increases for this case. For sounds such as [s] where $r_1<0$, decreasing r_1 decreases V_1. However, for other unvoiced sounds where $0<r_1<.5$, decreasing r_1 could either increase or decrease V_1 depending on how much r_1 is decreased. The general impression that one gets upon monitoring the normalized error is that preemphasis by differencing makes the normalized error an unreliable measure of voicing.

Computing the values of the autocorrelation function for the differenced signal (e.g. in order to see the effect of differencing on r_1) is possible from the autocorrelation of the undifferenced signal. Let R'_k be the autocorrelation function of the differenced signal. Then, by definition:

$$R'_k = \sum_{n=-\infty}^{\infty} s'_n \, s'_{n+k} \qquad (5\text{-}68)$$

Substituting (5-63) in (5-68) we obtain:

$$R'_k = \sum_{n=-\infty}^{\infty} (s_n - s_{n-1})(s_{n+k} - s_{n+k-1})$$

$$= \sum_{n=-\infty}^{\infty} (s_n \, s_{n+k} - s_n \, s_{n+k-1} - s_{n-1} \, s_{n+k} + s_{n-1} \, s_{n+k-1})$$

$$= R_k - R_{k-1} - R_{k+1} + R_k$$

$$\text{and} \quad R'_k = 2R_k - R_{k-1} - R_{k+1} \quad , \qquad (5\text{-}69)$$

$$\text{or} \quad R'_k = -[(R_{k+1} - R_k) - (R_k - R_{k-1})]$$

$$= -[d(R_{k+1}) - d(R_k)]$$

$$\text{and} \quad R'_k = -d^2(R_k) \quad . \qquad (5\text{-}70)$$

(5-70) says that the autocorrelation of a differenced signal is equal to the negative of the second difference of the autocorrelation of the original signal. This result is analogous to the analog domain property that the autocorrelation of a differentiated continuous signal is equal to the negative of the second derivative of the autocorrelation of the original signal (see for example, Papoulis, 1965, p. 317). As an example, r'_1 for the differenced signal is equal to:

$$r'_1 = \frac{R'_1}{R'_0} = \frac{1}{2}\left[\frac{r_1 - r_2}{1 - r_1} - 1\right] \quad . \qquad (5\text{-}71)$$

(Remember that $R_{-k} = R_k$, for all k.)

5.51 Using r_1 as a Voicing Detector

It has become clear that what makes the normalized error a good voicing detector for high quality speech is the fact that most voiced sounds have a high energy concentration at low frequencies while unvoiced sounds have the energy more spread out or partly concentrated at high frequencies. This spectral balance, when disturbed (e.g. by preemphasis) causes the normalized

error to be an unreliable voicing detector. We have explained some of the reasons for this above, where we appealed to an analysis in terms of r_1 and its effect on V_1. In particular, we observed that for a differenced signal $r_1' < r_1$, while the value for V_1 had no such consistent relation. This suggests the use of r_1 as a voicing detector.

For an unpreprocessed signal, r_1 should work as well as the normalized error. From the limited data we have examined for a single male speaker, $r_1 > .8$ for voiced sounds and $r_1 < .6$ for unvoiced sounds worked very well as a voicing detector. Furthermore, when the speech signal was preemphasized by differencing we noted that r_1' was always less than r_1, but the amount changed with the particular sound. Front vowels exhibited a large drop as might be expected. (For example, one [i] sound had $r_1 = .95$ and $r_1' = .2$.) However, most sounds remained separable between voiced and unvoiced, although we do not expect the reliability to be as high as with r_1. If preemphasis is performed before the signal is digitized then one could just use r_1'. However, if the signal is to be differenced digitally, one need not use r_1'; r_1 would still be available and relatively cheap computationally; all that is needed is to compute R_0 and R_1 from the original signal before it is differenced.

There is nothing sacred or magical about using the normalized error or r_1 as a voicing detector, especially if the signal was

processed in some special way. In that case one could perform a suitable weighting on the spectrum and get a measure that would correlate well with voiced or unvoiced sounds. r_1 uses a cosine weighting; this is only one of an infinite number of different weightings that could be used. Furthermore, no single method for the detection of voicing will work all the time. It is normally advisable to have at least two methods at hand, and the two should be based on different properties of the signal.

5.6 Optimum Number of Predictor Coefficients

It was stated in Section 4.3 that for certain applications we wish to approximate the envelope of the signal spectrum $P(\omega)$ by an all-pole spectrum $\hat{P}(\omega)$ whose parameters are the predictor coefficients a_k, $1 \le k \le p$. Also, we were assured that by minimizing the error in (4-16) we obtain a spectrum $\hat{P}(\omega)$ which (for some p) is a good estimate of the spectral envelope of $P(\omega)$. The question that remains is for what value(s) of p will $\hat{P}(\omega)$ indeed be a good spectral envelope. We know that such a value of p (or range of values) must exist, because for very low values of p, $\hat{P}(\omega)$ is a very crude fit to $P(\omega)$, while as $p \to \infty$, $\hat{P}(\omega)$ becomes identical to $P(\omega)$. Somewhere in between there should be a value of p that would be satisfactory for a good envelope fit. In Section 2.4 we obtained a rough idea of what p should equal for some sounds from theoretical considerations. Here we shall give an empirical method to determine

the optimum value of p for each soun

Figures 5-2, 5-5 and 5-9 show error curves corresponding to different spectra. Each of the error curves starts at 1 for p=0 and monotonically decreases to its own V_{min} as $p \to \infty$. Also, each of the curves exhibits what might be called the "knee" of the curve. This is a region of the curve after which the curve slopes very slowly towards its asymptote. For example, in Fig. 5-2, starting at p=7 for [s] and at p=11 for [æ], the error curve falls off gently. Our physical explanation for this "knee" is that around that value of p the approximate spectrum $\hat{P}(\omega)$ is the optimum approximation to the envelope of the signal spectrum $P(\omega)$. A lower value of p results in a grosser approximation to the spectral envelope while a larger value of p will superimpose fine structure information on the spectral envelope. This explanation is based on the properties of the error measure (4-16) which were discussed in Section 4.3.

Therefore, for each frame of the signal one could find the knee of the error curve and choose the optimal value of p as that place where the error curve begins to fall off slowly towards its asymptote. This method is, of course, quite approximate. It should be clear that the optimal value of p will vary a good deal depending on the particular sound. For many applications this process is cumbersome and a fixed value of p would be more desirable. In general, increasing p beyond its optimal value has a

a less drastic effect than if p is decreased. Therefore it is usually sufficient to set p to a fixed value that is the upper limit necessary to describe the spectral envelopes of the different sounds in the signal. For speech signals bandlimited to 5 kHz and sampled at 10 kHz, a value of p between 10-14 is chosen depending on the application. This agrees with the speech production considerations of Section 2.4.

In Section 6.2 the above results will be extended to other linear prediction methods, and will be useful in determining the value of p which leads to accurate formant information.

CHAPTER VI

FORMANT ANALYSIS AND PITCH EXTRACTION

In an analysis-synthesis system based on linear prediction, the synthesis part of the system is normally based on the speech production model shown in Fig. 2-1. We have discussed in Chapters III and IV several methods for the computation of the predictor parameters. In Chapter V we discussed methods for the detection of voicing. One important remaining parameter is the pitch τ, for those sounds judged to be voiced. We define pitch to be the time interval between consecutive glottal pulses. The instantaneous fundamental frequency F_0 is then defined as the inverse of the pitch, $F_0 = \frac{1}{\tau}$. The first section in this chapter discusses briefly methods of pitch extraction (estimation) based on linear prediction. It should be emphasized that the discussion in this chapter applies to both the Covariance and Autocorrelation methods of linear prediction.

For other applications, such as formant-based synthesis and speech recognition, it is desired to estimate the formants of the vocal tract as well. The formants are estimated from the poles of $\hat{S}(z)$ in the speech production model. The extent to which the formant values thus obtained reflect the actual resonances of the vocal tract depends on several factors. We discuss the adequacy

of the all-pole model for formant extraction (estimation), the effect of the number of poles p in $\hat{S}(z)$, the dependency on the specific method of linear prediction used, and the importance of the signal frame width and frame positioning. The last factor is discussed in terms of pitch-synchronous and pitch-asynchronous analysis. A discussion of windowing is included in pitch-asynchronous analysis.

Finally, we discuss peak picking of the linear prediction spectrum as a means of formant extraction. Preemphasis of the speech signal and computing the spectrum along a contour inside the unit circle are suggested as two efficient and effective methods to improve the performance of peak picking in formant extraction.

6.1 Pitch Extraction

If we assume that the model in Fig. 2-1 is accurate for the production of voiced speech, then by passing the speech signal s(nT) into a filter that is the inverse of $\hat{S}(z)$, we should obtain a signal that is close to u(nT), which consists of a sequence of impulses. Except for the gain factor A, the filter H(z) defined in (2-3) is the inverse filter to $\hat{S}(z)$. From Fig. 4-1 we see that passing the signal s(nT) through the filter H(z) produces the error signal e(nT). Therefore, e(nT) should be related to u(nT) by a multiplicative constant for any one frame of speech,

i.e. $e(nT) \cong A\, u(nT)$. The error signal, then, should exhibit impulses corresponding to the pitch pulses. The separation of these pulses in time would then be the pitch period, whose inverse is the instantaneous fundamental frequency F_0.

After the predictor coefficients a_k are computed by any desired method, the error signal e(nT) is obtained from the original signal by using (3-2), which is repeated here:

$$e_n = s_n - \sum_{k=1}^{p} a_k\, s_{n-k} \,. \qquad (6\text{-}1)$$

e_n is simply the difference between the original signal and the predicted signal. It is a measure of the inaccuracy in assuming a linear prediction model. In the direct Autocorrelation method the original signal is usually windowed before the coefficients are computed. In that case (6-1) could be applied either to the windowed signal or to the original signal. In the direct Autocorrelation method windowing is necessary in order to obtain better estimates of the coefficients a_k. However, once this is done, the computed coefficients a_k are supposed to apply to the original signal as well.

Although the coefficients a_k are computed from a specific frame of the signal, one could compute (6-1) for a time interval that is larger than that used for computing the coefficients a_k.

In a quasi-steady-state situation, the same coefficients a_k should continue to apply to a portion larger than the frame used for the analysis.

Figure 6-1 shows examples of error signal analysis using the direct Autocorrelation method for four types of voiced speech segments. Each example shows three signals, each 25.6 msec long. s(nT) is the original signal. The predictor coefficients a_k are computed from a Hamming-windowed s(nT), then the error signal e(nT) in the figure is obtained by applying (6-1) to the original unwindowed signal s(nT). $R_e(nT)$ is the autocorrelation of e(nT). In Fig. 6-1, e(nT) is normalized with respect to the maximum error in the frame. Also, the first p values of e(nT) have been set to zero since e(pT) is the first value we compute. $R_e(nT)$ is normalized with respect to the maximum value in the frame other than $R_e(0)$, which is known to be greater than all other autocorrelation coefficients. In fact, $R_e(0)$ is not shown in the examples in Fig. 6-1.

In comparison with Fig. 6-1, Fig. 6-2 shows the error autocorrelation functions for the same four frames, except that the error signal is obtained from the windowed signal. The computations were performed in the frequency domain as follows:

$$R_e(nT) = \frac{T}{2\pi} \int_{-\pi/T}^{\pi/T} |E(\omega)|^2 \, e^{jn\omega T} \, d\omega \, , \qquad (6\text{-}2)$$

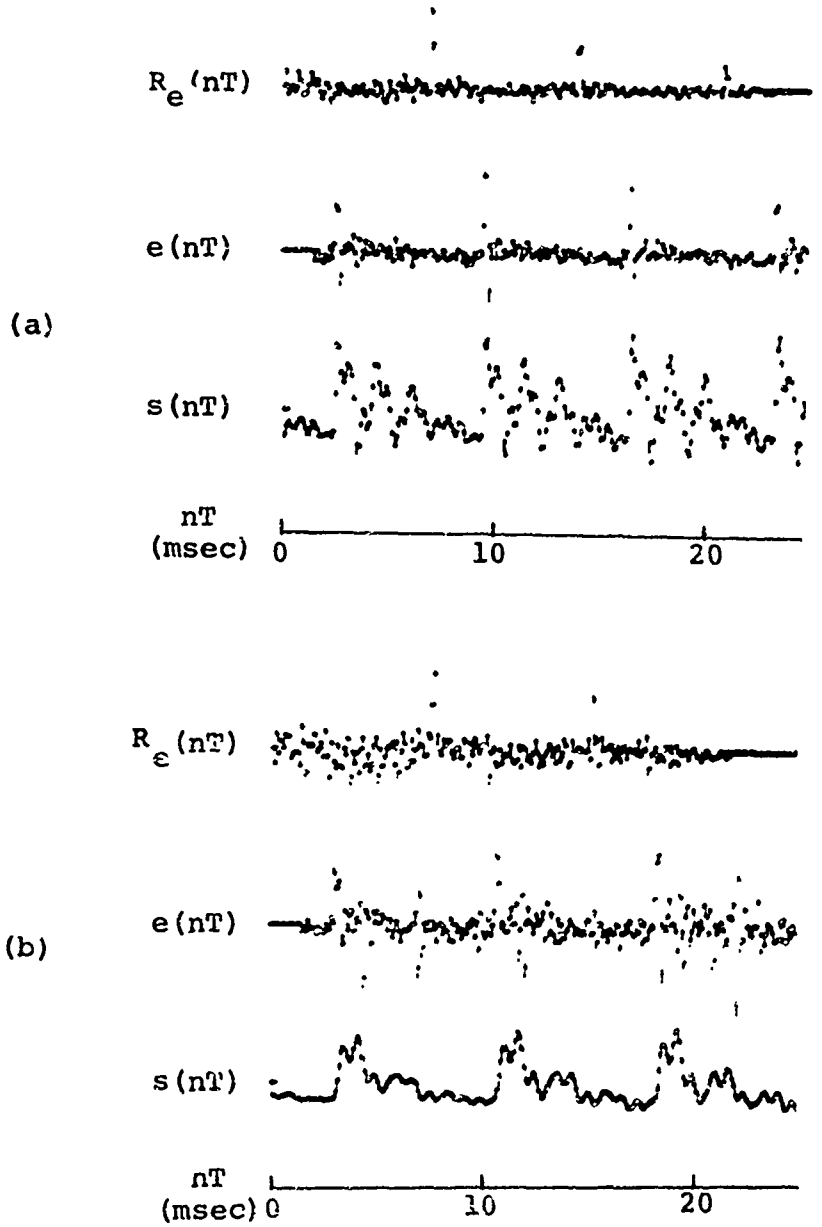

Fig. 6-1. Analysis of error signal for pitch extraction.
(a) The vowel [æ] in "potassium".
(b) The liquid [r] in "rubidium".

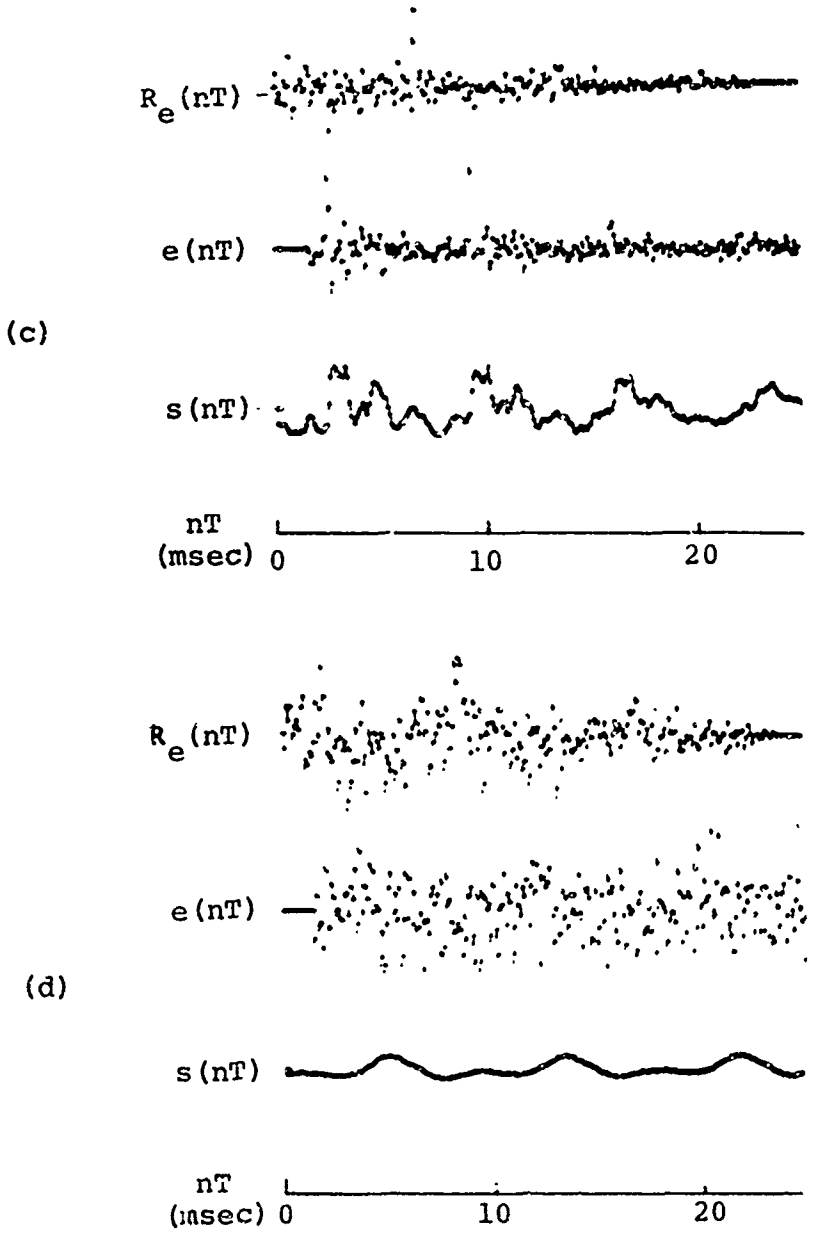

Fig. 6-1. (Cont'd) Error signal analysis for pitch extraction.
(c) The [æ]-[s] transition in "potassium".
(d) The voicing in the voiced stop [b] in "rubidium".

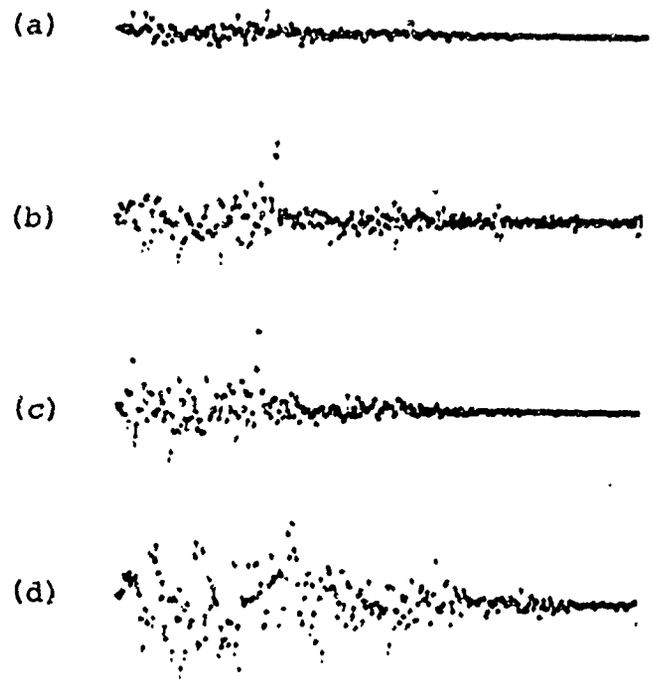

Fig. 6-2. Error autocorrelation functions $R_e(nT)$ for the same four frames shown in Fig.6-1, except thac the error signal here is obtained from the windowed signal.

and $$|E(\omega)|^2 = |S(\omega)|^2 \, |H(\omega)|^2$$

$$= \frac{P(\omega)}{A^2 \, \hat{P}(\omega)} \quad , \qquad (6\text{-}3)$$

where $P(\omega)$ is the power spectrum of the windowed signal, $\hat{P}(\omega)$ is the power spectrum corresponding to $\hat{S}(\omega)$, and A^2 is the minimum error in (3-37). $P(\omega)$ and $\hat{P}(\omega)$ are computed via the FFT, as described in Appendix C. Then, (6-2) is computed by an inverse FFT. (Note that if the speech signal is N samples long, then one should append at least an equal number of zeros and compute 2N-point FFT's, in order to obtain the complete autocorrelation function.)

We mentioned earlier that the error signal e(nT) for a voiced sound should exhibit impulses that correspond to the pitch pulses. The error signal in Fig. 6-1a shows a typical case where the prominent peaks can be associated with pitch pulses. The corresponding error autocorrelation function shows a sharp peak at a lag equal to the pitch period. Although Fig. 6-1a is quite typical for many voiced sounds, there exist a number of important exceptions. Fig. 6-1b shows an error signal with more than one peak within a single pitch period. (The prominent peak is associated with excitation due to closing of the glottis while the secondary peak in the middle of the pitch period can be associated with excitation due to the opening of the glottis.) The error autocorrelation in Fig. 6-1b still shows a prominent peak at the pitch period.

An important case is shown in Fig. 6-1c during a vowel-consonant transition. As the voicing decays, the pitch pulses seem to disappear. The same is true during consonant-vowel transitions. During both types of transitions the sound is clearly voiced, yet the error signal does not show any prominent peaks that could be associated with pitch pulses. Fig. 6-1d shows the same phenomenon during the voicing in a voiced stop. (Note that e(nT) in each example has been normalized to the maximum error in that frame. That is why e(nT) in Fig. 6-1d seems to be excessively large compared to the other examples; in reality it is not.) The above-mentioned cases have in common the fact that the signal is not rich in harmonics as is normally the case during sustained vowels. Another way of stating this is that the signal tends to become sinusoidal in nature in those cases. This is very evident for s(nT) in Fig. 6-1d. Now, the linear prediction model works very well for sinusoidal signals. In fact, a pure sine wave can be generated digitally with each sample being equal to a linearly weighted summation of the preceeding two samples, and this can go on indefinitely in time. Therefore, for a sine wave, the linear prediction error signal would be zero for all time (except for the very first sample), and there would exist no pulses to delineate pitch periods. The implication for cases such as in Figs. 6-1c and 6-1d is that the error signal ceases to be a good source for measuring pitch. All is not lost, however, because pitch can now be

estimated from the signal s(nT) itself, since it is quasi-sinusoidal. This can be done by any number of ways, including peak picking of the signal itself or its autocorrelation. (Note in Fig. 6-1d that although e(nT) is very erratic, the autocorrelation $R_e(nT)$ still exhibits a peak at the pitch period.) It is clear from Fig. 6-2 that the autocorrelation of the error signal obtained from the windowed speech signal can also be used for pitch extraction.

In summary, pitch can be extracted in most cases from either the error signal or its autocorrelation. In cases where the speech signal is not rich in harmonics, pitch can be extracted directly from the speech signal or its autocorrelation. The combination of methods to use depends on the properties of the signal as well as on the specific application.

The examples shown in Fig. 6-1 were obtained using the Autocorrelation method. The same sounds when analyzed using the Covariance method did not show any significant deviation in the error signal or its autocorrelation. This was also true for all the sounds we have examined thus far.

6.2 Formant Analysis

In an analysis-synthesis system using linear prediction, where the synthesizer is of the form shown in Fig. 2-1b, it is necessary to know the values of the predictor coefficients a_k, but it is

not necessary to know the poles of the filter $\hat{S}(z)$ which is shown in Fig. 2-1a and given below (except perhaps to check for possible instability of the filter):

$$\hat{S}(z) = \frac{A}{1 - \sum_{k=1}^{p} a_k z^{-k}} . \qquad (6\text{-}4)$$

However, for applications such as speech recognition and formant synthesis, it is necessary to compute the poles of $\hat{S}(z)$ in order to be able to deduce the formants of the vocal tract. The poles of $\hat{S}(z)$ can be computed by setting the denominator of $\hat{S}(z)$ in (6-4) to zero and solving the resultant polynomial equation in z for its roots. (We have successfully used a variation on the POLRT routine in the IBM Scientific Subroutine Package, 1968. The variations included elimination of all double precision computations, raising error tolerances, and modifying the starting point for each root to be a random point on the unit circle.) Since the coefficients a_k are real, some or none of the roots are real and the rest are complex conjugate pairs. Conversion to the s-plane can be achieved by setting each root $z_k = e^{s_k T}$, where $s_k = \sigma_k + j\omega_k$ is the corresponding pole in the s-plane. If the root $z_k = z_{kr} + jz_{ki}$, then:

$$\omega_k = f_s \arctan \frac{z_{ki}}{z_{kr}} \qquad (6\text{-}5)$$

$$\sigma_k = \frac{f_s}{2} \log (z_{kr}^2 + z_{ki}^2) \qquad (6\text{-}6)$$

where f_s is the sampling frequency.
In the s-plane the poles will also be either real or in complex conjugate pairs.

If the speech spectrum can be approximated by poles only, then the formants can be obtained from the poles of $\hat{S}(z)$ by noting that:

a) A formant consists of a pair of complex conjugate poles.

b) A formant normally has a high ratio between its frequency and bandwidth. Complex conjugate poles with very wide bandwidths can be regarded as contributing to general spectral shaping only.

c) The frequency range of a particular formant is usually known.

d) Peak picking can be performed on the approximate spectrum as a double check on the formant values.

e) Continuity of formant values from one spectral frame to another can always be invoked, keeping in mind that very fast formant transitions do exist in speech.

The extent to which the formant values thus obtained reflect the actual resonances of the vocal tract depends on at least the following factors:

a) Adequacy of the all-pole model.

b) Number of poles p.

c) Method of analysis (e.g. Autocorrelation or Covariance method).

d) Frame width: number of samples in one frame of the signal; and frame positioning (e.g. whether pitch synchronous or asynchronous, etc.).

Ideally, these factors would be taken into consideration separately for each frame of interest. However, this can be very expensive computationally, so in practice, tradeoffs are made between cost and reliability of the desired results. We shall discuss briefly the above-mentioned factors and point out some of these tradeoffs.

We wish to emphasize here that the discussion below applies to the Covariance as well as the Autocorrelation method, unless specifically stated otherwise.

6.21 Adequacy of the All-Pole Model

This issue has already been discussed in Section 2.3. We have argued there that the all-pole model seems be quite adequate for speech synthesis. The question here is the adequacy of the model for formant extraction. For the purposes of speech recognition, for example, one would ideally want to be able to compute the transfer function of the vocal tract. This means that the antiformants as well as the formants may be needed. It is reasonable to assume that the all-pole model would be adequate for formant extraction of vowels. (This assumption is based on another

assumption, namely that the glottal spectrum and radiation can be approximated by poles only.) However, for sounds such as nasals and fricatives, whose spectra are known to have antiformants, the all-pole model might not yield accurate results for the resonances of the vocal tract. Figure 6-3 shows the signal spectrum and the linear prediction spectrum (p=14) for the second [n] in the word "anyone" for a male speaker. The problem in looking at a spectrum like this is in deciding where the formants and antiformants are. There is no good way of making this decision in general, unless one has some knowledge about the system that produced the signal whose spectrum is under analysis. In fact, the spectral fit in Fig. 6-3 is very adequate, and it is quite reasonable to assume that some all-pole system has those characteristics. However, from our knowledge of the acoustics of the human speech production system, we know that if the spectrum in Fig. 6-3 is that of the sound [n], it must have zeros as well as poles. But even if we knew this, how would the linear prediction all-pole approximation help us in determining the values of the formants and antiformants? Some of the poles will correspond approximately to nasal formants, which can be obtained as described earlier in this section, but we know of no simple manner in which the antiformants can be determined from the poles of the linear prediction spectrum. The problem is that the same poles must approximate the effects of both the formants and the antiformants. This is clear from the fact that the

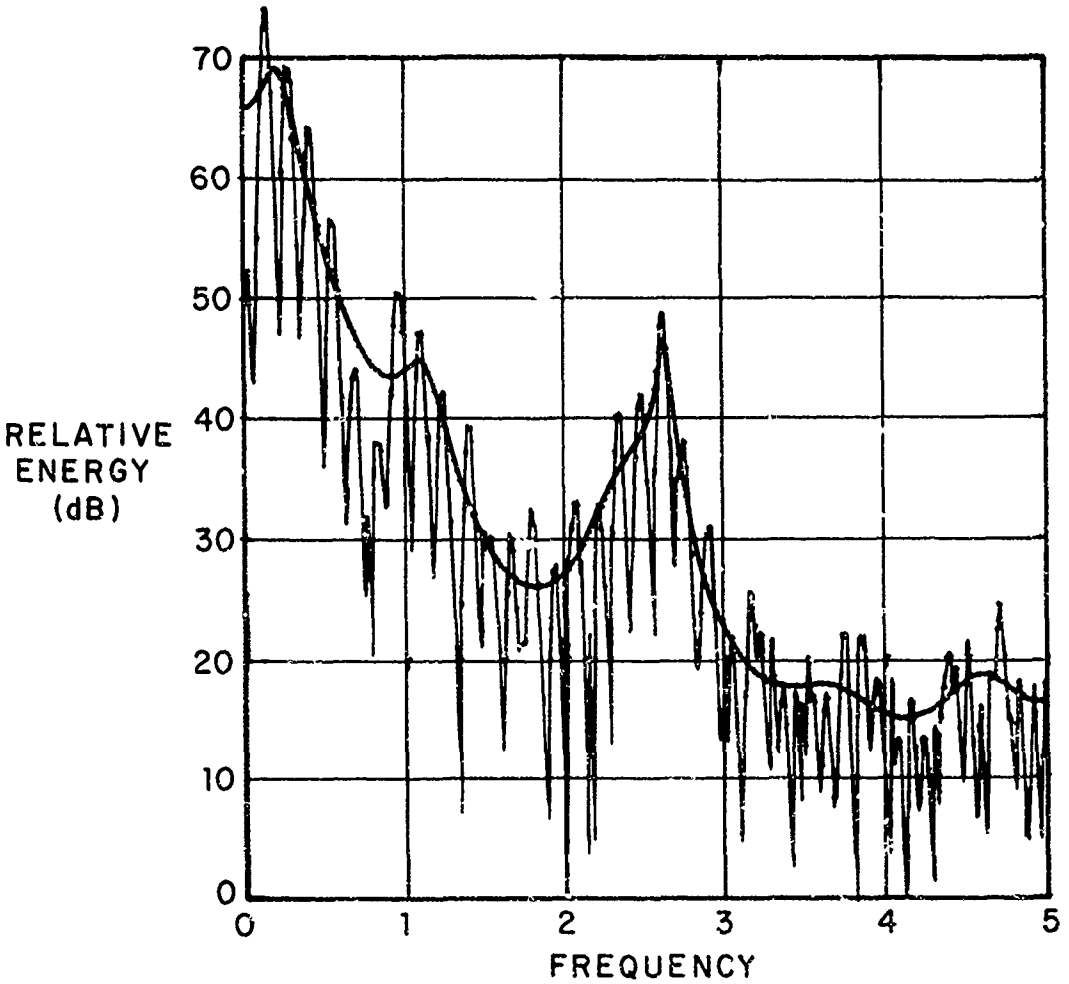

Fig. 8-3. Signal spectrum and linear prediction spectrum (p=14) for the second [n] in the word "anyone". Period of analysis is 25 msec.

linear prediction spectral matching process performs equally well at all frequencies irrespective of the shape of the speech spectral envelope (see Section 4.3). Another consequence is that the positions and more so the bandwidths of the extracted formants will often be very different from their "actual" values, depending on the position of each formant with respect to the antiformants. Formants that are far from the nearest antiformant are well approximated, while those that are close to an antiformant are often poorly approximated. A formant that is close to an antiformant can appear as a very wide-bandwidth peak which might go undetected. With nasals, the first formant is normally well approximated since it is separated from the nearest antiformant by at least one other formant. Other extracted formants may or may not be reliable depending on the speaker and the particular sound (i.e. in general unreliable). For example, in Fig. 6-3 the first and second formants seem to be adequately approximated. The third peak at 2.6 kHz is probably the fourth nasal formant. Between the second and fourth formants there should be a formant cluster, i.e. a cluster of two formants and one antiformant (see Section 2.4). The antiformant may be around 1.8 kHz, but it is not clear where the two formants are exactly.

Analysis of fricatives run into the same problems as nasals, if one is interested in determining the zeros as well as poles. At least the first two formants are heavily damped for all fricatives, due to neighboring antiformants. Pronounced formant peaks

at mid to high frequencies (2.5 - 6 kHz) occur for [s] and [š] only (Heinz and Stevens, 1961); these formants are usually attainable by linear prediction. Also, certain stop bursts, especially that of [k], are well represented. However, there is always the problem of pairing the formant peaks with the formant numbers, i.e. whether a particular peak corresponds to the third formant or the fourth formant, etc. This problem can be particularly important in speech recognition.

We have assumed in much of the above that one is interested in extracting most of the formants and antiformants for a particular sound. However, for speech recognition, all of this might not be necessary. For example, given a relatively weak voiced sound with a formant structure, such that the first formant is very low, and the spectral transitions to and from this sound are abrupt, one can safely recognize that as a nasal much of the time. Formant transitions to or from this nasal could then be used to determine the place of articulation of the nasal. All this can be done without knowing whether there are zeros or not in the spectrum under analysis. Similar considerations exist for the recognition of fricatives. However, a major problem arises with nasalized vowels. The introduction of zeros into a vowel spectrum can be disastrous. The reason is that we depend heavily on the exact positions and the bandwidths of the extracted formants for the recognition of the vowel, and the introduction of zeros plays havoc with the real formant frequencies and bandwidths. We know

of no good solution for this problem using the linear prediction model.

In the above we have seen that the linear prediction model is inadequate for the extraction of formants and antiformants from a spectrum containing zeros as well as poles. In these cases one could use other methods such as analysis-by-synthesis that includes zeros as well as poles in the approximate spectrum. Of course, one must first know whether the spectrum is likely to have zeros or not. This can be done from separate considerations, such as we have suggested above for the recognition of nasals. Therefore, one must first perform some form of class recognition on the sound under analysis. If that sound is recognized to be, say, a nasal or a fricative, then the alternate analysis-by-synthesis method can be used. Similarly, if a vowel is next to a nasal, one can assume that the vowel might be nasalized, then resort to the other method to determine formant positions more accurately.

6.22 Optimum Number of Poles p

Assuming that the all-pole model is adequate for a particular speech segment, the confidence and accuracy in relating certain poles of the linear prediction model to actual resonances of the vocal tract depends to a good extent on the total number of poles p. If the value of p is too small, there may not be enough poles to represent all the resonances in the frequency range of

interest. On the other hand, if p is too large, there will be extraneous poles which might be mistaken for formants of the vocal tract. It is clear that between the two extremes, there must exist some value (or range of values) of p which is optimal for the accurate extraction of formants. In fact, the value of p should be set such that the linear prediction transfer function $\hat{S}(z)$ approximates the transfer function of the vocal tract (including the effects of the glottal flow and radiation). We have seen from the last two chapters that this approximation occurs in the power spectral domain. Namely, the linear prediction spectrum $\hat{P}(\omega)$ (or 2D-spectrum $\hat{Q}(\omega,\omega')$) approximates the signal spectrum $P(\omega)$ (or 2D-spectrum $Q(\omega,\omega')$). In particular, we want the linear prediction spectrum to approximate the envelope of the signal spectrum. (Hereafter, the word "spectrum" will refer to both the one-dimensional stationary spectrum used in the Autocorrelation method and the two-dimensional nonstationary spectrum used in the Covariance method.) What we are claiming is the following:

> **A value of p that results in an optimal spectral envelope fit, also results in an optimal number of poles many of which can be related, with good confidence and accuracy, to the resonances of the vocal tract.** (6-7)

That is, the optimal value of p gives the best confidence and accuracy relative to that obtained by other values of p. The remaining question is how to find this optimal value for p.

The reader is referred to Section 5.6 where the optimal p is deduced from the normalized error curve. There, the discussion was restricted to the Autocorrelation method. Here we shall extend the results of Section 5.6 to the Covariance method as well. We shall define the normalized error V_p in the Covariance method as equal to

$$V_p = \frac{E_p}{\phi_{00}} = 1 - \sum_{k=1}^{p} a_k \frac{\phi_{0k}}{\phi_{00}} \quad \text{(Covariance Method)} \quad (6\text{-}8)$$

where E_p is the minimum total-squared error in (3-19), and ϕ_{00} is the energy in N samples of the signal. We have found that the behavior of V_p in the Covariance method is very similar to that in the Autocorrelation method. In both methods the error curve exhibits a "knee" after which the curve slopes down at a slow rate. The optimal value of p is that point where the error curve begins to fall off slowly. This method has been corroborated by informal observations. However, we have seen that the bandwidths of the resulting formants were less accurate and more variable than the formant frequencies.

Statement (6-7) and the above procedure for finding the optimal value for p are correct only if the all-pole model is adequate. For purposes of speech synthesis this is generally the case. However, as we have seen above, if relatively accurate formant (or antiformant) information is needed, then the all-pole model is not adequate for sounds with antiformants, such as

nasals and fricatives. In these cases it is not clear how one would choose an optimal value for p, if such a value exists. We shall illustrate this problem by an example. Figure 6-4 shows the normalized error curve for the nasal [n] in the word "nickel" by the same speaker associated with Fig. 6-3. (The analysis was done using the direct Autocorrelation method, but the discussion here also applies to the Covariance method.) The point after which the error curve slopes down slowly is around p=12. For this value of p we show the approximate and signal spectra in Fig. 6-5. Only the first and fourth formants appear in the approximate spectrum. In the signal spectrum one can clearly see in addition two other formants between the first and fourth. In order for these two other formants to appear in the approximate spectrum we must increase the value of p. From Fig. 6-4 we see that at p=18 there is a noticeable decrease in the error curve from the value at p=12. We interpret such a change in the error curve as reflecting a correspondingly noticeable change in the approximate spectrum. This change is evident in Fig. 6-6 where the two formants between the first and fourth are now evident in the approximate spectrum. Unfortunately, this caused side effects around the first formant and at high frequencies. The position of the first peak moved closer to that of the first harmonic and another wide bandwidth pole was introduced next to it; it is no longer clear where the first formant really is. At frequencies higher than 3 kHz it

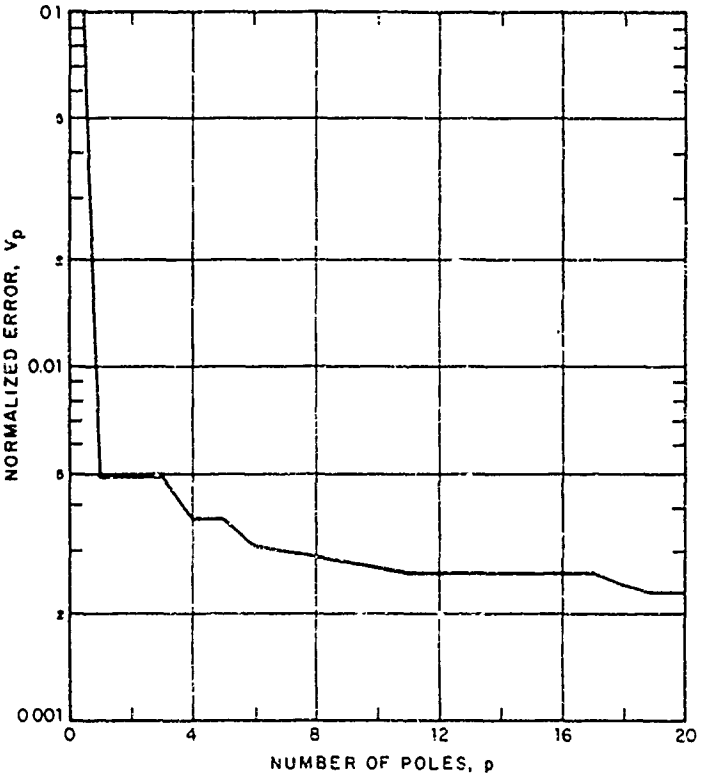

Fig. 6-4. Normalized error curve for [n] in the word "nickel". Window width is 25 msec, 10 kHz sampling.

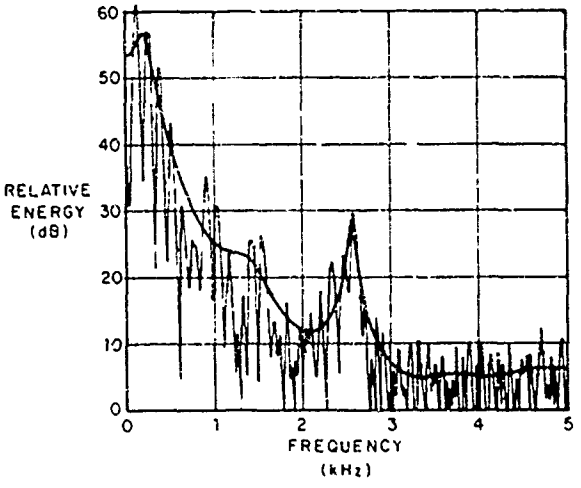

Fig. 6-5. Approximate spectrum (p=12) and signal spectrum for [n] in the word "nickel".

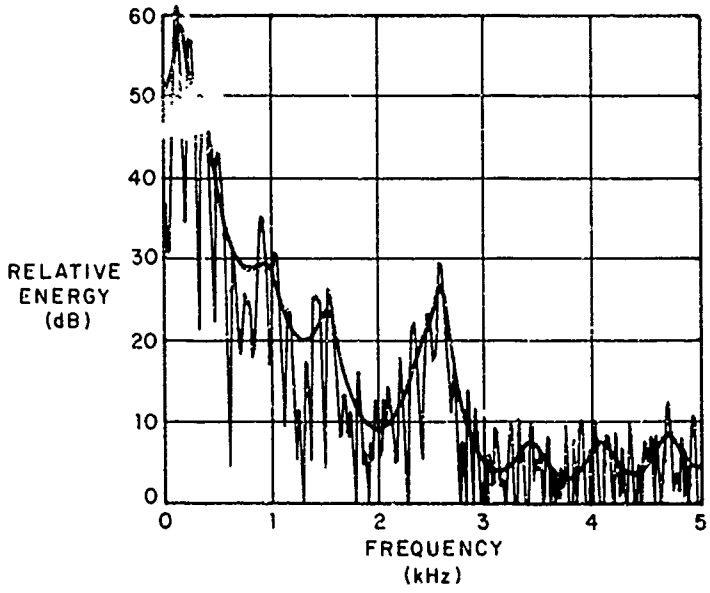

Fig. 6-6. Approximate spectrum (p=18) and signal spectrum for [n] in the word "nickel".

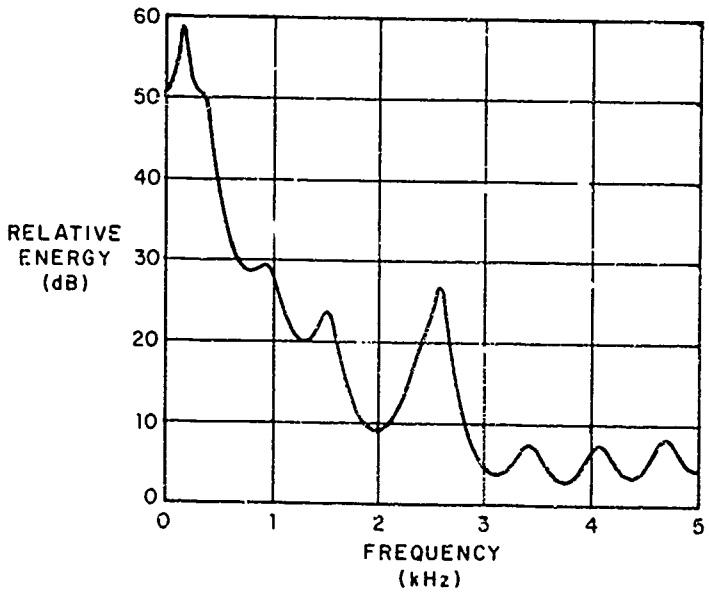

Fig. 6-7. Linear prediction spectrum (p=18) using the Covariance method for [n] in the word "nickel".

looks as if we have three extra peaks, which most probably do not correspond to actual resonances of the nasal tract, since that region of the spectrum is at the noise level. In summary, in order to have the linear prediction spectrum show the formants evident on the signal spectrum, there are two problems: (a) one must somehow determine the necessary value of p, and (b) even if that value of p is known, the results of the formant extraction may or may not correspond to resonances of the speech production mechanism, depending on the particular sound.

6.23 Method of Analysis

From a purely theoretical point of view, the assumptions underlying the Covariance method are superior to those underlying the Autocorrelation method. The Covariance method assumes that the signal in the frame of interest is nonstationary, while the Autocorrelation method assumes that the signal is stationary. Speech is a nonstationary process and therefore the assumption of nonstationarity is superior to that of stationarity. However, in any single frame of interest, the signal can be considered to be quasi-stationary. In that case, the assumption of stationarity is not a bad one, but the assumption of nonstationarity is still a better one.

It can be shown that if a signal is generated from an all-pole source, the Covariance method can recover these poles exactly

by using only a finite number of samples of the signal (Portnoff, Zue and Oppenheim, 1972). The same is not true for the Autocorrelation method unless the infinite signal is considered. However, very good approximations to the poles can be obtained from only a finite portion of the signal. Our experience with real speech has been that if the period of analysis is on the order of a pitch period or greater, the poles resulting from both methods are very close to each other. For example, Fig. 6-7 shows the linear prediction spectrum (using the Covariance method) for the same conditions as those of Fig. 6-6.

Another point of comparison is in how the two methods compare in an analysis-synthesis system. Thus far we have not made such a comparison. However, Atal (personal communication) claims that the Covariance method produces higher quality speech in an analysis-synthesis system.

6.24 Frame Width and Position

In the speech production model in Section 2.1, we defined a frame as an interval of time within which the human vocal tract can be assumed to be fixed. This interval is usually on the order of 10-25 msec. A specific choice for a frame width and position depends on several factors:

(a) The type of signal to be analyzed.

(b) The application for the analysis.

(c) Whether one uses the direct or indirect method of analysis.

We shall be discussing the above three factors interchangeably, but first we must explain what we mean by the direct and indirect method of analysis. In Section 4.4 the terms "direct" and "indirect" were applied to the Autocorrelation method to refer to whether the autocorrelation coefficients were computed from a windowed signal, or from an apparent autocorrelation function which was computed from a finite portion of an unwindowed signal, respectively. In Section 4.6, the Covariance method was reformulated in an analogous manner into a direct and an indirect method. Therefore, the term "direct" implies that the signal has been appropriately windowed, i.e. the resulting signal is infinite in extent but is zero outside the frame of interest, while the term "indirect" refers to the fact that a finite unwindowed frame of the signal is used in the analysis without making any assumptions about the signal outside that frame. It so happens that the two popular methods defined in Chapter I are the direct Autocorrelation and indirect Covariance methods. However, we wish to emphasize here that the issue of direct versus indirect analysis is independent of the issue of Autocorrelation versus the Covariance method which we have already discussed. One important issue that faces the direct method is a proper choice of the window to be used in each case.

There are instances during the analysis of a speech utterance when the frame position and width are critical factors and must be chosen judiciously. For example, in analyzing a stop burst, it

is best to have the frame positioned to include the burst and nothing more. During rapid transitions (such as certain vowel-nasal transitions), the frame width should be small enough so that the sharp transition can be detected. In general, the frame width and position should be chosen such that the assumption that the vocal tract is fixed during that time interval remains valid.

For fricatives, the frame width and position are not critical factors in the analysis. Thus, any "effective" frame width on the order of 10-25 msec can be used with generally similar results. (The effective frame width is discussed in Section 6.242.) On the other hand, for sonorants, the frame width and position can be important factors, depending on the particular application for the analysis. Below, we shall restrict the discussion to the analysis of sonorants. It is hoped that from the method of presentation one can extrapolate the results to other situations. We shall differentiate between two major types of analysis: pitch-synchronous and pitch-asynchronous.

6.241 Pitch-Synchronous Analysis

Pitch-synchronous analysis implies that one is somehow able to detect pitch, and then delineate each pitch period for analysis. (For example, one could perform a pitch-asynchronous analysis and detect pitch pulses, as in Fig. 6-1a, then reanalyze intervals between adjacent pitch pulses.) Let us assume for the moment that

the frame of analysis is defined to be the whole pitch period. This case is of special interest because a pitch period represents (approximately) the impulse response of the combined effects of the glottal source, the vocal tract and radiation. The word "approximately" was used because the signal in a pitch period includes contributions (though small) from past vocal tract excitations whose effects have not completely decayed as yet. These contributions increase with increased pitch (i.e. shorter pitch period, as for females and children) causing the approximation to be worse. This is a basic loss of information that cannot be recovered without adding some compensatory information. We shall resort to the frequency domain to explain what we mean by the last statement. The impulse response under discussion is theoretically infinite (though practically it dies within 30 msec), and its power spectrum is a continuous function of frequency. The power spectrum of the response due to a periodic train of unit pulses, at a rate of F_0 pulses per second, contains energy only at multiples of the fundamental, i.e. at $f=nF_0$. This discrete spectrum has an infinity of possible envelopes. Two of these envelopes are the impulse response spectrum and the spectrum of a single pitch period. In other words, the pitch period spectrum is guaranteed to be equal to the impulse response spectrum only at multiples of F_0. To the extent that the pitch period spectrum is not equal to the impulse response spectrum for $f \neq nF_0$, we say that information

has been lost. It is easy to see that as F_0 increases, the loss of information is likely to increase. It is in this sense that female or children's speech (with higher pitch), relatively speaking, contains less information about the response of the articulatory mechanism than does male speech (with lower pitch). This loss of information is irrecoverable unless extra information is supplied from an independent source. We shall argue that linear prediction supplies extra information which hopefully recovers part of the information lost.

Given the spectrum of a single pitch period, the problem is to estimate the spectrum of the impulse response. In linear prediction the information takes the form of an assumption about the nature of the impulse response spectrum, namely that it is all-pole. To the extent that the all-pole model is correct, we have succeeded in adding the needed compensatory information. Thus, recovery of lost information is bound to be more successful with vowels (which are well modelled by poles) than with nasals (which are best modelled by a combination of poles and zeros). Supplying additional information by judiciously assuming a model is the basic idea and power behind the general method of spectral analysis-by-synthesis. Linear prediction is a special case of analysis-by-synthesis where the assumed model is restricted to be all-pole.

We conclude from the above discussion that if one wishes to use the direct method of analysis over a pitch period, then the

window to be used should be rectangular and should coincide in position and width with the pitch period under analysis. In other words, the samples over a pitch period should be left intact. Any window other than rectangular will introduce unwanted distortion in the signal spectrum and consequently in the linear prediction spectrum approximating the impulse response spectrum.

Thus far we have assumed that the frame for analysis consists of the whole pitch period. There are applications for which it is desirable to perform the analysis on only a portion of the pitch period. The portion of the signal during which the glottis is closed is of particular interest. It is well known that the major excitation of the vocal tract occurs at the closing of the glottis. Thus, during the first portion of a pitch period the glottis is closed. The vocal tract is excited again as the glottis opens, but to a lesser degree. The vocal tract resonances are different in the closed- and open-glottis conditions. When the glottis is closed, the subglottal tract is decoupled from the system and the resonances are those of the vocal tract proper. When the glottis is open, there is coupling to the subglottal tract, thus causing changes in the over-all system resonances. In particular, bandwidths tend to be larger when the glottis is open. Coupling to the subglottal tract could also introduce extra zeros and poles in the signal spectrum. By analyzing the whole

pitch period, one is actually averaging out the closed- and open-glottis characteristics. The result is often reflected in variability of the formant bandwidths and, to a lesser extent, the formant frequencies. Therefore, in order to obtain accurate formant information for the vocal tract, it is best to perform the analysis on the portion of the signal when the glottis is closed (see Pinson, 1963). The problem here is to know when the glottis is closed in relation to the signal. The only thing we are sure of is that the glottis is closed during the first portion of the pitch period. This interval can be anywhere between zero to a few milliseconds, depending on the condition of phonation. Although we cannot be sure of the glottis condition it would still be more accurate, on the average, to analyze the first portion of the pitch period than to analyze the whole pitch period.

Analyzing a portion of the pitch period is best done using the indirect method. The direct method is bound to give gross errors (see the discussion on windowing below). We note here that the indirect Covariance method as well as one of the indirect Autocorrelation methods require a minimum interval of analysis equal to 2p samples, where p is the number of predictor coefficients.

6.242 Pitch-Asynchronous Analysis and Windowing

As "pitch-asynchronous" suggests, the frame width and position are here independent of pitch information. This poses no serious problems if the indirect method is used, and the results would vary little from those obtained using pitch-synchronous analysis, especially if the frame width is on the order of a pitch period or larger. However, if the direct method is to be used, the results could vary a great deal depending on the frame width and the window shape used. We shall now discuss the problem of windowing in the direct method of analysis. The discussion will be detailed and rigorous because we feel that the subject of windowing has not been treated with enough rigor in the past, when applied to speech analysis.

In discussing pitch-synchronous analysis with the direct method, we saw that a rectangular window over the whole pitch period is best, because we are then certain that the signal spectrum would equal the impulse response spectrum at least at multiples of the fundamental frequency F_0. The best we can hope for in pitch-asynchronous analysis is that the signal spectrum approximate, as well as possible, the spectral values of the impulse response spectrum at $f=nF_0$. This is the purpose of windowing. We shall again resort to the frequency domain to show how our objective can be accomplished by proper windowing. For simplicity, the discussion will be carried on for continuous time

signals, but the results will apply also to discrete or sampled signals.

Let $x(t)$ be a periodic signal with period $\tau = \frac{1}{F_0}$ and Fourier integral transform $X(f)$. Let $s(t)$ be the signal obtained by multiplying $x(t)$ by a window function $w(t)$:

$$s(t) = w(t)\, x(t). \tag{6-9}$$

Then the Fourier transform of $s(t)$ is the convolution of the transforms of $w(t)$ and $x(t)$:

$$\begin{aligned} S(f) &= W(f) \otimes X(f) \\ &= \int_{-\infty}^{\infty} W(f-\lambda)\, X(\lambda)\, d\lambda, \end{aligned} \tag{6-10}$$

where $S(f)$ and $W(f)$ are the Fourier Transforms of $s(t)$ and $w(t)$, respectively, and the symbol $\otimes$ represents convolution.
Since $x(t)$ is a periodic signal, its Fourier transform $X(f)$ is a line spectrum that can be represented by

$$X(f) = \sum_{n=-\infty}^{\infty} Z(f)\, u_0(f-nF_0), \tag{6-11}$$

where $u_0(f)$ is the unit impulse function defined in (4-40), and $Z(f)$ is some envelope function whose values are specified at $f = nF_0$, but can be arbitrary otherwise. (For example, one

can think of Z(f) as the transform of the impulse response of the vocal tract, or as the transform of a single pitch period. The two transforms are equal at $f=nF_0$.)

Substituting (6-11) in (6-1[illegible] performing the integration, and replacing n by m, we obtain:

$$S(f) = \sum_{m=-\infty}^{\infty} W(f-mF_0)\ Z(mF_0), \tag{6-12}$$

and

$$S(nF_0) = \sum_{m=-\infty}^{\infty} W(nF_0-mF_0)\ Z(mF_0). \tag{6-13}$$

Our objective is to specify possible window functions such that

$$S(nF_0) = Z(nF_0), \text{ for all } n, \tag{6-14}$$

or as nearly so as possible. This is equivalent to our earlier statement saying that the signal spectrum should equal the impulse response spectrum at $f=nF_0$.

If s(t) consists of an integral number of pitch periods, M, then it is well known that S(f) satisfies (6-14). This can be seen by noting that s(t) in that case is equivalent to multiplying x(t) by a rectangular window whose width is equal to M pitch periods. The rectangular window is given by:

$$w(t) = \begin{cases} \frac{1}{M\tau}, & |t| \le \frac{M\tau}{2}, \\ 0, & \text{otherwise}, \end{cases} \tag{6-15}$$

and $$W(f) = \frac{\sin(\pi Mf/F_0)}{\pi Mf/F_0} . \qquad (6\text{-}16)$$

Substituting (6-16) in (6-13), we obtain:

$$S(nF_0) = \sum_{m=-\infty}^{\infty} \frac{\sin[\pi M(n-m)]}{\pi M(n-m)} Z(mF_0). \qquad (6\text{-}17)$$

Note that the window term in (6-17) is equal to zero for all values of m except for m=n, when it is equal to 1. Therefore, (6-17) reduces to

$$S(nF_0) = Z(nF_0) , \qquad (6\text{-}18)$$

which is identical to (6-14). Therefore, (6-14) is exactly satisfied for a rectangular window whose width is equal to an integral number of pitch periods. In particular, it is true for a single pitch period, a result that we already know.

The above result clearly satisfies (6-14), which is our objective, but it suffers from one major drawback, namely that the window depends on the exact length of a pitch period. Thus, it is really a pitch-dependent window, which is of little use in pitch-asynchronous analysis. We need a pitch-asynchronous window, one whose width does not depend on the exact length of the pitch period, and which satisfies (6-14) as well as possible.

We note again that what allowed us to reduce (6-17) to (6-18) was the important fact that the window term was equal to zero for all values of m except for m=n, when it was equal to 1. In other words, we have $W(0)=1$, and $W(nF_0)=0$ for all n. If we could find window functions such that $W(0)=1$ and $|W(nF_0)|<\varepsilon$ for all n, where $\varepsilon<<1$, then (6-14) would be approximately satisfied. Going further, if $|W(f)|<\varepsilon$ for all $f\geq F_0$, then clearly $|W(nF_0)|<\varepsilon$ is satisfied, and our objective is also achieved. A value of W(0) different from 1 merely introduces a multiplicative constant to (6-14), which can be easily corrected for. What is important in specifying a window is the relative amplitude of W(f) with respect to W(0). Therefore, our only condition that a window function must satisfy is:

$$\left|\frac{W(f)}{W(0)}\right|<\varepsilon \ , \quad |f|\geq F_0 \ , \ \varepsilon<<1 \ . \tag{6-19}$$

One often picks $\varepsilon\leq 0.02$ for good results. This is equivalent to W(f) being at least 34 dB below the peak W(0) for $f>F_0$. We shall now give a few examples of window functions that have been suggested. These functions have the property that they are even functions of time. Although this property is not required for our application, it clearly does no harm.

There are two major families of window functions that are in use today. The first is what we shall call the Cosine family.

These functions are raised cosines or convolutions of raised cosines. The two most popular Cosine window functions are the Hanning and Hamming windows (Blackman and Tukey, 1958, pp. 95-99). These are given by:

$$\underline{\text{Hanning}}: \quad w_H(t) = \frac{1}{2T_w}\left(1+\cos\frac{\pi t}{T_w}\right) u_{-1}\left(1-\frac{|t|}{T_w}\right), \tag{6-20}$$

$$\underline{\text{Hamming}}: \quad w_h(t) = \frac{1}{1.08T_w}\left(0.54 + 0.46\cos\frac{\pi t}{T_w}\right) u_{-1}\left(1-\frac{|t|}{T_w}\right), \tag{6-21}$$

where $$\tau' = 2T_w \tag{6-22}$$

is the <u>window size</u> or <u>width</u>, and $u_{-1}(x)$ is the unit-step function defined by:

$$u_{-1}(x) = \begin{cases} 0 \ , & x<0, \\ 1 \ , & x\geq 0. \end{cases} \tag{6-23}$$

Both windows in (6-20) and (6-21) have been normalized such that $W(0)=1$.

The other major family of window functions is what we shall call the SINC^n family, because their Fourier transforms are of the form $\left(\frac{\sin \pi x}{\pi x}\right)^n$, and the function $\frac{\sin \pi x}{\pi x}$ is often referred to as sinc x. This family is generated in the time domain by (n-1) convolutions of the rectangular window, with the appropriate normalization to keep the window size equal to τ'. This family is

represented in the frequency domain by:

$$W_n(f) = \left[\frac{\sin(2\pi f T_w/n)}{2\pi f T_w/n}\right]^n , \qquad (6\text{-}24)$$

where n is the order of the window. Thus, $W_1(f)$ is the rectangular window, $W_2(f)$ is the triangular, etc. It has been shown that the corresponding time domain window $w_n(t)$ is given by (Makhoul, 1970a):

$$w_n(t) = \frac{(n/2)^n}{T_w(n-1)!} \sum_{k=0}^{\left[\frac{n-1}{2}\right]} (-1)^k \binom{n}{k} \left(1-\frac{2k}{n} - \frac{|t|}{T_w}\right)^{n-1} u_{-1}\left(1-\frac{2k}{n} - \frac{|t|}{T_w}\right), \qquad (6\text{-}25)$$

where n is any positive integer,

$$\binom{n}{k} = \frac{n!}{k!\ (n-k)!}$$

and $\left[\frac{n-1}{2}\right] \equiv$ integer portion of $\frac{n-1}{2}$.

A window that is of particular interest is $w_4(t)$, which is sometimes called the Parzen window, given by:

$$w_4(t) = \frac{8}{3T_w}\left[\left(1-\frac{|t|}{T_w}\right)^3 u_{-1}\left(1-\frac{|t|}{T_w}\right) - 4\left(\frac{1}{2}-\frac{|t|}{T_w}\right)^3 u_{-1}\left(\frac{1}{2}-\frac{|t|}{T_w}\right)\right]. \qquad (6\text{-}26)$$

In order to see how (6-19) might apply, we shall discuss three windows: the rectangular, Parzen, and Hamming windows.

The three windows are shown in Fig. 6-8, along with a summary of their spectral characteristics. A plot of the power spectrum for each window is shown in Fig. 6-9. We shall first discuss the Hamming window spectrum shown in Fig. 6-9b. We note that for $f \geq 2f_0$, $|W_h(f)|$ is at least 40 dB below $W_h(0)$, and hence (6-19) will apply with $\varepsilon = .01$ if the following condition holds:

$$2f_0 \leq F_0 \ , \tag{6-27}$$

where

$$f_0 = \frac{1}{\tau'} = \frac{1}{2T_w} \ , \tag{6-28}$$

and

$$F_0 = \frac{1}{\tau} \ .$$

(τ is the pitch period and τ' is the window size.)
From (6-27) and (6-28) we obtain the desired relation:

$$\tau' \geq 2\tau \ . \qquad \text{(Hamming)} \tag{6-29}$$

(6-29) says that in order to guarantee that the signal spectrum be very nearly equal to the impulse response spectrum for $f = nF_0$, the window size τ' must be at least twice the pitch period. Since we know the general range of pitch periods for human voices, it is easy to satisfy (6-29) most of the time. As a rule of thumb, when using a Hamming window, a window size of at least 20 msec should give good results (this corresponds to τ = 10 msec).

The same analysis can be applied to the Parzen window spectrum

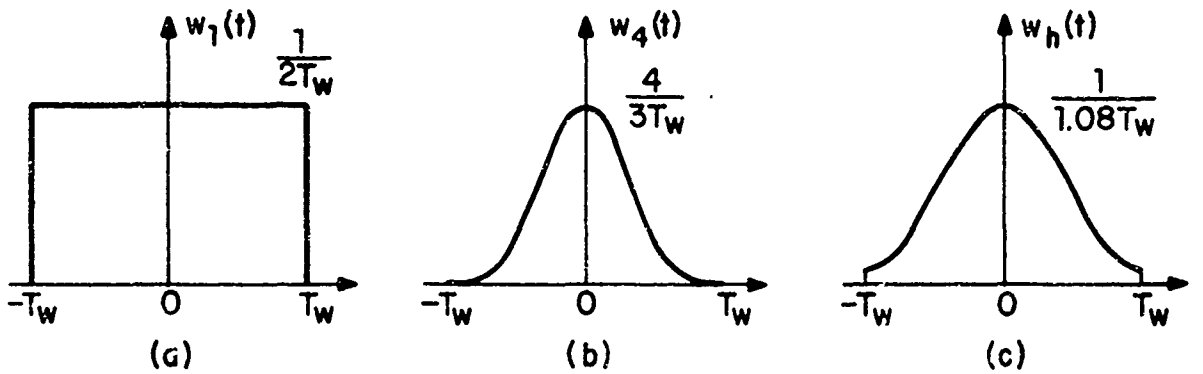

WINDOW	3 dB BANDWIDTH	LARGEST SIDELOBE RELATIVE TO MAIN LOBE	HIGH-FREQUENCY ROLL-OFF
RECTANGULAR	0.9 f_0	−13.3 dB (1st SIDELOBE)	−6 dB/OCT
PARZEN	1.8 f_0	−53.1 dB (1st SIDELOBE)	−24 dB/OCT
HAMMING	1.33 f_0	−43 dB (4th SIDELOBE)	−6 dB/OCT

(d)

Fig. 6-8. (a) Rectangular window.
(b) Parzen window.
(c) Hamming window
(d) Summary of spectral characteristics for the three windows. $f_0 = \frac{1}{\tau'} \approx \frac{1}{2T_w}$.

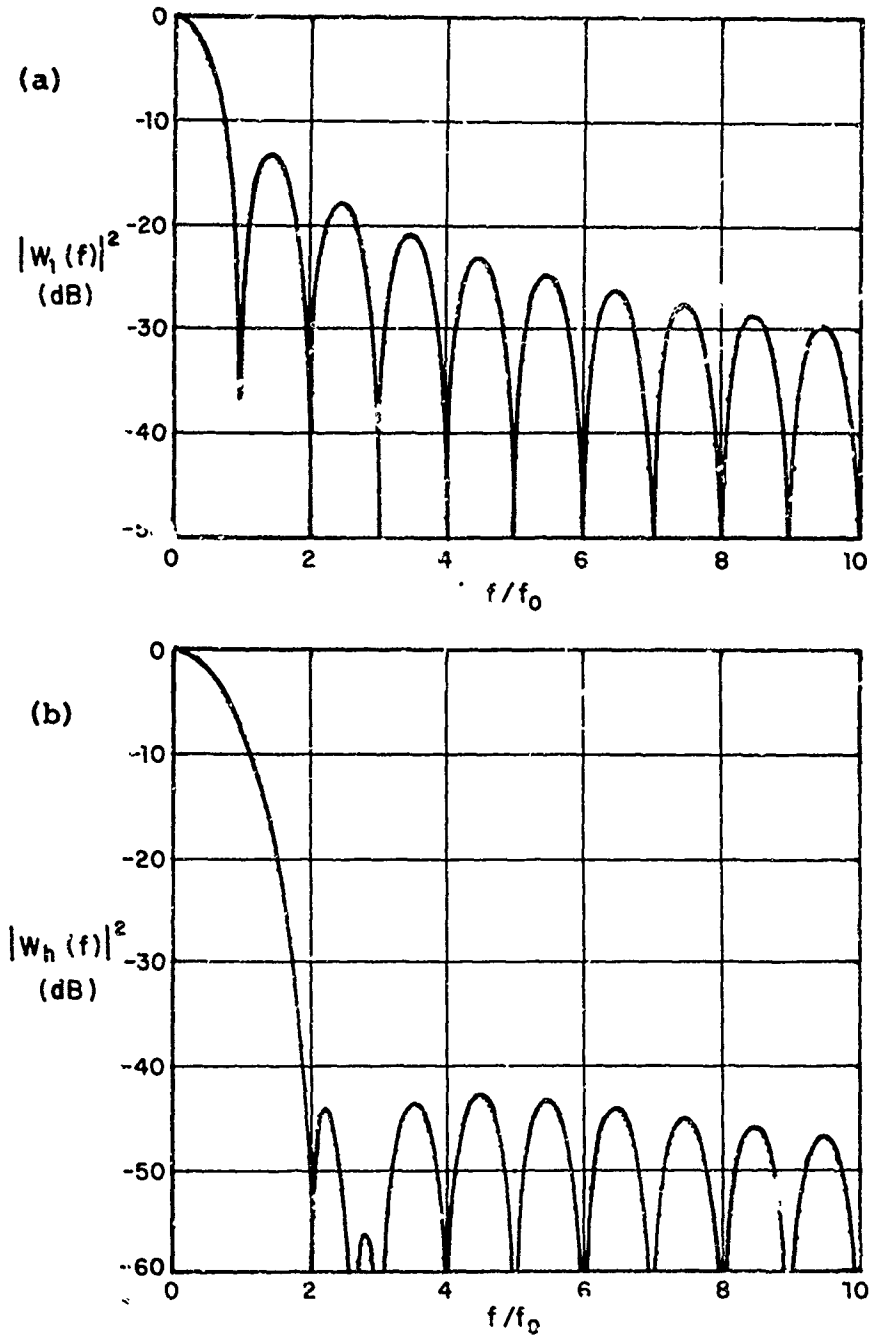

Fig. 6-9. (a) Power spectrum of rectangular window.
(b) Power spectrum of Hamming window.

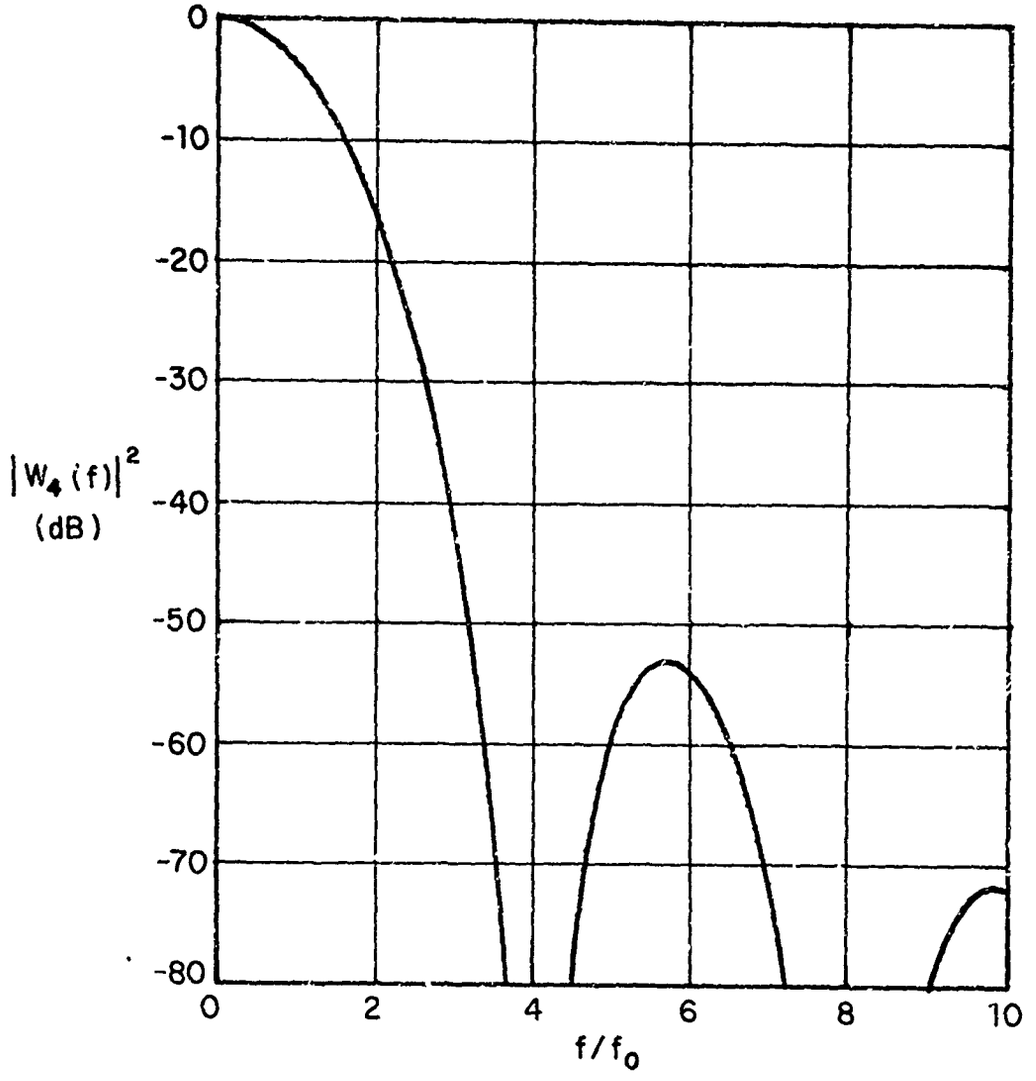

Fig. 6-9. (Cont'd)
(c) Power spectrum of Parzen window.

in Fig. 6-9c, and we obtain the relation:

$$\tau' \geq 3\tau \ , \quad \text{(Parzen)} \tag{6-30}$$

with $\varepsilon = .01$ (40 dB). This means that if the Parzen window is used, the window should equal at least three pitch periods if very good results are desired. Conditions (6-29) and (6-30) can be relaxed by about 20% with generally adequate results.

Returning to the power spectrum of the rectangular window in Fig. 6-9a, we see that (6-19) cannot apply with $\varepsilon = .02$ (34 dB) for $\frac{f}{f_0} \leq 10$. In fact, the best that can be achieved is an $\varepsilon = .03$ for $\frac{f}{f_0} \geq 10$. This is bad for two reasons: a) ε is on the high side, and therefore the approximation will be worse, and b) $\frac{f}{f_0} \geq 10$ means that $\tau' \geq 10\tau$, i.e. the window size is 10 times the pitch period, which is far greater than the frame size that our model allows (for good results). The best compromise is $\varepsilon = 0.1$ (20 dB) for $\frac{f}{f_0} \geq 4$. But this ε is quite high. The conclusion is that the rectangular window is not a good window for pitch-asynchronous analysis.

One conclusion we can draw from the above discussion is that the frame width should be on the order of at least 2 pitch periods if one is to obtain good results with pitch-asynchronous analysis using the direct method. This explains why analyzing a portion of a pitch period using the direct method is not recommended.

Below we shall make use of the notion of the "effective" width

of a window. Although an actual window width is equal to τ', its effective width is generally less than that, because the signal samples are weighted by the window. (We are assuming here that the area under the window is always constant and is equal to 1, i.e. $W(0) = 1$.) It is reasonable to assume that the effective width of a rectangular window is equal to its actual width τ'. We shall assume further that the effective width of any window is inversely proportional to its bandwidth. From the last two assumptions, we can define the effective width, τ_e', of a window to be equal to:

$$\tau_e' = \tau' \frac{B_1}{B} , \qquad (6\text{-}31)$$

where B_1 is the bandwidth of the rectangular window, and B is the bandwidth of the window whose effective width is desired. From Fig. 6-8d we see that $B_1 = 0.9f_0 = \frac{0.9}{\tau'}$. Substituting for B_1 in (6-31), we obtain:

$$\tau_e' = \frac{0.9}{B} ,$$

where B is measured in Hz and τ_e' in sec.

For example, the bandwidth of the Hamming window from Fig. 6-8d is $B = 1.33f_0 = \frac{1.33}{\tau'}$. From (6-31), $\tau_e' = 0.68\tau'$, and the effective width of a Hamming window is about two-thirds its actual width. We must stress here that (6-31) is but one of many other

reasonable definitions.

We have thus far discussed methods of windowing that would lead to good results when using the direct method. The question now is how the direct method compares with the indirect method in pitch-asynchronous analysis. In order to do the comparison fairly, the "effective" frame width for both types of analysis should be the same. We have already discussed above how to find the effective frame width in the direct method. In many formulations of the indirect method, the signal samples are weighted equally, hence the effective frame width is equal to the actual frame width. Therefore, if a Hamming window is used, for example, on a 20 msec frame, the effective frame width is 20 x 0.68 = 13.6 msec. Therefore, the frame width corresponding to the N samples in the indirect method should be 13.6 msec. It is reasonable to assume that the 13.6 msec frame would be centered within the 20 msec frame.

Given the above basis for comparison we have found that the direct Autocorrelation method and the indirect Covariance method gave practically the same results for the poles of $\hat{S}(z)$ for effective frame widths larger than a pitch period.

As a general rule of thumb, the indirect method works well for almost any frame size, but the direct method works well only for a frame size of at least one pitch period, with a proper choice of window shape.

6.25 Formant Extraction by Peak Picking

In the beginning of Section 6.2 we indicated how one might deduce formant values from the poles of $\hat{S}(z)$ in (6-4). We mentioned then that peak picking could be performed on the approximate spectrum $\ddot{P}(\omega)$ as a double check on the formant values. In this section we shall discuss briefly the possibility of formant extraction by peak picking alone, avoiding the computation necessary to solve a p-th degree polynomial (where p is usually greater than 10).

Most formants show up as peaks in the approximate spectrum because they usually have a high Q (ratio of frequency to bandwidth). However, there are cases when peaks don't show up very well, usually because the formant has low Q, and in addition may be close to another formant with a dominating peak. Below, we shall discuss two methods for improving the shape of the approximate spectrum so that peak picking will give good results for most cases. We should point out here that peak picking has one inherent drawback, namely that the formant values obtained are only approximately equal to those that would be obtained by finding the poles of $\hat{S}(z)$. This is due to the fact that the formant peak does not occur exactly at the formant frequency. That difference becomes smaller as the formant bandwidth decreases. In addition, the position of a formant peak is also dependent on the positions of neighboring formants. However, for many applications, peak picking

can give adequate accuracy for formant values.

6.251 Preemphasis

One method that usually improves the effectiveness of peak picking is preemphasis. We have already discussed some of the properties of preemphasis by differencing in Section 5.5. We saw that differencing attenuates the energy at very low frequencies and enhances the energy at high frequencies at the rate of approximately +6dB/octave. The positive effect of this type of preemphasis on peak picking is two-fold: a) Attenuation of the energy at low frequencies eliminates peaks due to the glottal source, peaks that otherwise might be mistaken for vocal tract formants, and b) because of the resulting increase in the spectral slope, formants that are overshadowed by neighboring higher amplitude formants would now appear as peaks. One disadvantage of preemphasis is that it causes shifts in computed formant frequencies and bandwidths. This effect is most noticeable with the first formant. However, these shifts are not significant in general, and can be disregarded for many applications.

We saw in Section 5.5 that preemphasis by differencing is equivalent to introducing a zero at zero frequency (z=1) in the signal spectrum. This zero should approximately cancel one of the low frequency poles, and hence one less pole would be needed in the linear prediction all-pole approximation. We have

found that if a certain value of p is optimal (in the sense given by (6-7)) for some signal, then a value of (p-1) is optimal for the differenced signal.

We shall demonstrate some of the above properties by an example. Figure 6-10a shows the original and linear prediction spectra for [w] in the word "anyone" [ɛniwʌn]. The analysis was done using the direct Autocorrelation method on a 25 msec Hamming-windowed signal, with p=12. The corresponding analysis for the differenced signal is shown in Fig. 6-10b with p=11 (p was reduced by 1 according to the above discussion). The low frequency effect due to the glottal source is evident in Fig. 6-10a but disappears in Fig. 6-10b. The second formant does not form a peak in Fig. 6-10a but its peak is quite clear in Fig. 6-10b. In order to see the differences in computed formant frequencies we refer to Fig. 6-11. Figure 6-11a shows the formant frequencies obtained by peak picking from 256-point FFT-computed spectra (i.e. 128 spectral values over 5 kHz). The value of the frequency at which a peak occurred was refined by using a parabolic fit to the three points around the peak. Figure 6-12 shows an example of such curve fitting. Given three points around the peak, the position of the peak can be shown to be at:

$$x_m = \frac{1}{2} \frac{\Delta_1 + \Delta_2}{\Delta_1 - \Delta_2}, \qquad (6\text{-}32)$$

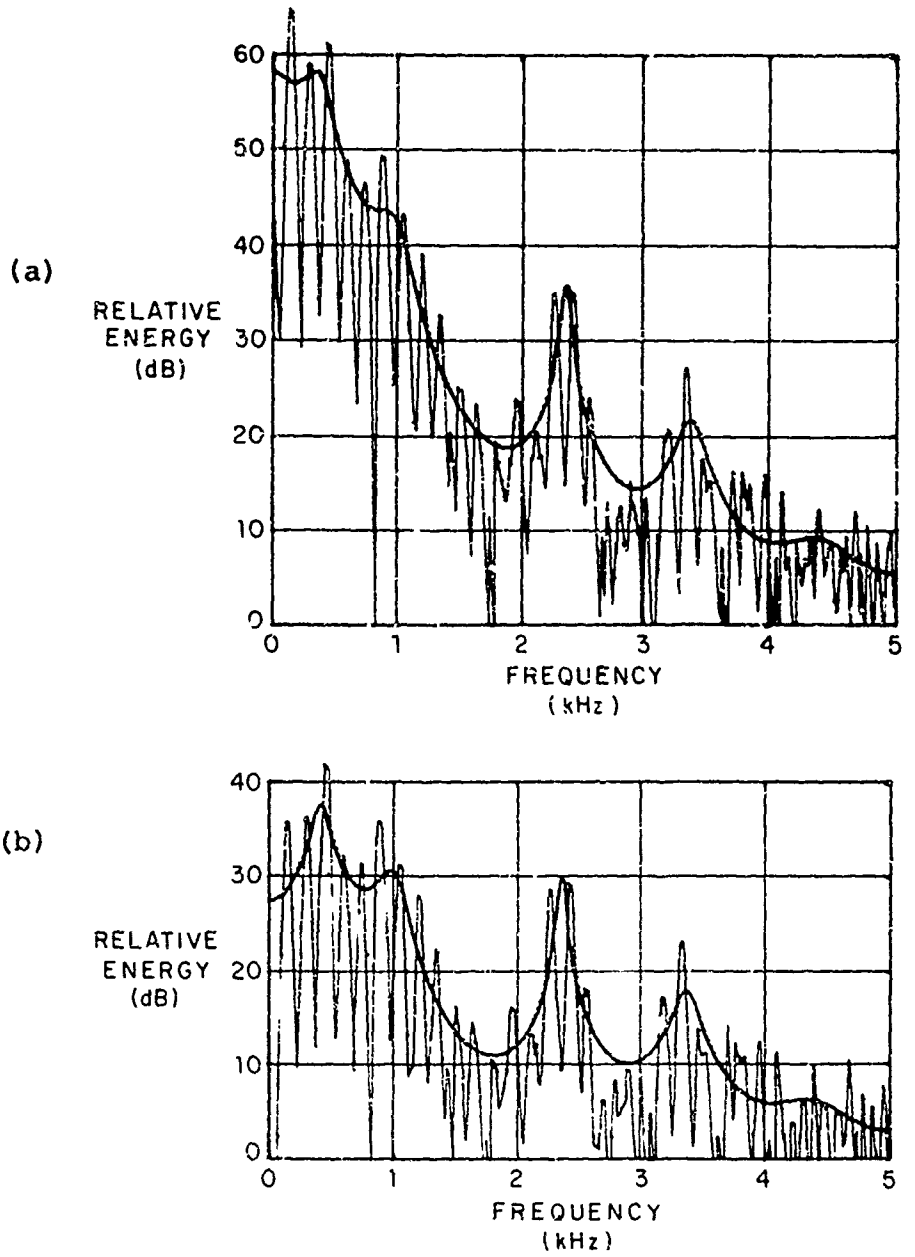

Fig. 6-10. (a) Analysis of [w] in the word "anyone", using the Autocorrelation method. Window size is 25 msec, p=12.
(b) Analysis of the differenced signal, p=11.

	Original	Differenced
F_1	346	421
F_2	---	980
F_3	2383	2382
F_4	3389	3388

(a)

	Original Signal		Differenced Signal	
n	F_n	B_n	F_n	B_n
1	387	220	420	173
2	1008	273	1013	233
3	2385	75	2382	74
4	3396	225	3393	232

(b)

Fig. 6-11 Formant values for the signal associated with Fig.6-10.
(a) Formant frequencies obtained by peak picking with parabolic interpolation.
(b) Formant frequencies and bandwidths obtained from the poles of $S(z)$.

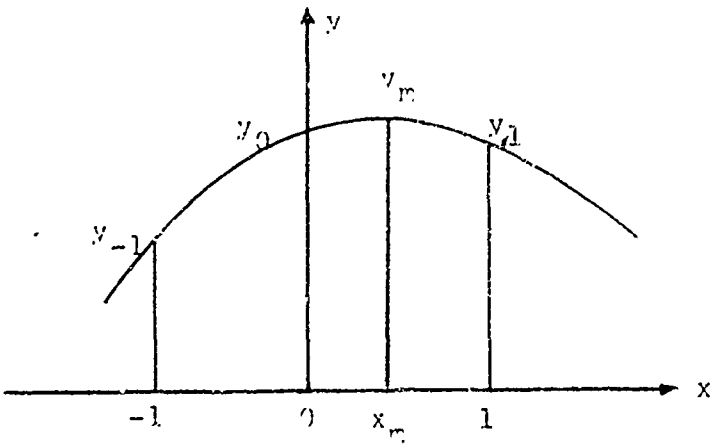

Fig. 6-12 Refining of peak estimation by parabolic curve fitting. (x_m, y_m) are the coordinates of the hypothesized peak.

where $\Delta_1 = y_0 - y_{-1}$,

and $\Delta_2 = y_1 - y_0$.

The peak-picked formant frequencies shown in Fig. 6-11a are to be compared with those obtained from the poles of $\hat{S}(z)$ and shown in Fig. 6-11b, where the formant bandwidths are shown in addition. These formant values are computed from the poles of $\hat{S}(z)$ as follows:

$$F_n = \frac{\omega_n}{2\pi}$$

$$B_n = \frac{|\sigma_n|}{\pi} \qquad (6\text{-}33)$$

where ω_n and σ_n are computed from (6-5) and (6-6). (The definition of bandwidth in (6-33) is not exactly equivalent to the 3-dB definition, but it gives similar results for high-Q formants.) We note from Fig. 6-11a that a peak-picked formant frequency is closer to the computed frequency in Fig. 6-11b when the formant bandwidth is small, as is the case with the third formant in this example. We also note that the largest relative change in frequency between the formant values for the original signal and those of the differenced signal occurs for the first formant.

Although we have not done so here, it is also possible to estimate the formant bandwidths from the approximate spectrum by simply measuring (with interpolation) the frequency interval between

the -3 dB points below each peak. Accurate values would result only for high-Q formants.

Although the application of preemphasis to the speech sign might improve the results of formant extraction by peak picking, it involves a distortion of the signal (by differencing in our case) which has some bad side effects, e.g. the normalized error becomes useless as a voicing detector (see Section 5.5). We shall now describe a second method that improves the results of peak picking without affecting the signal in any way.

6.252 Off-Axis Spectrum

We know that formants with small bandwidths show up very well as peaks in the approximate spectrum $\hat{P}(\omega)$ because the poles corresponding to these formants lie close to the contour along which the spectrum is computed (the unit circle in the z-plane or the $j\omega$-axis in the s-plane). Therefore, for those formants whose peaks do not show up in the spectrum, one could enhance the peaks by moving the contour along which the spectrum is computed closer to these formant poles. In order to see how this might be done efficiently and effectively, we shall first define a more general linear prediction "spectrum" $\hat{P}(\sigma,\omega)$ given by:

$$\hat{P}(\sigma,\omega) = |\hat{S}(z)|^2, \quad z = e^{(\sigma+j\omega)T},$$

$$\hat{P}(\sigma,\omega) = \frac{A^2}{\left|1 - \sum_{k=1}^{p} a_k e^{-k(\sigma+j\omega)T}\right|^2} ,$$

$$= \frac{A^2}{\left|1 - \sum_{k=1}^{p} \left(a_k e^{-k\sigma T}\right) e^{-jk\omega T}\right|^2} . \qquad (6\text{-}34)$$

If $\sigma = 0$, $\hat{P}(\sigma,\omega)$ reduces to $\hat{P}(\omega)$ defined in (4-6a). If σ is a constant ($\sigma = \sigma_0$), then (6-34) reduces to:

$$\hat{P}(\sigma_0,\omega) = \frac{A^2}{\left|1 - \sum_{k=1}^{p} d_k e^{-jk\omega T}\right|^2} \qquad (6\text{-}35)$$

where $$d_k = a_k g^k , \quad 1 \le k \le p , \qquad (6\text{-}36)$$

and $$g = e^{-\sigma_o T} \cong 1 - \sigma_o T, \text{ for } |\sigma_o T| << 1. \qquad (6\text{-}37)$$

$\hat{P}(\sigma_o,\omega)$ in (6-35) has the form of a regular spectrum (see Appendix C on how to compute such a spectrum) computed from a new sequence of coefficients d_k which are obtained by multiplying the coefficients a_k by an exponential, as shown in (6-36) and (6-37). Since $\sigma = \sigma_o$ defines a line parallel to the $j\omega$-axis in the s-plane, we call $\hat{P}(\sigma_o,\omega)$ an <u>off-axis spectrum</u>. It is equivalent to computing the spectrum in the z-plane along a circle of radius $r = \frac{1}{g}$ concentric with the unit circle. An illustration of the peak enhancing ability of the off-axis spectrum is presented

below.

The locations in the s-plane of the first four formants of the original signal in Fig. 6-11b are shown in Fig. 6-13. The off-axis spectrum for $\sigma_o = -2\pi \times 75$ ($g = 1.048$) is shown in Fig. 6-14. This is to be compared with the regular spectrum shown in Fig. 6-10a. The second formant now shows up as a definite peak in the off-axis spectrum. Also, the peaks corresponding to F_1 and F_4 have become sharper (more peaked), while the F_3 peak remained about the same. Sharper peaks, of course, mean that the new peak-picked formant frequencies are closer to the actual formant locations.

One should be able to estimate the formant bandwidths by adding $\frac{-\sigma_o}{\pi}$ to the 3 dB bandwidths of the peaks in the off-axis spectrum. This indeed gives correct results for F_1, F_2 and F_4 in this case, but not for F_3, because F_3 now lies to the right of the σ_o-axis. For such poles, the estimated bandwidth is obtained by subtracting the measured 3 dB bandwidth from $\frac{-\sigma_o}{\pi}$. Unfortunately, there is no way to tell whether a formant lies to the right or to the left of the σ_o-axis from the off-axis magnitude spectrum. (Note that the same is also true for the regular spectrum, except in that case we already know that all poles must lie to the left of the $j\omega$-axis.) Now we see why the F_3 peak was about the same in Figs. 6-10a and 6-14: F_3 is equally distant from the $j\omega$-axis and

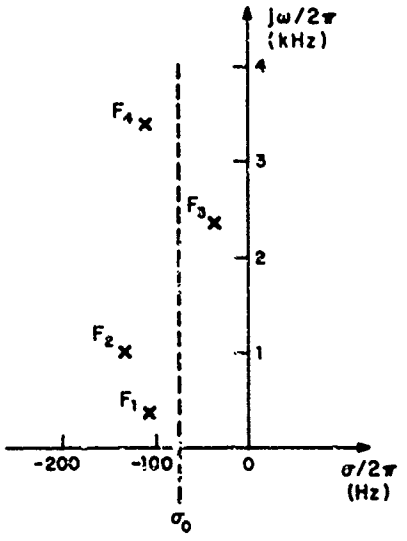

Fig. 6-13. Location in the s-plane of the formants shown in Fig. 6-11b for the original signal.

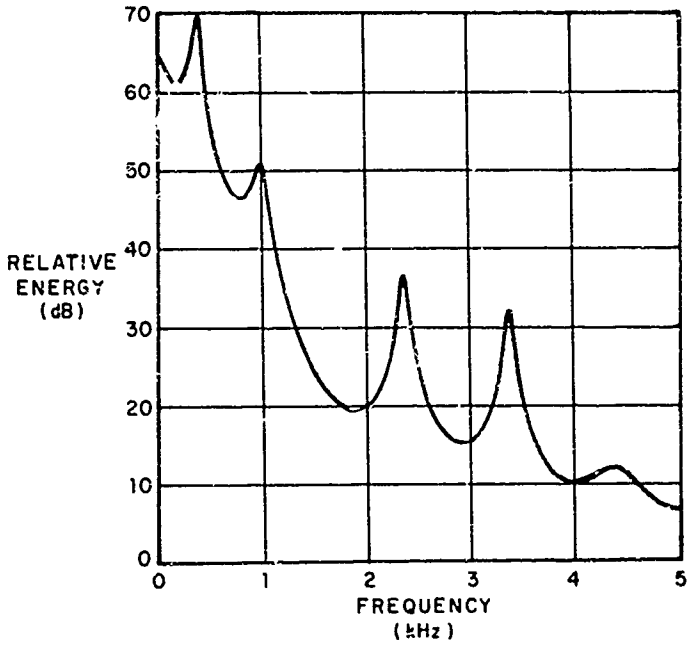

Fig. 6-14. The same linear prediction spectrum shown in Fig. 6-10a except that here the spectrum was computed inside the unit circle (σ_0=-2πx75).

the σ_o-axis, as shown in Fig. 6-13. Therefore, the off-axis-spectrum method has the disadvantage that some bandwidth information might be lost. However, it is easy to see that such bandwidth information can be retained by also computing the regular magnitude spectrum or a phase spectrum.

For formant peak enhancement, we wish to use a value of σ_o which is closer to the poles of interest, on the average, than is the $j\omega$-axis. Since we expect the first four formants to have bandwidths in the range 0-300 Hz, a value of σ_o corresponding to a formant bandwidth of 150 Hz (i.e. $\sigma_o = -2\pi \times 75$) should work well. We have found this value to be effective.

A line parallel to the $j\omega$-axis is only one of many possible contours that would be effective in improving the results of formant extraction by peak picking. Another possibility is to compute the spectrum along an arbitrary straight line in the s-plane. (The corresponding contour in the z-plane is a spiral.) Such a spectrum can be computed using the chirp z-transform (CZT) (Rabiner, Schafer and Rader, 1969). This type of contour makes sense in speech analysis because, generally speaking, formant bandwidths increase with frequency. Unfortunately, computing the CZT is quite expensive, and it is not clear that it would be cost-effective. We would like to point out here that the off-axis spectrum would be a special case where the arbitrary line happens to be parallel to the $j\omega$-axis. However, in that case, the method described in

equations (6-35) through (6-37) is much more efficient than computing the CZT.

6.26 Comparison with the Cepstral Smoothing Method

Schafer and Rabiner (1970) have developed a system for formant analysis by a peak-picking algorithm applied to a cepstrally-smoothed spectrum (i.e. a low-pass filtered log spectrum), and in cases where formants were believed to be very close to each other, they applied the CZT to the cepstrum in order to enhance the formant peaks and separate the formants. It is of interest to compare that method to linear prediction.

First, it should be pointed out that applying the CZT to the cepstrum corresponding to the approximate spectrum $\hat{P}(\omega)$ is equivalent to computing $\hat{P}(\sigma,\omega)$ in (6-34) using the CZT, because $\hat{S}(z)$ is minimum-phase (Schafer and Rabiner, 1970, Appendix B). We have seen that the enhanced peaks in the resulting spectrum correspond to the formant frequencies which could be obtained more accurately by solving for the poles of $\hat{S}(z)$. Therefore, unlike the method with a cepstrally-smoothed spectrum where the CZT is useful in obtaining extra information about formant locations, applying the CZT in linear prediction adds no information.

Another point of comparison is that both types of spectra are smoothed versions of the original signal spectrum. One method does it by actually low-pass filtering the log spectrum, and the other

by reducing the number of poles of an all-pole approximate spectrum. The two types of smoothing are not equivalent, however, because in linear prediction the spectral fitting is based on an all-pole model of speech which, for non-nasal sonorants, corresponds to the usual model of the vocal tract transfer function. For those sounds, we would expect linear prediction to give a better spectral fit. Figure 6-15a shows a spectrum of a Hamming weighted 25 msec of the vowel [a] obtained from 10 kHz sampled telephone speech, and superimposed on it is the smoothed spectrum obtained by linear prediction with p = 14. Figure 6-15b shows the corresponding cepstrally-smoothed spectrum. (The cepstrum has unity weighting up to 1.5 msec and cosine weighting up to 3.0 msec.) Note that a simple peak picking algorithm in Fig. 6-15b would result in a false third formant at 2 kHz. Because we know the spectral characteristics of the vowel [a], the third formant is more likely at 2.8 kHz as shown in Fig. 6-15a.

High-pitched speech normally gives rise to problems in formant tracking due to the fact that for voiced sounds the spectral harmonics are widely separated. We have seen in Section 6.2 that this results in a basic loss of information about the formant structure, a loss that cannot be recovered even by pitch-synchronous analysis, unless new information is added. We have also suggested that the method of linear prediction should perform quite well (with nonnasal sonorants) because of the fact that we assume an

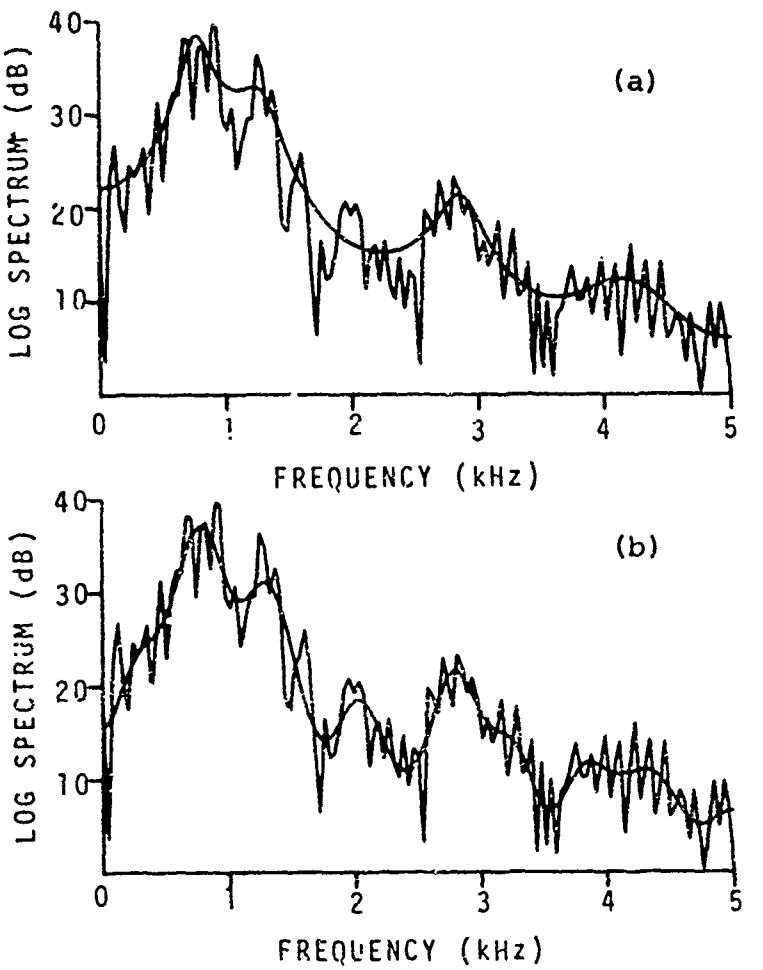

Fig. 6-15. Spectral smoothing of a spectrum of the vowel [a] obtained from 10 kHz sampled telephone speech (a) by linear prediction with p=14, and (b) by cepstral smoothing with unity weighting up to 1.5 msec and a cosine weighting up to 3.0 msec.

all-pole model, which amounts to additional information. In cepstral smoothing the cut-off point of the low-pass filter is placed below the pitch peak, which for high-pitched speech can mean a further loss of information about the formant structure. In linear prediction, the formant locations are less affected by the pitch because the harmonics are forced to fit the all-pole model. This is a well-known property of analysis-by-synthesis methods. (Mermelstein (1967) has suggested a method for smoothing the spectrum by subtracting an approximation to the effects of the fine structure from the spectrum, thus bypassing the problems that arise from low-pass filtering the spectrum.)

Although for nonnasal sonorants linear prediction is expected to give more accurate formant values than the cepstral smoothing method, the same is not necessarily true for other sounds such as nasals and fricatives, whose spectra are known to have antiformants as well as formants. The problems involved have been discussed in Section 6.21.

CHAPTER VII

CONCLUSIONS

Linear prediction is an autocorrelation-domain analysis. Therefore, it can be approached either from the time or frequency domain. Although the actual computations are performed in the time domain, we chose to derive the most general formulations for linear prediction from the frequency domain because of the dominance of spectral analysis in speech research. We have shown that all least-squares methods of linear prediction can be derived from a single general concept, namely that of generalized analysis-by-synthesis. Here the 2D-spectrum (two dimensional spectrum) of a nonstationary signal (such as speech) is to be approximated by another 2D-spectrum, where the error to be minimized is proportional to the integral of the ratio of the signal spectrum to the approximate spectrum. This error criterion was shown to be very desirable for a good spectral envelope fit. In the special case when the approximate spectrum consists of poles only, the generalized method reduces to the general Covariance method of linear prediction. If, in addition, the signal is assumed to be stationary, the 2D-spectrum is replaced by the ordinary power spectrum, and the Covariance method reduces to the Autocorrelation method of linear prediction.

The linear prediction speech production model assumes the vocal tract to be fixed in shape within a portion of the speech

signal (a frame) on the order of 10-25 msec. Within each frame, the speech signal is assumed to be nonstationary in the Covariance method and stationary in the Autocorrelation method. In general, the assumption of nonstationarity is a better assumption for speech signals. However, within a frame, the speech signal can be considered to be quasi-stationary, so the assumption of stationarity in the Autocorrelation method is not a bad one. In general, one would expect the Covariance method to give better results than the Autocorrelation method, especially with analysis-synthesis systems. However, for other speech applications, the advantages of one method over the other do not seem to be significant.

In computing the predictor coefficients from a single frame we defined two basic methods: the direct and indirect methods. In the direct method, the signal is weighted by a window that is zero outside the frame, and the resulting signal is considered to be infinite. In the indirect method, an unwindowed finite portion of the signal is used. The most popular and useful methods are the direct Autocorrelation and indirect Covariance methods. As a general rule of thumb, the indirect method works well for almost any frame size, but the direct method works well only for a frame size of at least one pitch period, with a proper choice of window shape. We have developed criteria that a window function must satisfy in order to give good results.

The direct Autocorrelation method was discussed in detail because, with this method, it was possible to examine in what manner the all-pole linear prediction spectrum approximated the signal spectrum. For example, from the normalized error curve it was possible to set general guidelines to help determine the number of poles in the linear prediction spectrum that would best approximate the envelope of the signal spectrum. As the number of poles approached infinity, the linear prediction spectrum became identical to the signal spectrum, while the linear prediction transfer function became the minimum-phase counterpart to the signal transfer function. Several methods were suggested for computing the minimum-phase sequence corresponding to the original signal.

The study of the normalized error in the direct Autocorrelation method led to some interesting and important results. First, we showed that the normalized error was equal to the ratio of the geometric mean of the linear prediction spectrum to its arithmetic mean. The arithmetic mean of the spectrum is equal to the energy in the signal, while the geometric mean is equal to the exponential of the zero quefrency component, c_0, of the cepstrum. Thus, the normalized error measure is a form of normalization of c_0 with respect to the energy in the signal, and the resulting ratio is a function of only the shape of the spectrum. The properties of the normalized error are a reflection

of the properties of c_0. One such property is the usefulness of the normalized error in the detection of voicing. It was shown that such usefulness depended completely on the spectral shapes of the sounds. Any processing of the signal that changed its spectral characteristics was seen to have a possible detrimental effect on the usefulness of the normalized error as a voicing detector. Speech preemphasized by differencing, and telephone speech, were given as examples of such processing. Under these circumstances, it was suggested that the first autocorrelation coefficient would be a better voicing detector.

Filtering the speech signal by the linear prediction inverse filter results in an error signal. For voiced sounds, this error signal often shows distinct pulses at the start of each pitch period. These "pitch pulses" can be used for pitch extraction. In cases where the signal is not rich in harmonics, e.g. during sonorant-nonsonorant transitions and for voicing of stops and fricatives, pitch pulses are likely not to be prominent, and therefore pitch would have to be estimated by some other means, such as peak picking of the speech signal itself.

Another application of linear prediction is in the estimation of formants of the vocal tract. These formants are estimated from the poles of the linear prediction transfer function. We discussed several factors that influence the extent to which

extracted formant values correspond to actual resonances of the vocal tract. We concluded that formant extraction by linear prediction works well with nonnasal sonorants. However, if the transfer function of the vocal tract contains antiresonances as well as resonances, as is the case for nasals and fricatives, then linear prediction is inadequate for the extraction of the formants and antiformants.

Because computing the poles of the linear prediction transfer function is expensive, we discussed formant tracking by peak picking of the linear prediction spectrum as an alternate inexpensive method. Unfortunately, not all formants are represented by peaks in the spectrum. Two methods were discussed to render peak picking more effective. The first method involves preprocessing the speech signal by preemphasis. Preemphasis by differencing was seen to be effective, except that it had some undesirable side effects, such as shifts in formant positions, especially the first formant. The second method did not involve any preprocessing of the signal. One merely computes the linear prediction spectrum along a circle inside the unit circle (which corresponds to a line parallel and to the left of the $j\omega$-axis). The resulting "off-axis spectrum" has proven to be both efficient and effective.

One issue of importance to most types of speech analysis is the choice of frame width and position. This issue was discussed

in terms of pitch-synchronous and pitch-asynchronous analysis. The latter type of analysis included a detailed discussion of windowing.

APPENDIX A

ON THE z-TRANSFORM AND FOURIER SERIES

In this appendix we shall define the z-transform, its inverse, and their relation to Fourier series and the Laplace transform.

A.1 Definition and Properties of z-Transforms

Given a sampled sequence x(nT), defined for all n, where n is an integer and T is the sampling interval, the z-transform of x(nT) is defined as:

$$X(z) = \sum_{n=-\infty}^{\infty} x(nT)\ z^{-n} \ . \qquad \text{(A-1)}$$

The operator z is, in general, complex and is defined in terms of the Laplace operator s as follows:

$$z = e^{sT} = e^{(\sigma+j\omega)T} \qquad \text{(A-2)}$$

where $\omega = 2\pi f$ is the radian frequency in rad/sec,

σ is the damping factor in rad/sec,

$T = \frac{1}{f_s}$ is the sampling interval in seconds,

and f_s is the sampling frequency in Hz.

x(nT) could in general be complex but is often real in actual applications.

The inverse z-transform of X(z) is then x(nT) and can be shown to be equal to (Gold and Rader, 1969, pp. 26-27):

$$x(nT) = \frac{1}{2\pi j}\oint X(z)\ z^{n-1}\ dz\ , \qquad \text{(A-3)}$$

where the path of integration encloses the region of convergence of X(z).

The relation between s and z in (A-2) defines a mapping between the s-plane and the z-plane. It is very important to understand the nature of this mapping for a thorough understanding of z-transforms. The s-plane shown in Fig. A-1a has been divided by horizontal dashed lines into strips of width $\omega=\frac{2\pi}{T} = 2\pi f_s$. There are, of course, an infinite number of these strips in the s-plane. According to (A-2), each strip of width $2\pi f_s$, as shown in Fig. A-1, maps into the entire z-plane. Therefore, the mapping from the s-plane to the z-plane is an infinity-to-one mapping. For a particular configuration in the z-plane (see Fig. A-1b), the s-plane consists of an infinity of repeating strips of identical configurations. Each pole (or zero) in the z-plane maps into an infinite number of poles (or zeros) in the s-plane separated by $\omega = 2\pi f_s$. This is shown in Fig. A-1 for the poles a, b, $\bar{b}$, and c, where the over-bar denotes complex conjugate. As can be seen from (A-2) and Fig. A-1, the $j\omega$-axis ($\sigma=0$) maps into the unit circle $z=e^{j\omega T}$ in the z-plane. The left half of the s-plane maps into the region inside the unit circle, while the right half of

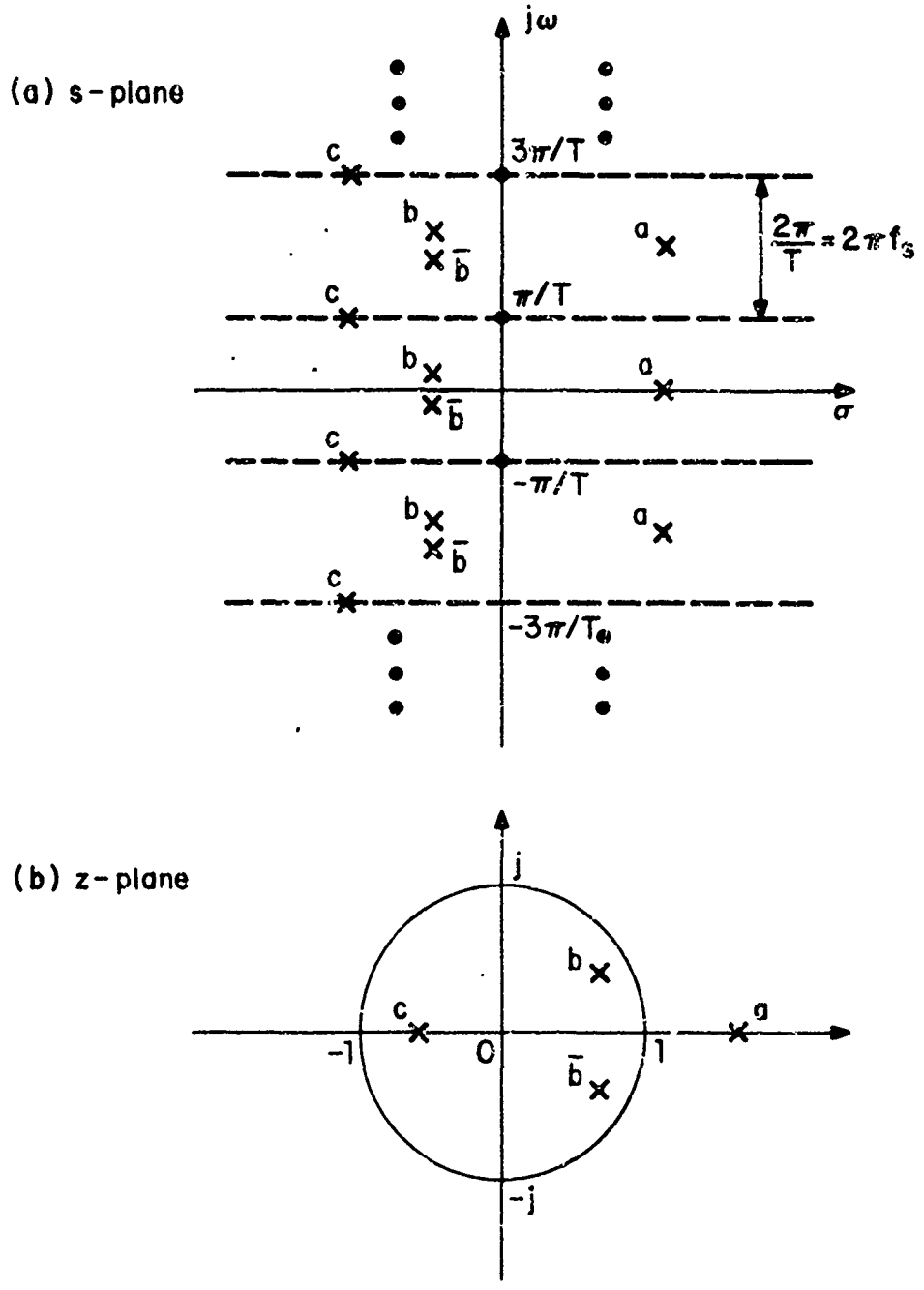

Fig. A-1. Mapping of the z-plane onto the s-plane.

the s-plane maps into the region outside the unit circle. A vertical line at $\sigma=\sigma_0$ in the s-plane maps into a circle defined by $z=e^{\sigma_0 T}e^{j\omega T}$. A horizontal line at $\omega=\omega_0$, as well as lines at $\omega_0 + \frac{2\pi k}{T}$ in the s-plane, map into a radial half-line emanating from the origin of the z-plane and defined by $z = e^{\sigma T}e^{j\omega_0 T}$. In particular, the real-axis ($\omega=0$) in the s-plane maps into the positive real half-line (z real and >0) in the z-plane. The negative real half-line (z real and <0) of the z-plane maps into horizontal lines at $\omega = (2k+1)\frac{\pi}{T}$ in the s-plane. These horizontal lines form the boundary lines between strips in the s-plane. This latter mapping is quite unique in the context of z to s mapping. This can be seen by examining how the poles in the z-plane shown in Fig. A-1b map into corresponding poles in the s-plane. Also, we shall concentrate on the center strip in the s-plane ranging from $\frac{-\pi}{T}$ to $\frac{\pi}{T}$. The positive real-axis pole a in the z-plane maps into a real-axis pole in the s-plane. The complex poles b and $\bar{b}$ in the z-plane map into corresponding complex poles in the s-plane. However, the negative real pole c in the z-plane maps into complex poles in the s-plane. Figure A-2c shows a single period of the amplitude frequency response for a single negative real pole in the z-plane ($z_c = -0.6$). Compare that with Fig. A-2a for a positive real pole ($z_a = 1.7$), and with Fig. A-2b for a complex conjugate pair of poles ($z_b = 0.4(1+j\sqrt{3})$, $\bar{z}_b = 0.4(1-j\sqrt{3})$).

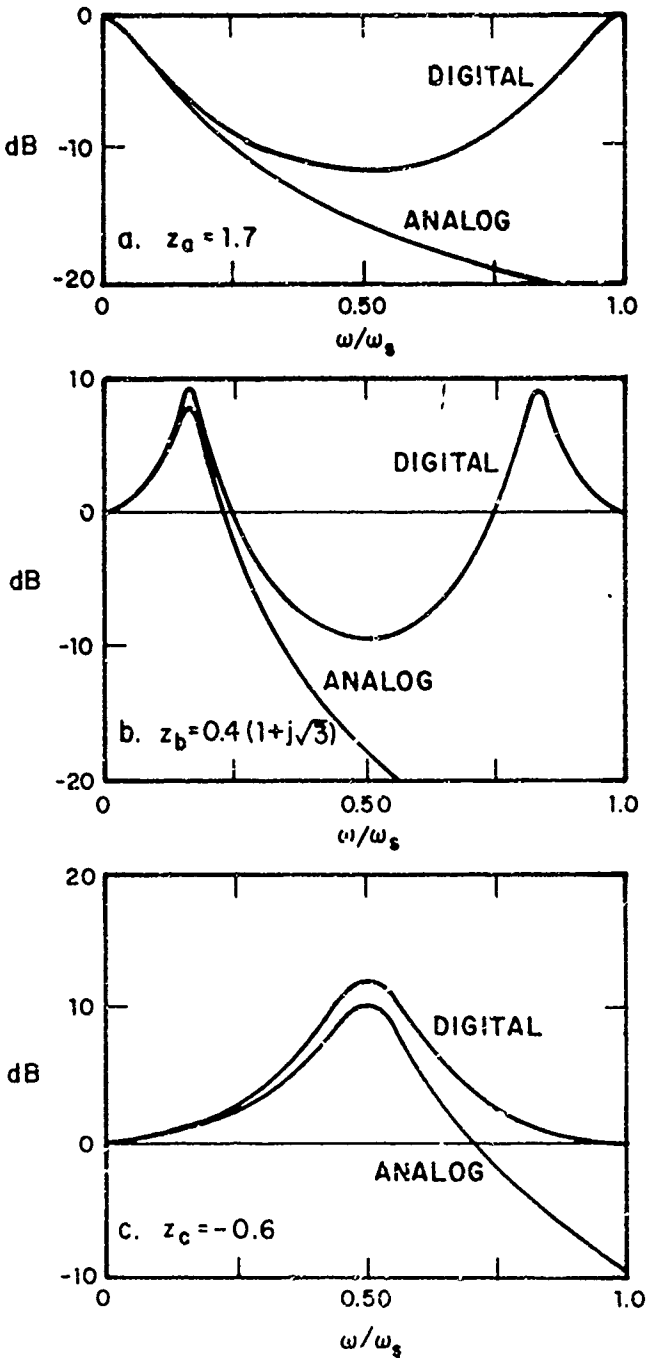

Fig. A-2. Amplitude frequency responses for the poles shown in Fig. A-1.

Also, compare the digital frequency response in each case with the corresponding analog (s-plane) response which is the response of the poles that are in the center strip $\frac{-\pi}{T} \leq \omega \leq \frac{\pi}{T}$ in Fig. A-1a.

A.2 z-Transform and Fourier Series

In order to relate z-transforms to Fourier series we let $\sigma=0$ in (A-2), resulting in $z = e^{j\omega T}$. Substituting for z in (A-1) we obtain:

$$X(\omega) = \sum_{n=-\infty}^{\infty} x(nT)\ e^{\ jn\omega T} \qquad \text{(A-4)}$$

where $X(\omega)$ stands for $X(e^{j\omega T})$.

The inverse transform of $X(\omega)$ is obtained by substituting $z = e^{j\omega T}$ in (A-3) and taking the path of integration around the unit circle. The result can be easily shown to be:

$$x(nT) = \frac{T}{2\pi} \int_{-\pi/T}^{\pi/T} X(\omega)\ e^{jn\omega T}\ d\omega. \qquad \text{(A-5)}$$

Equations (A-4) and (A-5) can be viewed simply as the ordinary Fourier series transform pair, but with time and frequency interchanged. In traditional Fourier series analysis the time function is normally continuous and periodic while the frequency domain is discrete (i.e., the transform exists only at multiples of the fundamental); in other words, the frequency function is sampled. On the other hand, in z-transform analysis, the time function is

sampled while the frequency function is continuous and periodic. Therefore, we can make the general assertion that sampling in one domain corresponds to periodicity in the transform domain. We have, as a corollary, that if a function in one domain is both sampled and periodic, then the transform function must also be both sampled and periodic. Another way of stating this is that if a time function is sampled and its frequency transform is also sampled, then both functions must also be periodic. Indeed, this is one of the principal properties of the discrete Fourier transform (Gold and Rader, 1969, Ch. 6).

We have seen above that the z-transform with $\sigma = 0$ reduces to the Fourier series transform. We also know that the Laplace transform with $\sigma = 0$ reduces to the Fourier integral transform. Therefore, we can say that the z-transform is to Fourier series what the Laplace transform is to Fourier integrals. This analogy can be very useful in understanding the workings of the z-transform.

We shall give one example where the result is obtained by analogy to Fourier series. Consider a continuous and periodic function of time $x(t)$ with period T, having a transform in the frequency domain $X\left(\frac{n}{T}\right)$. Then, the energy in one period of the signal can be obtained from the time domain as well as the frequency domain as follows:

$$\text{Energy} = \frac{1}{T}\int_{-T/2}^{T/2} |x(t)|^2\, dt = \sum_{n=-\infty}^{\infty} \left|X\left(\frac{n}{T}\right)\right|^2. \qquad \text{(A-6)}$$

This is a special case of Parseval's theorem (Lee, 1960, p. 11). Now, by carefully interchanging time and frequency in (A-6) we have:

$$\text{Energy} = \frac{T}{2\pi}\int_{-\pi/T}^{\pi/T} |X(\omega)|^2\, d\omega = \sum_{n=-\infty}^{\infty} |x(nT)|^2 \; . \qquad \text{(A-7)}$$

This says that the total energy in a sampled signal x(nT) can be obtained by integrating over a period of the power spectrum. Equation (A-7) can be, of course, also derived directly from (A-4) and (A-5), but we wanted to demonstrate how one might use the analogy with Fourier series.

APPENDIX B

THE AUTOCORRELATION METHOD AND ORTHOGONAL POLYNOMIALS

The inverse filter H(z) defined in (2-3) is a function of p, the number of predictor coefficients. Here we shall make this dependence explicit by writing:

$$H_p(z) = 1 - \sum_{k=1}^{p} a_k z^{-k} . \qquad \text{(B-1)}$$

In this appendix we shall use the results of Grenander and Szegö (1958) to show that $H_0(z)$, $H_1(z)$, ..., $H_p(z)$,... form a unique set of polynomials that is orthogonal on the unit circle with respect to the signal power spectrum $P(\omega)$. This will lead us to certain properties of $H_p(z)$, and to a derivation of the solution to the autocorrelation normal equations (3-17). We call this solution the Fast Autocorrelation method.

B.1 Orthogonal Polynomials on the Unit Circle

Let P(x) be a nonnegative and Lebesque-integrable function, i.e.

$$P(x) \geq 0, \text{ all } x, \qquad \text{(B-2a)}$$

and

$$\int_{-\pi}^{\pi} P(x)\, dx \leq C, \qquad \text{(B-2b)}$$

where C is some finite constant.

Also, let the inverse Fourier transform of P(x) be given by:

$$R_k = \frac{1}{2\pi} \int_{-\pi}^{\pi} P(x)\ e^{jkx}\ dx\ . \qquad \text{(B-3)}$$

We form a system of polynomials

$$\phi_0(z),\ \phi_1(z),\ \ldots,\ \phi_n(z),\ \ldots$$

of the complex variable z which are orthonormal on the unit circle $z=e^{jx}$, with the weight $\frac{1}{2\pi}\ P(x)$. These polynomials satisfy the following two conditions:

(i) $\phi_n(z)$ is a polynomial of degree n in which the coefficient of z^n is real and positive;

(ii) the inner product $(\phi_n(z),\phi_m(z))$ with respect to P(x) is given by:

$$(\phi_n(z),\phi_m(z)) = \frac{1}{2\pi}\int_{-\pi}^{\pi} \phi_n(z)\ \overline{\phi}_m(z)\ P(x)\ dx = \delta_{nm},\ z = e^{jx};\ n,\ m=0,1,2,\ldots \qquad \text{(B-4)}$$

where the over-bar denotes complex conjugate.

Grenander and Szegö (1958, pp. 12-14, 35-42) have shown that the set of polynomials $\{\phi_n(z)\}$ is <u>uniquely</u> determined by conditions (i) and (ii).

Each polynomial $\phi_n(z)$ is given by:

$$\phi_n(z) = (D_{n-1}D_n)^{-\frac{1}{2}} \begin{vmatrix} R_0 & R_1 & R_2 & \cdots & R_{n-1} & R_n \\ R_{-1} & R_0 & R_1 & \cdots & R_{n-2} & R_{n-1} \\ R_{-2} & R_{-1} & R_0 & \cdots & R_{n-3} & R_{n-2} \\ \vdots & \vdots & \vdots & & \vdots & \vdots \\ R_{1-n} & R_{2-n} & R_{3-n} & \cdots & R_0 & R_1 \\ 1 & z & z^2 & \cdots & z^{n-1} & z^n \end{vmatrix} \quad \text{(B-5)}$$

where $D_n = \det(R_{j-i})_0^n = \begin{vmatrix} R_0 & R_1 & \cdots & R_n \\ R_{-1} & R_0 & \cdots & R_{n-1} \\ \vdots & \vdots & & \vdots \\ R_{-n} & R_{1-n} & \cdots & R_0 \end{vmatrix}$. (B-6)

If we let

$$\phi_n(z) = k_n z^n + \ldots + \ell_n \quad \text{(B-7)}$$

where k_n is the coefficient of z^n and ℓ_n is the constant term, then the polynomial $\phi_n(z)$ is shown to obey the recurrence relation:

$$k_n \phi_{n+1}(z) = k_{n+1} z \phi_n(z) + \ell_{n+1} z^n \phi_n(z^{-1}) , \quad \text{(B-8)}$$

where we have assumed that the coefficients of $\phi_n(z)$ are real. From (B-8) one can compute $\phi_n(z)$ recursively given the following additional properties:

$$\phi_0(z) = R_0^{-\frac{1}{2}} , \tag{B-9}$$

$$k_n^2 = \frac{D_{n-1}}{D_n} = \sum_{i=0}^{n} |\ell_i|^2 . \tag{B-10}$$

B.2 Application to Linear Prediction

If we let $x = \omega T$ in $P(x)$, and let $P(\omega)$ be the power spectrum of a signal with finite energy, then conditions (B-2) are satisfied and R_k are the autocorrelation coefficients, which are real and even. From (B-5) we see that $\phi_n(z)$ must have real coefficients. Furthermore, by comparing (B-5) and (3-17), the autocorrelation normal equations, it can be shown that:

$$\phi_n(z) = \frac{z^n}{A_n} H_n(z) , \tag{B-11}$$

where $H_n(z)$ is the inverse filter defined in (B-1) and A_n is the gain factor defined in (2-3) and given by (3-37):

$$A_n^2 = E_n = R_0 - \sum_{k=1}^{n} a_k R_k . \tag{B-12}$$

A_n^2 is equal to the minimum total-squared error E_n. From (B-1), (B-11) and (B-7) it is clear that:

$$A_n = \frac{1}{k_n} . \tag{B-13}$$

Substituting (B-13) in (B-11) and the result in (B-8) we have:

$$k_n\, k_{n+1}\, z^{n+1}\, H_{n+1}(z) = k_n\, k_{n+1}\, z^{n+1}\, H_n(z) + \ell_{n+1}\, k_n\, H_n(z^{-1}). \quad \text{(B-14)}$$

Dividing (B-14) by $(k_n\, k_{n+1}\, z^{n+1})$ we obtain the recurrence relation:

$$H_{n+1}(z) = H_n(z) + K_n\, z^{-(n+1)}\, H_n(z^{-1}) , \quad \text{(B-15)}$$

where $$K_n = \frac{\ell_{n+1}}{k_{n+1}} . \quad \text{(B-16)}$$

From (B-10) we have:

$$k_{n+1}^2 = k_n^2 + \ell_{n+1}^2$$

or
$$k_n^2 = k_{n+1}^2 - \ell_{n+1}^2$$

$$= k_{n+1}^2 \left(1 - \frac{\ell_{n+1}^2}{k_{n+1}^2}\right) . \quad \text{(B-17)}$$

Substituting (B-16) and (B-13) in (B-17) we obtain a recurrence relation for A_n:

$$A_{n+1}^2 = A_n^2 \left(1 - K_n^2\right) . \quad \text{(B-18)}$$

We now show how to compute K_n (Markel and Gray, to be published). Take the inner product of $H_{n+1}(z)$ in (B-15) with $z^{-(n+1)}$. (The definition of the inner product of two polynomials is given by

the left-hand side of (B-4).)

$$\left(H_{n+1}(z),\ z^{-(n+1)}\right) = \frac{1}{2\pi}\int_{-\pi}^{\pi} H_{n+1}(\omega)\ e^{j(n+1)\omega T}\ P(\omega)\ d\omega T$$

$$= \frac{1}{2\pi}\int_{-\pi}^{\pi}\left[1 - \sum_{k=1}^{n+1} a_k\ e^{-jk\omega T}\right]\ e^{j(n+1)\omega T}\ P(\omega)\ d\omega T$$

$$= R_{n+1} - \sum_{k=1}^{n+1} a_k\ R_{n+1-k}\ . \qquad \text{(B-19)}$$

If we let i=p=n+1 in the autocorrelation normal equations (3-15), then (B-19) is equal to zero:

$$\left(H_{n+1}(z)\ ,\ z^{-(n+1)}\right) = 0\ . \qquad \text{(B-20)}$$

Therefore, from (B-15) and (B-20) we have:

$$K_n = -\frac{\left(H_n(z)\ ,\ z^{-(n+1)}\right)}{\left(z^{-(n+1)}H_n(z^{-1}),\ z^{-(n+1)}\right)}\ . \qquad \text{(B-21)}$$

By derivations similar to that given above, and making use of (B-12), it can be shown that:

$$K_n = -\frac{R_{n+1} - \sum_{k=1}^{n} a_k^{(n)} R_{n+1-k}}{A_n^2}\ , \qquad \text{(B-22)}$$

where $a_k^{(n)}$ are the predictor coefficients corresponding to $H_n(z)$.

Equations (B-15), (B-18) and (B-22) in addition to the initial conditions

$$H_0(z) = 1$$

$$\text{and} \qquad A_0^2 = R_0 \ , \tag{B-23}$$

give a complete recursive solution for the polynomials $H_n(z)$, and hence a solution to the autocorrelation normal equations (3-17).

Equation (B-15) can be expressed as a recurrence relation in terms of the predictor coefficients a_k. Substituting from (B-1) in (B-15) we have:

$$1 - \sum_{k=1}^{n+1} a_k^{(n+1)} z^{-k} = 1 - \sum_{k=1}^{n} a_k^{(n)} z^{-k} + K_n \, z^{-(n+1)} \left[1 - \sum_{k=1}^{n} a_k^{(n)} z^{k} \right]$$

$$\text{or} \quad \sum_{k=1}^{n+1} a_k^{(n+1)} \, z^{-k} = \sum_{k=1}^{n} a_k^{(n)} \, z^{-k} - K_n \, z^{-(n+1)} + K_n \sum_{k=1}^{n} a_k^{(n)} z^{k-n-1}$$

$$= \sum_{k=1}^{n} a_k^{(n)} \, z^{-k} + K_n \sum_{k=1}^{n} a_{n+1-k}^{(n)} z^{-k} - K_n z^{-(n+1)} . \tag{B-24}$$

By equating the coefficients of equal power of z on both sides of (B-24), we have:

$$a_{n+1}^{(n+1)} = -K_n$$

$$a_k^{(n+1)} = a_k^{(n)} + K_n \, a_{n+1-k}^{(n)} \ , \quad k=1,2,\ldots,n. \tag{B-25}$$

Therefore, the solution for (3-17) is given recursively by (B-23), (B-22), (B-18) and (B-25). A flow chart is given in Fig. B-1. If the computations in (B-25) are to be done in place, one must be careful not to destroy newly computed values as others are computed. One solution is to compute a_k and a_{n+1-k} at the same time since

$$a_{n+1-k}^{(n+1)} = a_{n+1-k}^{(n)} + K_n \, a_k^{(n)} \quad .$$

Another method is to use an extra array b_k where

$$b_k = a_{n+1-k}, \quad 1 \leq k \leq n,$$

then

$$a_k^{(n+1)} = a_k^{(n)} + K_n \, b_k^{(n)} \quad .$$

In Fig. B-1, AA is equal to A^2, the minimum total-squared error, at every stage of the computation. Therefore, $\frac{AA}{R_0}$ is equal to the normalized error V_n, which is discussed in Chapter V. If the autocorrelation coefficients are normalized with respect to R_0 before applying the algorithm in Fig. B-1, then AA will be equal to the normalized error at every stage. Normalization of the autocorrelation coefficients is especially recommended for those who are using a computer with only integer arithmetic capability.

The coefficients K_n in (B-22) are the same as the partial autocorrelation (PARCOR) coefficients of Itakura and Saito (1972).

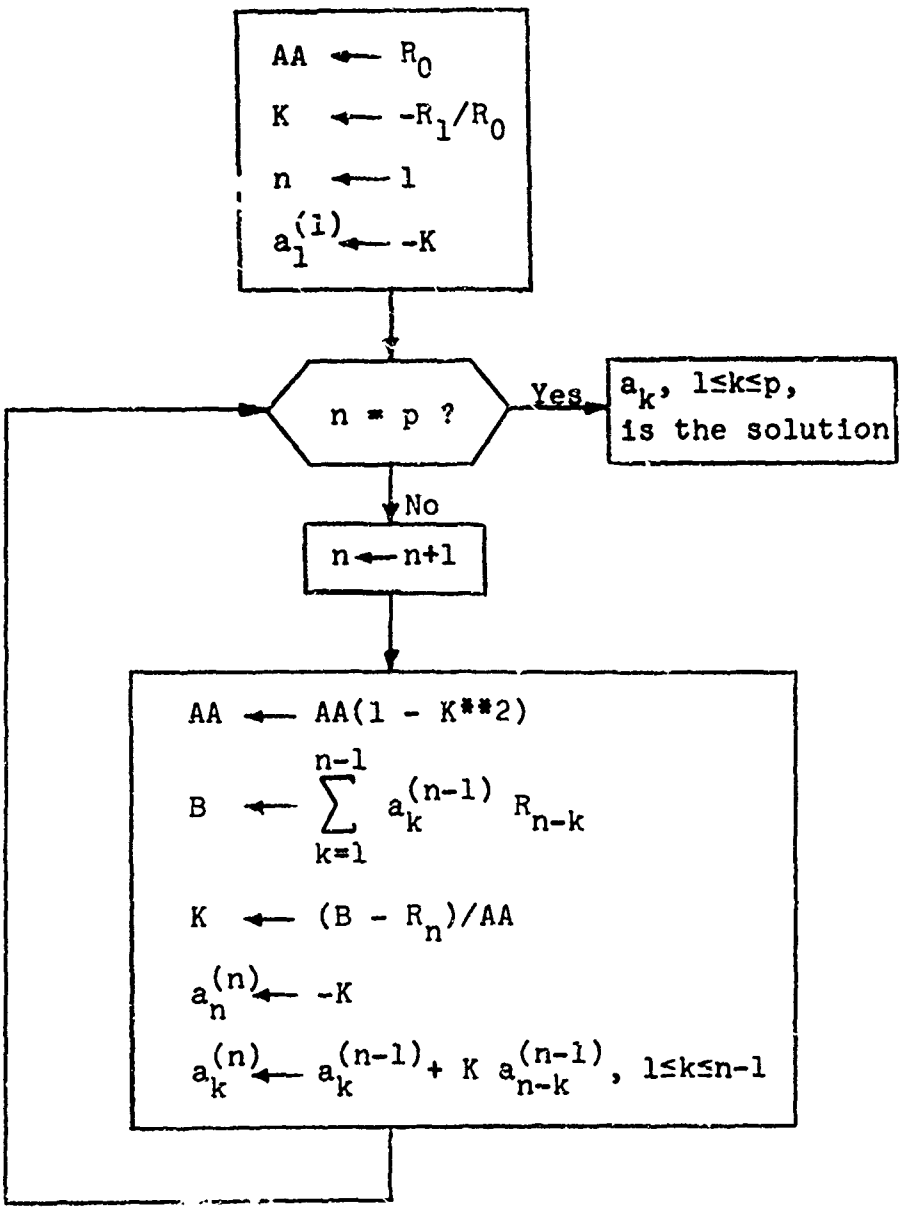

Fig. B-1 Flow chart for the solution of the autocorrelation normal equations (3-17). This is called the Fast Autocorrelation method.

Since the minimum total-squared error ($E_n = A_n^2$) is always positive, we conclude from (B-18) that K_n must obey the relation:

$$|K_n| < 1 \ . \qquad \text{(B-26)}$$

B.3 Properties of $H_p(z)$

(a) From (B-11) and (B-4) we have:

$$\frac{T}{2\pi} \int_{-\pi/T}^{\pi/T} \frac{H_n(\omega)}{A_n} \frac{\bar{H}_m(\omega)}{A_m} P(\omega)\, d\omega = \delta_{nm}, \quad n,m = 0,1,2,\ldots \qquad \text{(B-27)}$$

$\{H_n(z)\}$ is a complete set of polynomials orthogonal on the unit circle with A_n as the normalizing factor for $H_n(z)$. It should be remembered that (B-27) holds if and only if the coefficients R_k in (B-3) are positive-definite (see Section 4.4). This is guaranteed in the direct Autocorrelation method.

For $n = m = p$, (B-26) reduces to

$$\frac{T}{2\pi} \int_{-\pi/T}^{\pi/T} \frac{P(\omega)}{\hat{P}(\omega)}\, d\omega = 1, \qquad \text{(B-28)}$$

where $\hat{P}(\omega) = \dfrac{A_p^2}{|H_p(\omega)|^2} = |\hat{S}(\omega)|^2$ is the approximate spectrum. Note that (B-28) is identical to (5-3) which was derived in a different manner.

(b) The zeros of the orthogonal polynomials $H_p(z)$ all lie inside the unit circle (Grenander and Szegö, 1958, p. 40). In other words, the inverse filter $H_p(z)$ is minimum-phase and the all-pole filter $\hat{S}(z)$ is stable, as we have observed in Section 3.4. Again, this is true iff the coefficients R_k are positive-definite. An equivalent necessary and sufficient condition is given by (B-26). Another equivalent condition is that the minimum total-squared error be positive.

(c) Since the system of orthogonal polynomials $H_p(z)$ is complete, any polynomial in z^{-1} of degree p can be represented as a linear summation of the polynomials $H_0(z)$, $H_1(z),\ldots,H_p(z)$. In other words, any recursive filter of degree p can be realized as a linear summation of minimum-phase recursive filters $H_n(z)$ with degrees $\leq p$.

APPENDIX C

COMPUTATION OF SIGNAL AND APPROXIMATE SPECTRA

The signal power spectrum in the direct Autocorrelation method is given by:

$$P(\omega) = \left| \sum_{n=0}^{N-1} s_n \, e^{-jn\omega T} \right|^2 \qquad \text{(C-1)}$$

where s(nT) is the windowed signal.

The approximate or linear prediction spectrum $\hat{P}(\omega)$ can be defined for all methods of linear prediction as:

$$\hat{P}(\omega) = \frac{A^2}{\left| 1 - \sum_{k=1}^{p} a_k \, e^{-jk\omega T} \right|^2} \quad , \qquad \text{(C-2)}$$

where a_k , $1 \le k \le p$, are the predictor coefficients and A is the gain factor.

$P(\omega)$ and $\hat{P}(\omega)$ are both continuous, periodic, real and even functions of frequency. The periodicity is equal to $\frac{1}{T} = f_s$, the sampling frequency. Therefore, it is only necessary to compute the spectra from zero frequency to a frequency of $\frac{f_s}{2}$. Also, it is practical to compute the spectral values at only a finite number of frequencies. One method of doing this is to use the discrete Fourier transform (DFT) (Gold and Rader, 1969, Ch. 6) which

can be computed efficiently by fast Fourier transform techniques (FFT) (Cochran, et al., 1967). Computation times for the FFT can be cut approximately into half by using the fact that the signal s(nT) is real (see, for example, Makhoul, 1970b, Appendix B). Therefore, $P(\omega)$ is computed at discrete frequency intervals by taking the magnitude squared of the FFT of the signal s(nT). $\hat{P}(\omega)$ can be computed by dividing A^2 by the magnitude squared of the FFT of the sequence: $1, -a_1, -a_2, \ldots, -a_p$. Arbitrary resolution in the frequency domain can be obtained by simply appending an appropriate number of zeros to the sequence whose FFT is to be taken. If the number of zeros is large compared to the length of the original sequence (as is normally the case in computing $\hat{P}(\omega)$, where the number of frequency values desired is much larger than p), the FFT algorithm can be pruned (Markel, 1971) resulting in a saving in computation. (Markel's algorithm is based on a radix-2 FFT. We have implemented a radix-8 pruned FFT which saves time only if the number of points in the FFT is at least 8 times the length of the original sequence. For example, we have realized a saving of 32% over the regular radix-8 algorithm by computing a 256-point pruned FFT with p = 15.)

A more direct method of computing $\hat{P}(\omega)$ is obtained by noting that (C-2) can be rewritten as follows:

$$\hat{P}(\omega) = A^2 \Big/ \left| \sum_{k=0}^{p} a'_k \, e^{-jk\omega T} \right|^2$$

$$= A^2 \Big/ \left[\sum_{k=0}^{p} \sum_{i=0}^{p} a'_k \, a'_i \, e^{j(i-k)\omega T} \right]$$

and
$$\hat{P}(\omega) = \frac{A^2}{b_0 + 2\sum_{k=1}^{p} b_k \cos(k\omega T)} , \qquad \text{(C-3)}$$

where
$$a'_k = \begin{cases} 1, & k=0 , \\ -a_k, & \text{otherwise} , \end{cases} \qquad \text{(C-4)}$$

and
$$b_k = \sum_{n=0}^{p-k} a'_n \, a'_{n+k} , \quad k=0, 1, \ldots, p. \qquad \text{(C-5)}$$

The coefficients b_k are just the autocorrelation coefficients corresponding to the inverse filter $H(z) = 1 - \sum_{k=1}^{p} a_k z^{-k}$. These coefficients need be computed only once for use in (C-3). If for every frequency of interest we know $\cos(\omega T)$, then $\cos(k\omega T)$ can be computed recursively as follows:

$$\cos[(k+1)\omega T] = 2 \cos(\omega T) \cos(k\omega T) - \cos[(k-1)\omega T].$$

Another way of looking at this is to note that if $\cos(\omega T) = x$, then $\cos(k\omega T) = T_k(x)$, the Chebyshev polynomials. These polynomials obey the recurrence relation:

$$T_{k+1}(x) = 2x\, T_k(x) - T_{k-1}(x),$$

with $T_0(x) = 1$. Therefore, given $2x$, $T_{k+1}(x)$ can be computed by a single multiplication and subtraction. If we define a single computation as equal to a multiplication and an addition (or subtraction), then if we desire $\hat{P}(\omega)$ at M values of frequency, the total number of computations C needed is equal to:

$$C_d = \frac{p}{2}(p+3) + 2pM . \quad \text{(Direct Method)}$$

This is to be compared with

$$C_f = 2M(\log_2 M+1) \qquad \text{(Simple FFT)}$$

for the base-2 regular FFT. For $p = 14$ and $M = 128$, $C_d/C_f = 1.9$. C_d can be cut approximately in half if each $\cos(k\omega T)$ is already stored. However, we know that there exist algorithms which cut C_f by at least half. So, on the whole, the FFT is approximately twice as fast as the direct method. But, the efficient FFT algorithms compute the transform at M equidistant frequency points, where M is a power of 2. These restrictions do not apply to the direct method. If one is interested in computing $\hat{P}(\omega)$ along a nonlinear scale of frequencies, the direct method may prove to be more efficient.

REFERENCES

Atal, B.S., and Suzanne L. Hanauer, "Speech Analysis and Synthesis by Linear Prediction of the Speech Wave," J. Acoust. Soc. Am., vol. 50, No. 2 (Part 2), 637-655, Aug. 1971.

Bell, C.G., H. Fujisaki, J.M. Heinz, K.N. Stevens, and A.S. House, "Reduction of Speech Spectra by Analysis-by-Synthesis Techniques," J. Acoust. Soc. Am., vol. 33, No. 12, 1725-1736, Dec. 1961.

Bendat, J.S., and A.G. Piersol, Measurement and Analysis of Random Data, John Wiley & Sons, New York, 1966.

Blackman, R.B., and J.W. Tukey, The Measurement of Power Spectra, Dover Publications, Inc., New York, 1958.

Cochran, et al, "What is the Fast Fourier Transform?", IEEE Trans. on Audio and Electroacoustics, vol. AU-15, No. 2, 45-55, June 1967.

Cox, H., "Linear versus Logarithmic Averaging", J. Acoust. Soc. Am., vol. 39, No. 4, 688-690, 1966.

Fant, G., Acoustic Theory of Speech Production, Mouton & Co., 's-Gravenhage, The Netherlands, 1960.

Fejér, L., "Über trigonometrische Polynome", Journal für die reine und angewandte Mathematik, vol. 146, 53-82, 1915.

Flanagan, J.L., Speech Analysis Synthesis and Perception, Academic Press Inc., New York, 1965, Second Edition 1972.

Flinn, E.A., "Comments on 'Speech Analysis and Synthesis by Linear Prediction of the Speech Wave'", J. Acoust. Soc. Am., vol. 51, No. 1 (Part 1), 38, Jan. 1972.

Fujimura, O., "Analysis of Nasal Consonants," J. Acoust. Soc. Am., vol. 34, No. 12, 1865-1875, Dec. 1962.

Gold, B., and L.R. Rabiner, "Analysis of Digital and Analog Formant Synthesizers", IEEE Trans. on Audio and Elect., vol. AU-16, No. 1, 81-94, March 1968.

Gold, B., and C.M. Rader, Digital Processing of Signals, McGraw-Hill, New York, 1969.

Gradshteyn, I.S., and I.M. Ryzhik, Tables of Integrals, Sums, Sequences and Products, FIZMATGIZ, Moscow, 1963.

Grenander, U., and G. Szegö, Toeplitz Forms and their Applications, Univ. of California Press, Berkeley, 1958.

Heinz, J.M., and K.N. Stevens, "On the Properties of Voiceless Fricative Consonants", J. Acoust. Soc. Am., vol. 33, No. 5, 589-596, May 1961.

Hershey, R.L., "Analysis of the Difference Between Log Mean and Mean Log Averaging", J. Acoust. Soc. Am., vol. 51, No. 4 (Part 1) 1194-1197, April 1972.

Hildebrand, F.B., Introduction to Numerical Analysis, McGraw-Hill, New York, 1956.

IBM, IBM System/360 Scientific Subroutine Package (360A-CM-03X) version III, Programmer's Manual, 1968.

Itakura, F., and S. Saito, "A Statistical Method for Estimation of Speech Spectral Density and Formant Frequencies", Electronics and Comm. in Japan, vol. 53-A, No. 1, 36-43, 1970.

Itakura, F., and S. Saito, "Digital Filtering Techniques for Speech Analysis and Synthesis", Proc. 7th International Congress on Acoustics, Budapest, Paper 25C1, 261-264, 1971.

Itakura, F., and S. Saito, "On the Optimum Quantization of Feature Parameters in the PARCOR Speech Synthesizer", Conference Record, 1972 Conf. on Speech Comm. and Processing, Newton, Mass., 434-437, April 1972.

Klatt, D.H., "Acoustic Theory of Terminal Analog Speech Synthesis", Conference Record, 1972 Conference on Speech Comm. and Processing, Newton, Mass., 131-135, April 1972.

Koenig, W., H.K. Dunn, and L.Y. Lacey, "The Sound Spectrograph", J. Acoust. Soc. Am., vol. 18, 19-49, 1946.

Kolmogorov, A., "Sur l'interpolation et extrapolation des suites stationnaires", C.R. Acad. Sci., Paris, vol. 208, 2043-2045, 1939.

Kunz, K.S., Numerical Analysis, McGraw-Hill, New York, 1957.

Lee, Y.W., Statistical Theory of Communication, John Wiley & Sons, Inc., New York 1960.

Levinson, N., "The Wiener RMS (Root Mean Square) Error Criterion in Filter Design and Prediction", J. Math. Phys., vol. 25, No. 4, 261-278, 1947. Also in Appendix B of Extrapolation and Smoothing of Stationary Time Series by N. Wiener, M.I.T. Press, Cambridge, Mass., 1966.

Makhoul, J.I., "SINC^n - A Family of Window Functions", QPR No. 97, Res. Lab. of Electronics, M.I.T., Cambridge, Mass., 145-150, April 15, 1970. (1970a)

Makhoul, J.I., "Speaker-Machine Interaction in Automatic Speech Recognition", Technical Report 480, Res. Lab. of Electronics, M.I.T., Cambridge, Mass., Dec. 15, 1970.(1970b)

Markel, J.D., "FFT Pruning", IEEE Trans. Audio and Electroacoustics, vol. AU-19, No. 4, 305-311, Dec. 1971.

Markel, J.D., "Digital Inverse Filtering - A New Tool for Formant Trajectory Estimation", IEEE Trans. Audio Electroacoustics, vol. AU-20, No. 2, 129-137, June 1972. Also, SCRL Monograph 7 SCRL, Santa Barbara, Calif., 1971.

Markel, J.D., and A.H. Gray,Jr., "On Autocorrelation Equations as Applied to Speech Analysis", Submitted to IEEE Trans. Audio Electroacoustics.

Mártony, J., "Studies of the Voice Source", Quarterly Progress and Status Report 1/65, Speech Transmission Lab., Royal Institute of Technology, Stockholm, 4-9, 1965.

Mathews, M.V., Miller, J.E., and David, E.E., "Pitch Synchronous Analysis of Voiced Sounds", J. Acoust. Soc. Am., vol. 33, 179-186, 1961.

Matsuda, R., "Effects of the Fluctuation Characteristics of Input Signal on the Tonal Differential Limen of a Speech Transmission System Containing Single Dip in Frequency Response", Electronics and Comm. in Japan, vol. 49, No. 10, 54, Oct. 1966.

Mermelstein, P., "Extraction of the Spectrum Envelope for Voiced Speech Segments", J. Acoust. Soc. Am., vol. 41, 1595, 1967(A).

Mermelstein, P., "Speech Synthesis with the Aid of a Recursive Filter Approximating the Transfer Function of the Nasalized Vocal Tract", Conference Record, 1972 Conference on Speech Comm. and Processing, Newton, Mass., 152-155, April 1972.

Mersereau, R.M., and A.V. Oppenheim, "An Application of the Cepstrum as a Measure of the Amplitude of a Signal", QPR No. 104, Res. Lab. of Electronics, M.I.T., Cambridge, Mass., 240-243, Jan. 15, 1972.

Noll, A M., "Short-time Spectrum and Cepstrum Techniques for Vocal Pitch Detection", J. Acoust. Soc. Am., vol. 36, 296-302, 1964.

Olive, J.P., "Automatic Formant Tracking by a Newton-Raphson Technique", J. Acoust. Soc. Am., vol. 50, 661-670, 1971.

Oppenheim, A.V., and R.W. Schafer, "Homomorphic Analysis of Speech", IEEE Trans. Audio and Electroacoustics, vol. AU-16, 221-226, June 1968.

Papoulis, A., Probability, Random Variables, and Stochastic Processes, McGraw-Hill, New York, 1965.

Paul, A.P., A.S. House, and K.N. Stevens, "Automatic Reduction of Vowel Spectra: An Analysis-by-Synthesis Method and its Evaluation", J. Acoust. Soc. Am., vol. 36, No. 2, 303-308, Feb. 1964.

Pinson, E.N., "Pitch-Synchronous Time-Domain Estimation of Formant Frequencies and Bandwidths", J. Acoust. Soc. Am., vol. 35, No. 8, 1264-1273, Aug. 1963.

Portnoff, M., V. Zue, and A. Oppenheim, "Some Considerations in the use of Linear Prediction for Speech Analysis", QPR No. 106, Res. Lab. of Electronics, M.I.T., Cambridge, Mass., July 15, 1972.

Rabiner, L.R., R.W. Schafer, and C.M. Rader, "The Chirp z-Transform Algorithm", IEEE Trans. Audio and Electroacoustics, vol. AU-17, No. 2, 86-92, June 1969.

Ralston, A., A First Course in Numerical Analysis, McGraw-Hill, New York, 1965.

Robinson, E.A., "Predictive Decomposition of Time Series with Application to Seismic Exploration", Geophysics, vol. 32, No. 3, 418-484, June 1967. (1967a)

Robinson, E.A., Statistical Communication and Detection, Hafner Publishing Co., New York, 1967. (1967b)

Schafer, R.W., and L.R. Rabiner, "System for Automatic Analysis of Voiced Speech", J. Acoust. Soc. Amer., vol. 47, No. 2 (part 2) 634-648, 1970.

Treitel, S., and Robinson, E.A., "Introduction, Special Issue on the MIT Geophysical Analysis Group Reports", Geophysics, vol. 32, No. 3, 416-417, June 1967.

Weinstein, C.J., and A.V. Oppenheim, "Predictive Coding in a Homomorphic Vocoder", IEEE Trans. Audio and Electroacoustics, vol. AU-19, No. 3, 243-248, Sept. 1971.

Wiener, N., Extrapolation, Interpolation and Smoothing of Stationary Time Series, M.I.T. Press, Cambridge, Mass., 1966.

Wilkinson, J.H., and C. Reinsch, Handbook for Automatic Computation, vol. 2, Linear Algebra, Springer-Verlag, New York, 1971.

SYMBOL TABLE

This is a list of most of the symbols used in this report along with the page number where that symbol is first used or defined.

		PAGE
a_k	Linear predictor coefficient	3
A, A_p	Gain factor of linear prediction transfer function $\hat{S}(z)$	17
$b_n, b(nT)$	Minimum-phase sequence corresponding to s(nT)	93
B_n	Bandwidth of formant n	191
$B(z)$	z-transform of b(nT)	93
$c_n, c(nT)$	Cepstrum of s(nT)	98
$\hat{c}_n, \hat{c}(nT)$	Cepstrum of $\hat{s}(nT)$	98
$c'_n, c'(nT)$	Complex cepstrum of $\hat{s}(nT)$	98
d^i	Differencing operator	131
$D(z)$	z-transform of differencing operator	131
$e_n, e(nT)$	Linear prediction error sequence	31
E, E_p	Total-squared error	31
f_0	Inverse of window width T'	179
f_s	Sampling frequency	16
F_0	Fundamental frequency	141
F_n	Frequency of formant n	191
$H(z), H_p(z)$	z-transform of linear prediction inverse filter	17
p	Order of linear predictor	3
$P(\omega)$	Signal spectrum	54
$\hat{P}(\omega)$	Linear prediction or approximate spectrum	54
$\hat{P}(\sigma_0, \omega)$	Off-axis spectrum	193
$P_e(\omega)$	Error power spectrum	55
$P(\omega, t)$	Time-varying power spectrum	76
$Q(\omega, \omega')$	Two-dimensional signal spectrum	79
$Q_e(\omega, \omega')$	Two-dimensional spectrum of error signal	81

r_k	Normalized autocorrelation of signal	40
R_k	Autocorrelation of signal	34
R'_k	Autocorrelation of differenced signal	135
$\hat{R}_k$	Autocorrelation of impulse response of $\hat{S}(z)$	44
$\tilde{R}_k, \tilde{R}(kT)$	Apparent autocorrelation function	65
$R(t,t+\tau)$	Nonstationary autocorrelation function	76
s	Laplace operator	16
$s_n, s(nT)$	Signal to be analyzed	2
$s'_n, s'(nT)$	First difference of $s(nT)$	130
$\hat{s}_n, \hat{s}(nT)$	Impulse response of $\hat{S}(z)$	44
$S(z)$	z-transform of $s(nT)$	17
$\hat{S}(z), \hat{S}_p(z)$	Transfer function of discrete p-pole linear prediction speech production model	17
$\tilde{s}_n, \tilde{s}(nT)$	Linear prediction approximation to $s(nT)$	30
T	Sampling interval	3
T_i	Toeplitz form	71
$u_0(x)$	Impulse function	78
$u_{-1}(x)$	Step function	177
$u_n, u(nT)$	Excitation sequence for speech production model	17
$U(z)$	z-transform of $u(nT)$	17
V	Ratio of spectral geometric mean to arithmetic mean	115
V_m	Lower bound on V	116
V_{min}	V_p for $p = \infty$	104
V_p	Normalized error	40
$w_n, w(nT)$	Discrete window function	65
$w(t)$	Continuous window function	173
$W(f)$	Fourier transform of $w(t)$	173
z	Complex variable of sampled-data frequency domain	16
δ_{nm}	Kronecker delta	44
$\Gamma(\omega,\Omega)$	Alternate two-dimensional spectrum	76

σ	Damping factor (real part of s)	16
τ	(1) Time lag for autocorrelation	75
	(2) Pitch period	141
τ'	Window width	177
τ'_e	Effective window width	184
ϕ_{ik}	Covariance coefficient	5
$\phi_n(z)$	Polynomials orthogonal on the unit circle	216
ω	Radian frequency (imaginary part of s)	16
ω_s	Radian sampling frequency	77
ω'	Radian frequency in 2D-spectrum	79
Ω	Radian frequency in alternate 2D-spectrum	77